ELECTROCHEMICAL DETECTION OF DENGUE VIRUS USING NANOPOROUS MEMBRANE

PEH EN KAI ALISTER

(B.Sci.(Hons.), NUS)

A THESIS SUBMITTED FOR THE DEGREE OF DOCTOR OF PHILOSOPHY OF SCIENCE

DEPARTMENT OF CHEMISTRY

NATIONAL UNIVERSITY OF SINGAPORE

2013

Declaration Page

I hereby declare that this thesis is my original work and it has been written by me in its entirety under the supervision of Professor Li Fong Yau, Sam (in the laboratory S5-02-05), Chemistry Department, National University of Singapore, between 03 Aug 2009 and 02 Aug 2013.

I have duly acknowledged all the sources of information which have been used in the thesis.

This thesis has also not been submitted for any degree in any university previously.

The content of the thesis has been partly published in:

1. Peh, A.E.K., Leo, Y.S., Toh, C.S. (2011) Current and nano-diagnostic tools for Dengue infection. *Front. Biosci. (Scholar edition) 3*, 806-821.

2. Nguyen, B.T.T., Peh, A.E.K., Chee, C.Y.L., Fink, K., Chow, V.T.K., Ng, M.M.L., Toh, C.S. (2012) Electrochemical impedance spectroscopy Characterisation of nanoporous alumina Dengue virus biosensor. *Bioelectrochemistry 88*, 15-21.

3. Peh, A.E.K., Li, S.F.Y. (2013) Dengue virus detection using impedance measured across nanoporous alumina membrane. *Biosens. Bioelectron. 42(1)*, 391-396.

Peh En Kai Alister		02 Aug 2013
Name	Signature	Date

Acknowledgements

It would not have been possible to write this thesis without the help and support of many kind people around me, to whom it is possible to give particular mention here.

Above all, I would like to express my deepest gratitude to my supervisor Professor Sam Li for his unwavering support throughout my Ph.D. course, his patience, motivation, encouragement and immense knowledge. Thank you so much for being there when I needed you.

My sincere thanks are extended to Professor Lee Hian Kee, Assistant professor Toh Chee-Seng, Dr Nguyen Thanh Thi Binh and Ms Yin Thu Nyine for their advice, help and guidance for the projects and for parting the knowledge of electrochemical techniques and porous membranes.

My heartfelt appreciation to my collaborators for providing me with the samples required by my projects; Professor Mary Ng and Ms Loy Boon Kheng for providing the West Nile virus; Dr Katja Fink, Ms Ying Xiu and Mr Joseph Ng for providing the Dengue virus; Professor Vincent Chow and Ms Kelly Lau for providing the Dengue and Chikungunya virus.

I would like to acknowledge the financial, academic and technical support of the Ministry of Education, National University of Singapore and its staff. I also thank the Department of Chemistry for their support and assistance

I am indebted to my honours year students: Judy Lee, Celine Chee and Yeo Xue Xin, fellow graduate students, research assistants and research fellows of the group for being understanding, for all the simulating discussion, support and help.

Lastly, I would like to thank my family members, friends and relatives for their unequivocal support, spiritually and emotionally.

Table of Contents

Summary

This thesis entails the development of membrane-based biosensors for the detection and serotyping of an infecting Dengue virus. The projects aim to explore sensing platforms which can possibly be miniaturised into a point-of-care diagnostic tool. Early disease diagnosis is particularly important since the fluid treatment and monitoring is currently the only way to fight against the disease. Anodic aluminum oxide (alumina) membrane is chosen because of its good mechanical stability and regularity in pore sizes. These nano-sized pores permit high throughput analysis, better sensitivity and selectivity due to their large surface-area-to-volume ratio and close intimation with biomolecules of similar sizes. Electrochemical techniques are employed as the detecting platform because they can be easily miniaturised and the data can be output into values easily understood by an end-user.

In chapter 1 we used a home-made alumina membrane to detect the presence of the Dengue virus. The membrane electrode was fabricated by anodising and etching the coated aluminum metal. Impedance studies of the system reveal that the electrode surface is insensitive to the Dengue virus. This phenomenon is different from the conventional electrodes reported. In addition, the channel's capacitance can be used to differentiate the Dengue virus from other flaviviruses. The antigen-antibody binding was found to follow the Freundlich isotherm which is commonly used to describe the binding within porous systems. The main disadvantage of the biosensor is the alumina layer dislodging during washing steps.

In chapter 2, we fabricated another alumina electrode sensor by coating a layer of conductive platinum metal onto a commercially available alumina membrane with a diameter of 13 mm and a thickness of 60 μm. This biosensor is mechanically more stable than the home-made one since neither the alumina membrane nor the platinum layer dislodges during the preparation and analysis process. In addition, the biosensor design is very neat as the membrane acts as the working and counter electrode. This biosensor can achieve a lower detection limit than the home-made biosensor with similar preparation conditions.

In the last chapter, we demonstrated a proof of concept that using a flow-based system, unknown Dengue viruses can potentially be differentiated and serotyped. The process involves manipulating the properties of nanofluidics where the redox probes are made to diffuse across the alumina membrane immobilised with unknown Dengue viruses. The analysis time is similar to the RT-PCR process but is generally less complicated and unlikely to suffer from contaminations. Besides, with simple assumptions that the diffusion of the redox probes follows the Fick's first law and these probes will foul the electrode surface, we can adequately simulate and fit the observed data.

List of Tables

Chapter 2

Chapter 3

Chapter 4

List of Figures

Chapter 1

Chapter 2

List of Abbreviations

AAO	Anodic aluminum oxide
APS	3-aminopropyltrimethoxysilane
BCA	bicinchoninic acid
BSA	Bovine serum albumin
C	Capsid protein
C	Capacitance
C	Concentration
CE	Counter electrode
CHIKV	Chikungunya virus
CPE	Constant phase element
DENV 1	Dengue serotype 1 virus
DENV 2	Dengue serotype 2 virus
DENV 3	Dengue serotype 3 virus
DENV 4	Dengue serotype 4 virus
DHF	Dengue Hemorrhagic Fever
DMSO	Dimethyl sulfoxide
DNA	Deoxyribonucleic acid
DPV	Differential pulse voltammetry
DSS	Dengue Shock Syndrome
E	Envelope protein
ED III	Envelope domain 3 protein

EDC	1-ethyl-3-[3 dimethylaminopropyl]carbodiimidehydrochloride]
EIS	Electrochemical impedance spectroscopy
ELISA	Enzyme-linked immunosorbent assay
ER	Endoplasmic reticulum
FBS	Fetal bovine serum
Fc	Ferrocene
FESEM	Field emission scanning electron microscopy
GC	Glassy carbon electrode
HI	Hemagglutination inhibition
ICP-MS	Inductively coupled plasma mass spectrometry
IgG	Immunoglobulin G
IgM	Immunoglobulin M
LC-MS	Liquid chromatography mass spectrometry
M	Membrane protein
MAC-ELISA	IgM antibody capture enzyme-linked immunosorbent assay
MOI	Multiplicity of infection
NC	Nucleocapsid
NHS	N-Hydroxysuccinimide
NS 1	Non-structural protein 1
NS 2a	Non-structural protein 2a
NS 2b	Non-structural protein 2b
NS 3	Non-structural protein 3
NS 4a	Non-structural protein 4a

NS 4b	Non-structural protein 4b
NS 5	Non-structural protein 5
PBS	Phosphate buffered saline
PC	Photonic crystals
PCR	Polymerase chain reaction
PET	Polyethylene terephthalate
PrM	Precursor form of membrane protein
PRNT	Plaque reduction neutralisation test
QCM	Quartz crystal microbalance
R	Resistance
RE	Reference electrode
RNA	Ribonucleic acid
RT-PCR	Reverse transcriptase polymerase chain reaction
SPR	Surface plasmon resonance
TGN	Trans-golgi network
W	Warburg diffusion
WE	Working electrode
WNV	West Nile virus

List of Symbols

K_{ct}	Heterogeneous rate coefficient
R	Gas constant
T	Temperature
F	Faraday constant
A	Area
A_t	Area at time (t)
A_0	Initial area of the surface
C_{bulk}	Concentration of the bulk solution
C_{feed}	Concentration of the feed solution
$C_{channel,feed}$	Concentration of the channel near the feed side
ρ_c	Channel resistivity
K	Binding constant between the antibody and antigen
K_a	Rate of adsorption
D	Diffusion coefficient
θ	Fraction coverage
R_1	Channel resistance
R_2	Charge transfer resistance
R_s	Solution resistance
R_p	Pore resistance
ΔR_p	Change in pore resistance
R_{et}	Electron transfer resistance
C_m	Membrane capacitance
CPE_1	Membrane-electrolyte capacitance

CPE_2	Electrode-electrolyte capacitance
t	Time
i	Current
i_t	Current at time t
i_0	Initial current
J	Flux
N	Total number of available binding sites
l_m	Length of the nanochannel/Thickness of the membrane
E_t	Potential at time (t)
E_0	Initial potential
ω	Radial frequency
Z_o	Magnitude of impedance
Z*	Overall impedance
Z'	Real impedance
Z"	Imaginary impedance
ϕ	Phase shift
n_1,n_2	Fractal order of reaction
m	Mass transfer coefficient

Chapter 1: General introduction of Dengue virus and the current state of art for Dengue detection

1.1. Dengue virus in general

Dengue is the most rapidly spreading, acute febrile mosquito-borne viral disease caused by the Dengue virus. Over the past 50 years, the incidence of Dengue had increased by approximately thirty folds, spreading across increasing number of countries as well as from the rural to urban regions. This disease is now endemic in most tropical and subtropical regions. An estimated number of about 50 million cases of Dengue fever occur per year with 500,000 cases of Dengue Hemorrhagic Fever and 22,000 deaths. Presently, about 2.5 billion people live in over 100 Dengue endemic countries (*1*). The presence of Dengue has inflicted significant health, social and economic burden on these endemic areas (*2*). Hence decreasing the number of outbreaks and if possible eliminating the disease will be of utmost importance. There are several factors that contribute to the occurrence of the disease, mainly the increases in international travel and human population, besides global climate change (*3*).

The Dengue virus belongs to the flavivirus genus of the flaviviridae family. The Dengue virus is transmitted to vertebrates by infected *Aedes aegypti* and *Aedes albopictus* mosquitoes when they feed on their blood. The Dengue virus is divided into four antigenically related but distinct serotypes; Dengue 1 (DENV-1), Dengue 2 (DENV-2), Dengue 3 (DENV-3) and Dengue 4 (DENV-4). The mature Dengue virus is spherical in shape and approximately

50-60 nm in size. It contains a single-stranded RNA of 11,000 nucleotide bases in length. This RNA resides within a nucleocapsid which is enclosed by a lipid bilayer containing three structural proteins (*4-6*). The RNA genome is organised into 2 basic and distinct regions. The first region codes for 3 structural proteins; capsid protein (C), precursor of the membrane protein (prM) and envelope protein (E). The next region codes for three large non-structural proteins: NS1, NS3 and NS5 and four smaller non-structural proteins: NS2a, NS2b, NS4a and NS4b. Overall, the sequence of RNA genome is as follows: 5'-C-prM-E-NS1-NS2a-NS2b-NS3-NS4a-NS4b-NS5-3' in terms of protein expression.

There are three major complexes within the flaviviridae family: the Tick-borne encephalitis virus, Japanese encephalitis virus and Dengue virus. All flaviviruses share similar morphology and a genomic structure, with a common antigenic determinant. As a consequence, the specific identification of a family member poses significant challenge for serological methods owing to extensive cross-reactivity of the antibodies in the serum. The situation is worst in Dengue virus since it comprises four serotypes. Despite this extensive cross-reactivity, infection by one of the Dengue serotype usually confers lifelong immunity against the homologous serotype but not the other three serotypes (*4*).

Dengue infection can be caused by any of the four serotypes with varying severity. Infection in human leads to a wide spectrum of illnesses, ranging from mild febrile illnesses to fatal hemorrhagic diseases. Dengue fever is usually characterised by a sudden onset of fever which normally last 2-7 days, together with a variety of nonspecific signs and symptoms such as high fever,

headache, nausea, vomiting, joint pain, fatigue and rashes. The entire course of the illness can be broadly divided into three phases; febrile, critical and recovery phase (*1*). During the critical phase, some individuals may progress to a severe plasma leakage in cases with Dengue Hemorrhagic Fever (DHF) or Dengue Shock Syndrome (DSS), severe haemorrhage and severe organ involvement (*1*, *7*). The warning signs for severe Dengue include persistent vomiting, mucosal bleeding, lethargy, abdominal pain or tenderness, clinical fluid accumulation, restlessness, liver enlargement of more than 2 cm and an increase in the hematocrit count with a rapid decrease in platelet count (*1*). Shock ensues when a critical volume of the plasma is lost through leakage. A prolonged shock may lead to coagulopathy and multiorgan failure. Careful monitoring of the blood counts, the assessment of hemodynamic status and recognition of these warning signs allow early treatment intervention. Appropriate fluid management and supportive care are vital to the recovery (Fig. 1.1).

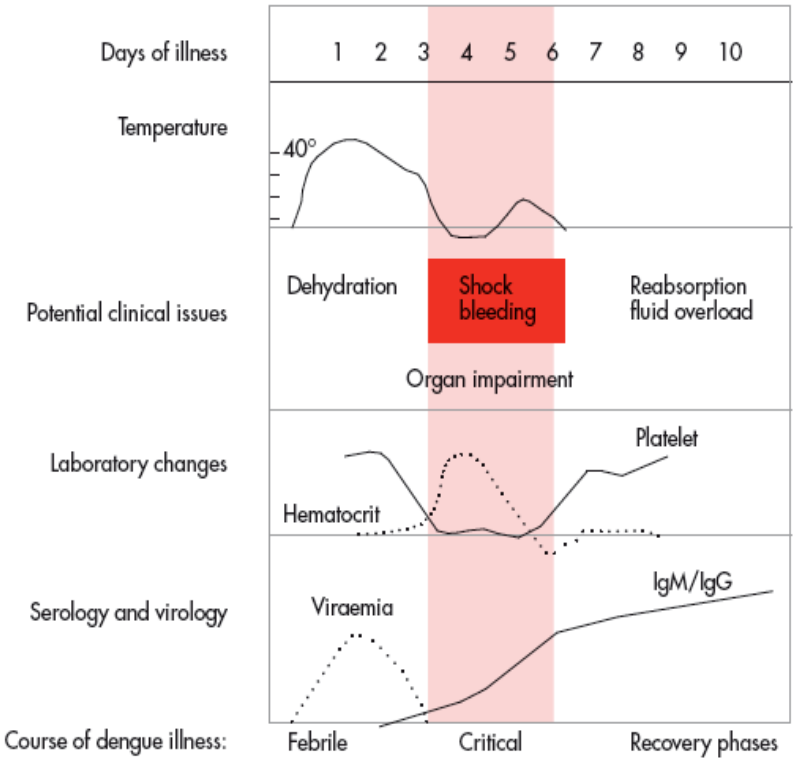

Fig. 1.1 Development of the disease adopted from ref (*1*).

Currently, there are no effective vaccines or drugs to prevent or treat Dengue infection. Hence, the most effective way to reduce the spread of the disease is to control vector multiplication (*5, 8*). However, the global attention to this issue is required since migration and geographical expansion can lead to the transportation of the virus from one place to another (*6*). Until a global cooperation of the vector control can be achieved or an effective vaccine becomes available, early diagnosis remains an important tool for case confirmation and clinical care. Relying solely on clinical diagnosis can be problematic since the symptoms of Dengue infection are nonspecific, in particular during the early febrile phase (*5*). Laboratory diagnosis methods relying on genome and antigen detection as well as serological methods have been widely applied. Conventional serological methods include hemagglutination inhibition **(**HI), plaque reduction neutralisation test **(**PRNT) and enzyme-linked immunosorbent assay (ELISA) whereas antigen detection methods are virus isolation and reverse transcriptase polymerase chain reaction (RT-PCR).

1.2. Conventional methods for the detection of Dengue infection

Hemagglutination inhibition **(**HI) is a modification of the hemagglutination test. Instead of measuring the amount of agglutination when the antigens are mixed with the red blood cells, the method measures the amount of anti-Dengue antibodies in the sera required to displace the agglutination. Details of the method had been neatly summarised by Clarke and Casals (*9*). Optimally, the HI test requires paired sera obtained in the acute- and

convalescent-phase with an interval of more than 7 days. Primary and secondary infection can be resolved by measuring the relative amount of antibodies in the paired sera collected. Primary infection is characterised by a low level of antibodies in the acute serum followed by a slow rise in the convalescent phase. While in secondary infection, antibody titers rise rapidly and usually exceed a 1:1280 value. The test is sensitive, simple to carry out and requires minimal equipment. However, it lacks specificity to distinguish between the flaviviruses and the four Dengue serotypes owing to cross-reactivity of the antibodies (*5*).

Plaque reduction neutralisation test **(**PRNT) is usually performed by adding a known amount of Dengue virus to the serum sample that has been subjected to serial dilution. This mixture is incubated and subsequently inoculated onto a sensitive cell monolayer. Each virus that initiates an infection forms a plaque. The plaques formed are subsequently counted and compared to the starting concentration of the virus to determine the percentage reduction in the total virus infectivity (*10*). This method is the most specific serological test that can differentiate the flaviviruses and the Dengue serotypes and it is more sensitive than the HI method. But it is time consuming, labour intensive and has relatively low throughput (*5*).

Enzyme-linked immunosorbent assay (ELISA) is a biochemical method to detect the presence of antigens or antibodies in the sample. There are two general forms of ELISA which are commonly carried out. The sandwich ELISA uses monoclonal antibodies to detect the presence of target antigens in the sample, followed by enzyme labelled antibodies which will bind to the target

antigens in a sandwich configuration. The indirect ELISA uses immobilised antigens to detect the presence of target antibodies in the sample, followed by binding of the target antibodies to added enzyme labelled antibodies. In both forms, after the formation of the immunocomplexes, the detection of the immunocomplexes is carried out by enzyme conjugated-monoclonal or polyclonal antibodies that will transform the colourless substrate into a coloured product, measured with a spectrophotometer. ELISA methods are generally simple, rapid and only require a basic equipment setup.

Immunoglobulin M-antibody capture ELISA (MAC-ELISA) is the commonest and widely used serological test. It is a sandwich ELISA method based on detecting the Dengue specific immunoglobulin M (IgM) which appears ~5 days after the onset of fever and last ~30-60 days. The MAC-ELISA can be carried out with either one serum or paired sera from the patient (*1*). Positive diagnosis of the patient with one serum sample indicates a probable Dengue case. Though MAC-ELISA using one serum sample does not confirm that the patient has Dengue infection, the rapid analysis time allows mass screening and immediate classification of suspected patients especially during epidemics.

The sensitivity of this method often depends on the point of time during which the sample was tested. If the test is carried out too early, or carried out on elderly and immunocompromised patients, the level of IgM may be below the detection limit. The method is considered to have good sensitivity and specificity only when it's used five or more days after the onset of fever.

Diagnosis with MAC-ELISA can be challenging because Dengue IgM antibodies also cross-react to some extent with other flaviviruses. In addition, MAC-ELISA test with a single acute-phase serum sample had been reported to give significantly more false negative results compared to false positive results (*6*). The MAC-ELISA assay is not useful for Dengue serotypes determination owing to cross-reactivity of the antibodies (*1*).

An immunoglobulin G (IgG) ELISA using the indirect method is usually used for the determination of past infection as well as to differentiate a primary infection from a secondary infection. The Dengue specific immunoglobulin G (IgG) usually appears ~7 days after the onset of fever and last for months to years. Due to the late appearance of the IgG antibodies, detection of IgG is not useful as a diagnostic tool. Past infection can be determined since IgG antibodies remain in the body for years. Primary and secondary infection can be determined in a similar way as in HI. A negative IgG in the acute-phase serum and a positive IgG in the convalescent-phase serum collected indicate a primary infection. While a positive IgG in the acute-phase serum and a four-fold rise in the IgG titer in the convalescent-phase serum suggest a secondary infection. Alternatively, the simultaneous determination of the IgG and IgM using the IgG and IgM capture ELISA allows primary and secondary infections to be distinguished too. In general, a IgM/IgG ratio greater than 1.2 or 1.4 (using patient's sera dilution of 1/100 or 1/20) is indicative of a primary infection and a ratio less than this reference number confirms a secondary infection (*1*). This ratio may vary between laboratories, thus standardisation of the test is required.

This IgM/IgG ratio method is more commonly used than the HI and IgG ELISA methods.

As mentioned above, an early detection of the Dengue infection is very important for epidemiological strategies, clinical management and administrating of appropriate treatment to the patients. Most of the serological methods are not suitable for routine early diagnosis since Dengue antibodies usually appear much later after the infection. Accuracy of serology methods is often hampered by patient suffering from secondary infection. Not to mention, serological methods are time consuming owing to cultivating of virus in PRNT or collecting of the serum in the convalescent phase in HI and ELISA. Nevertheless, serological methods are still important in retrospective studies. Presently, MAC-ELISA is the only serological method useful in clinical diagnosis. This is because, a lot of times people only seek treatment few days after the infection which coincide with the appearance of the IgM antibodies in the serum.

Virus isolation method depends on the cultivation of virus isolated from the patient's serum sample, followed by the subsequent detection of the virus using an immunofluorescence technique. Serum to be used for the analysis should be collected during the acute phase of the illness, coinciding with ~4-5 days of the disease for successful isolation of the Dengue virus. The Dengue virus can also be isolated from tissues such as the liver, spleen and lymph node (*11*). The mosquito cell line (C6/36) is most commonly used to cultivate the isolated Dengue virus in replacement of the traditional mosquito inoculation

method. This method is rapid, sensitive and economical, making it perfect for the diagnosis of large number of samples and for routine virological surveillance. Even though it is less sensitive than the mosquito inoculation method, the disadvantage is offset by the ease in which large amount of samples can be processed (*4*). The virus cultivated is identified using immunofluorescence technique with serotype-specific monoclonal anti-Dengue antibodies on the infected cells. Virus isolation is recognised as the 'gold standard' for the detection of Dengue virus and should be carried out whenever in doubt of the serological tests such as HI and ELISA. However, in comparison to the serological methods, virus isolation method is often slow, labour intensive, expensive and dependent on sample handling and transportation conditions (*4*). Thus, it has been gradually replaced by the reverse transcriptase polymerase chain reaction (RT-PCR) method.

In reverse transcriptase polymerase chain reaction (RT-PCR), reverse transcriptase enzyme is added to produce the complementary DNA sequence from a specified region of the viral RNA genome. Subsequently, the complementary DNA is amplified through repeated denaturation, annealing and elongation processes using the polymerase chain reaction (*5*). The amplicons produced are separated by agarose gel electrophoresis and detected with ethidium bromide or fluorescence. This is a rapid and sensitive method that is applicable to most viruses. It has comparable cost and better sensitivity compared to the virus isolation method (*1*). In addition, the result of this method is less affected by the handling and storage of the serum samples as well as the presence of any antibodies (*4*). With a careful selection of the specific primers

used, RT-PCR can be extremely useful for detecting and serotyping of the Dengue virus, thus allows rapid identification of existing or new serotypes in endemic areas (*5*). Though the RT-PCR method is gradually replacing the virus isolation method, it is still far from being a simple diagnostic tool. Prior knowledge of the viral genome sequence must be known in order to synthesise the specific primer. Also, sample preparations must be done carefully to reduce false negative results caused by contaminations (*5*). Various modifications of this method such as nested RT-PCR, real-time RT-PCR and quantitative RT-PCR had also been used for the diagnosis of Dengue infection. The advantages and disadvantages of these modified methods compared to the conventional RT-PCR had been clearly summarised by Ratcliff *et al. (12).*

Recently, a sandwich ELISA detection method for the non-structural protein 1 (NS1), had also been used to confirm Dengue infection cases (*13*). The NS1 protein can be detected in the blood serum from day one after the onset of fever up to day nine. It can also be detected after the viremia period when RT-PCR shows negative test for the viral RNA and when IgM antibodies are found in the serum sample (*13*). Thus, choosing the NS1 protein as the biomarker for Dengue infection has a clear advantage over the other serological methods which in addition, has shown good selectivity amongst other flaviviruses. The NS1 detection presently cannot differentiates the different Dengue serotypes (*1*).

Antigen detection methods are definitely more appealing since they permit early diagnosis with confidence (Fig. 1.2) compared to serological detection methods, and thus render early treatment possible. Conventional

antigen detection methods are sensitive and useful for serotyping of the infecting Dengue virus. However, they are too costly to be employed for routine diagnostic use. They are commonly used after the patient is screened and tested positive with the MAC-ELISA. The introduction of NS1-ELISA has made early detection of Dengue infection possible and more affordable for hospital usage. This method is only confounded by the limitations of the ELISA method which are time consuming, laboratory based and requires expertise to carry out the test.

The method of detection changes according to the development of the disease. During the first few days of the infection, also known as the viraemia stage (0-5 days), antigen detection methods provide the most accurate result. After 4-5 days, MAC-ELISA is preferred because the amount of viruses remaining in the blood serum begins to decrease due to the appearance of the IgM antibodies. From day 6 onwards, a combination of ELISA and PCR-based methods would be ideal for accurate results. The choice of diagnostic methods often depends on the purpose of testing, the type of laboratory facilities, technical expertise available, the analysis cost, as well as the time of sample collection. Most of the time, diagnosis is less straightforward as patients tend to delay in seeking treatment. Thus, WHO (World Health Organisation) recommended the use of a mixture of an antibody detection method with an antigen detection method for case confirmation. Alternative diagnostic systems that can detect the Dengue virus or related biomarkers during the early phase of the infection with comparable sensitivity, selectivity, diagnosis time as the current methods and can be operated by non-experts would be ideal. The main aim is to bring diagnostic device into clinical and home-based usage such that

patient down with fever can do a quick test and seek treatment immediately if the tested result is positive. This act is very favourable since it reduces the need to do a duo test for confirmation which will in turn save resources.

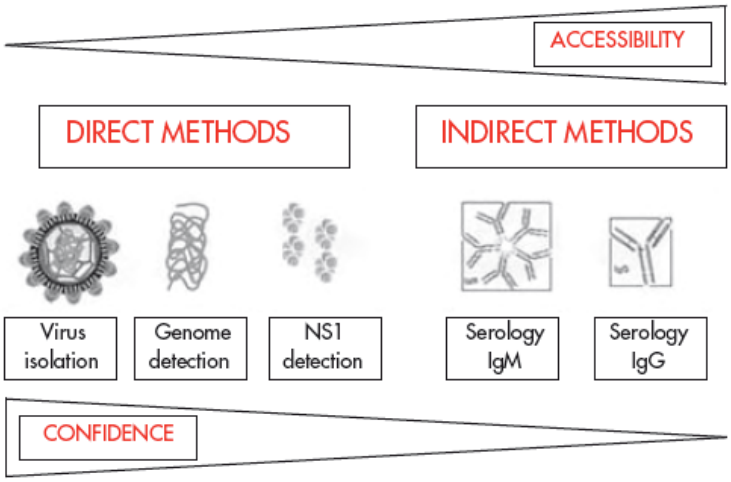

Fig. 1.2. Comparison of diagnostic tests according to their accessibility and confidence adopted from ref (*1*).

1.3. Advanced methods fabricated for the detection of Dengue infection

Recent reports have described an increase use of high sensitivity methods for virus detection with detection limits in range of ng mL^{-1} (*14, 15*) or pg mm^{-2} (*16, 17*) and as such, have been broadly described as nanotechnological advancements (*18*). In general, these methods rely on optical, electrical or electrochemical signals to detect minute changes in the physicochemical properties of the sensing element which often comprises micrometer to nanometer size particulate, film or membranous materials. We observe that these methods can be further classified into those relying significantly on sensitive instrument-based biosensor design such as the quartz crystal microbalance (QCM), surface plasmon resonance (SPR), photonic crystals (PC) and electrochemical impedance spectroscopy (EIS) as opposed to those which

focus on nanoscale material-based biosensor design such as using of nanowire, nanopore and liposome to amplify signal (Fig. 1.3). The use of impedance technique and nanoporous membrane will be elaborated in details in the following chapters. Besides showing a proof of concept that these novel systems can be used for sensitive Dengue detection, these systems can potentially be miniaturised and developed into point-of-care diagnostic tools.

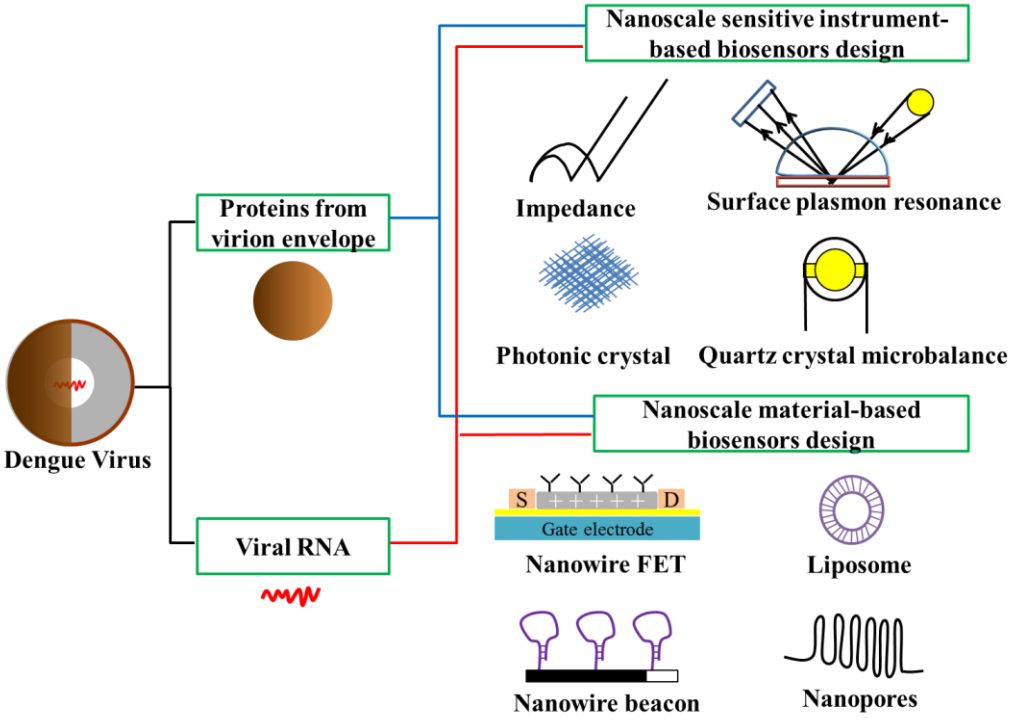

Fig. 1.3. Overview of the nanoscale sensitive instrument-based biosensors and nanoscale material-based biosensors used for the detection of Dengue infection.

Quartz crystal microbalance (QCM) is a piezoelectric transducer which can measure mass changes per unit area by following the corresponding frequency change of the resonating quartz crystal when small amount of mass is added or removed from the crystal surface (*19*). Quartz crystal microbalance sensors are low cost sensors designed for real-time mass determination. This method is sensitive, precise and has a fast response time, with potential for

miniaturisation owing to its small size, making it ideal for diagnostic purposes (*20-22*). The major disadvantage of the method is the signal tends to be affected by vibrations caused by the environment and by the viscosity drag in the liquid phase (*23*). The quartz crystal microbalance was used in kinetic research, medical diagnosis and the detection of pathogenic microorganisms (*23*).

Wu *et al.* developed a real-time and user-friendly QCM immunochip for the detection of the Dengue envelope protein and NS1 protein. With the aid of sample pretreatment using the cibacron blue 3GA gel-heat denature method, the detection limit of the envelope protein and NS1 protein was 1.727 μg mL^{-1} and 0.740 μg mL^{-1} respectively (*21*). In another work, Chen *et al.* developed a real-time and circulating-flow QCM useful for early diagnosis and epidemiology study of Dengue infection using nucleic acids identification (*22*). They had demonstrated that this method has comparable sensitivity and specificity to the fluorescent real-time PCR method. In addition, the method does not require expensive instrumentation, is label-free and highly sensitive, with a reported detection limit of 2 PFU mL^{-1} (*22*).

Photonic crystals are periodic optical nanostructure designed to affect the motion of the photons. Detection is achieved by measuring the wavelength of peak reflectance as a function of time or space. Photonic crystal is an appealing choice for making sensors since their optical properties can be modified under the influence of analytes (*24*). The photonic crystal sensor is a label-free method with typical detection limits in the range of pg mm^{-2}. It is able to produce reliable results even when the sensing area is in the micrometer to

millimeter range. This allows the crystals to be incorporated onto lab-on-a-chip devices for *in-situ* sensing of analytes (*24, 25*) including biological molecules (*24*). Huang *et al.* reported the detection of human anti-Dengue antibodies from serum samples using compact optoelectronics biosensors. The biosensor showed comparable detection sensitivity as ELISA but with shorter and simpler preparation steps (*26*). Mandal *et al.* presented a nanoscale optofluidic sensor array for the detection of Dengue virus which can carry out label-free, parallel detections of biomolecular interactions in aqueous environments with potential of achieving low mass detection limit (*27*).

Surface plasmon resonance (SPR) is an optical method which measures the changes in refractive index at the interface between the conductive layer and the external medium when an incident beam of p-polarised light strikes the surface. The major advantages of the surface plasmon resonance sensors include being a label-free method, able to characterise binding reactions in real-time, generate reproducible results with little effort and time (*28*) and give excellent detection limit in the range of pg mm^{-2} (*29*). In addition, the method has shown several advantages over the ELISA method such as lower detection limits, less false positive and negative results and rapid analysis times (*28, 30*). Kumbhat *et al.* had demonstrated that the surface plasmon resonance method can be used for the detection of Dengue virus and the sensor can be regenerated three times without showing significant deviation of the results (*30*).

In past decades, many scientists and engineers had been working toward improving the sensitivity and specificity of diagnostic tools as well as

miniaturising these systems such that they can be made portable for convenience use. This process of downscaling has led to the focus on the construction and utilisation of materials with sizes in the nanometer regime. These nanomaterials have unique physical and chemical properties owing to their nanometer size in one or more dimensions. For example, the large surface-to-volume ratio of the nanomaterials allows large number of biorecognition molecules to be attached. The close range interactions between the nanomaterials (which also function as transducers) and the attached biorecognition molecules can influence the physicochemical properties of these nanomaterials, especially in the presence of target analytes which bind to the biorecognition molecules (*31, 32*).

Nanowires are wires with diameters in the nanometer range. Nanowires used in various sensing strategies including optical, electrical, mass-dependent and in particular electrochemical methods, had been reported (*33*). They are very attractive sensing materials owing to their small sizes and high surface-to-volume ratio with unique electronic, optical or magnetic properties (*33*). In addition, nanowires can be readily functionalised with various biochemicals using appropriate linkage chemistries to produce nanosensors and nanocarriers with enhanced properties (*34*). Zhang *et al.* made use of an innovative silicon nanowire-based field-effect transistor sensor (Fig. 1.4) for label-free, specific, highly sensitive and rapid detection of RT-PCR products of Dengue 2 virus. The silicon nanowire biosensor was able to detect lower than 10 fM of amplicons within 30 min (*35*). Stoermer *et al.* had synthesised oligonucleotide sequence probes for the simultaneous detection of various viruses including the Dengue 2 virus. The nanowire was able to recognise the complementary DNA target

strands of the Dengue 2 virus and illustrated the exciting capability of barcoded nanowires as a multiplexing agent (*36*).

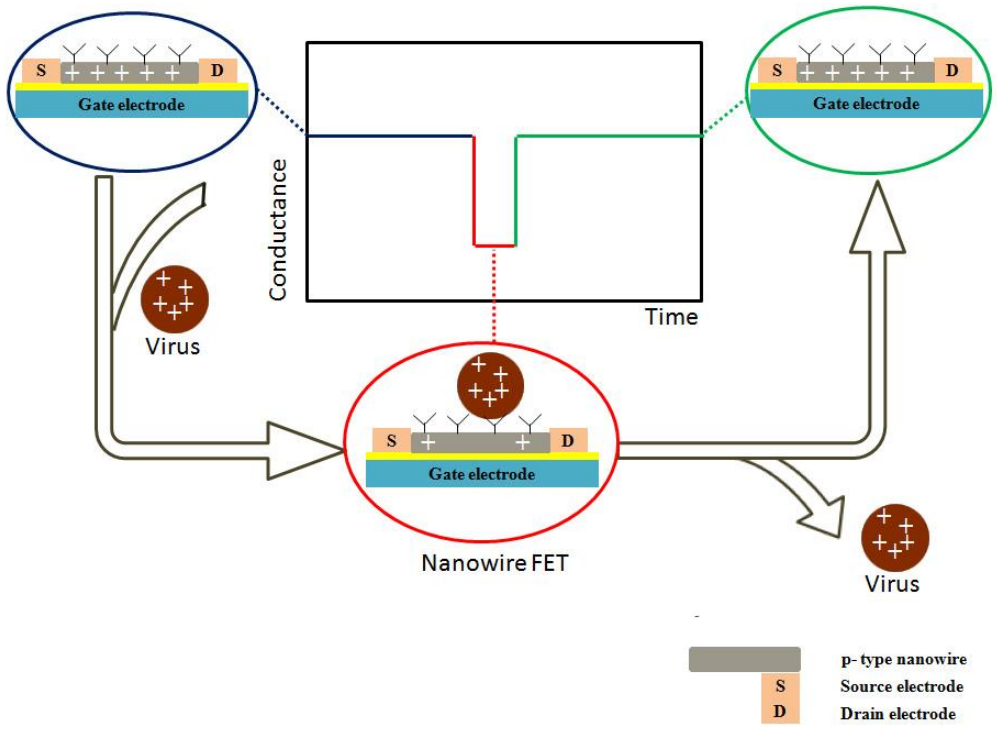

Fig. 1.4. Schematic diagram showing conductance measurement using a nanowire-based field-effect transistor sensor.

Liposomes are nanosized vesicles comprising one or more concentric lipid bilayers surrounding an internal aqueous compartment. They are formed spontaneously when phospholipids are dispersed in water and are usually biocompatible, non-toxic and biodegradable. These molecules are normally used as signal amplifier as they are capable of encapsulating a large quantities of a wide range of substances such as fluorophores and enzymes. The mode of detection depends on the type of marker molecules encapsulated within the liposomes (*37, 38*). Zaytseva *et al.* had created a microfluidic biosensor with fluorescence detection for the rapid, sensitive and serotype-specific detection of the Dengue virus. The fluorophores were carried by the liposomes which will

attached to the target. The fluorophores released allow fluorescence quantification of the hybridised complexes, with a reported excellent detection limit of 50 pM and analysis time of 20 min (*39*)(Fig. 1.5).

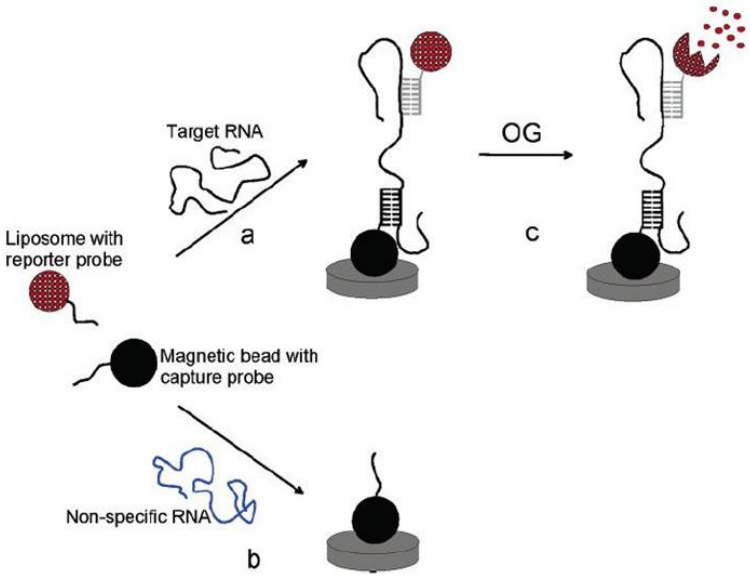

Fig. 1.5. Schematic diagram illustrating the recognition and detection of Dengue RNA using a liposome-based biosensor. (Re-printed with permission from *(39)*. Copyright (2005) American Chemical Society)

In general, those methods which rely on RNA and/or DNA detection are less useful for development into point-of-care diagnostic tools. The need to extract the RNA from the virus will definitely add time and cost to the analysis. In addition, RNA is a sensitive material which is encouraged to be handled only by trained personnel to minimise contamination or degradation of the RNA during the analysis process. Nevertheless, if these methods can be adapted and used for serotyping of the infecting Dengue serotypes, they can be employed to areas which cannot afford the expensive PCR equipment.

1.4. Scope of research

We have briefly described and illustrated some of the conventional and advanced methods fabricated for Dengue virus detection. In this thesis, we attempt to detect and differentiate the Dengue serotypes using different platforms of detection. First, we will demonstrate the use of the self-fabricated alumina membrane using the anodising and etching method for the detection of Dengue virus. The main focus is to understand the impedance circuit governing the alumina membrane. In the alumina membrane biosensor, majority of the biomolecules bind themselves to the wall of the nanochannels instead of the underlying electrode surface. As a consequence, Randles circuit which describes processes occurring at the working electrode cannot be applied here. This is somewhat different from most conventional biosensors. In addition, we also demonstrate that the constant phase element (CPE) describing the membrane can be used to differentiate the various flavivirus.

Next, we demonstrate that the commercially available alumina membrane can also be fabricated into a Dengue virus sensor. The good mechanical stability and high pore density of the alumina membrane make the sensor more robust and sensitive compared to the self-fabricated alumina electrode. A novel sensing platform is fabricated through making the membrane conductive and using it as the working and counter electrode. Randles circuit is not relevant in discussion because the working electrode is independent of the binding processes.

Finally, we show a proof of concept that electrochemical detection can be used to as a simpler tool to identify and differentiate the serotype of the Dengue virus. By taking advantage of diffusion as a form of transport in the nano-scaled pore size, the transport and binding of the redox labelled probes across the membrane bounded with the Dengue viruses together with the rate of fouling at the working electrode allow us to obtain a time-based graph. Through assuming that the diffusion of the probes across the membrane follows the Fick's first law and fouling occurs irreversibly at the working electrode due to simple Langmuir adsorption of the probes, we can adequately simulate the results obtained.

1.5. References

1. W.H.O. (2009) Dengue: guidelines for diagnosis, treatment, prevention and control - New Edition. Geneva, W.H.O. (World Health Organisation in Geneva).

2. Gubler, D. J. (2002) Epidemic Dengue/Dengue Hemorrhagic Fever as a public health, social and economic problem in the 21st century, *Trends Microbiol. 10*, 100-103.

3. Koh, B. K. W., Lee, C. N., Kita, Y., Choon, S. T., Li, W. A., Kit, Y. W., Lyn, J., and Kee, T. G. (2008) The 2005 Dengue epidemic in Singapore: Epidemiology, prevention and control, *Ann. Acad. Med. Singapore 37*, 538-545.

4. Gubler, D. J. (1998) Dengue and Dengue Hemorrhagic Fever, *Clin. Microbiol. Rev. 11*, 480-496.

5. Teles, F. R. R., Prazeres, D. M. F., and Lima-Filho, J. L. (2005) Trends in Dengue diagnosis, *Rev. Med. Virol. 15*, 287-302.

6. Guzman, M. G., Perez, A. B., Fuentes, O., and Kouri, G. (2008) Dengue, Dengue Hemorrhagic Fever, In International Encyclopedia of Public Health (Editor-in-Chief: Kris, H., Ed.), pp 98-119, Academic Press, Oxford.

7. W.H.O. (1997) Dengue Hemorrhagic Fever: diagnosis, treatment, prevention and control - 2nd edition. Geneva, W.H.O. (World Health Organisation in Geneva).

8. Callaway, E. (2007) Dengue fever climbs the social ladder, *Nature 448*, 734-735.

9. Clarke, D. H., and Casals, J. (1958) Techniques for hemagglutination and hemagglutination-inhibition with arthropod-borne viruses, *Am. J. Trop. Med. Hyg. 7*, 561-573.

10. Roehrig, J. T., Hombach, J., and Barrett, A. D. T. (2008) Guidelines for plaque-reduction neutralisation testing of human antibodies to Dengue viruses, *Viral Immunol. 21*, 123-132.

11. Guzmán, M. G., and Kourí, G. (2004) Dengue diagnosis, advances and challenges, *Int. J. Infect. Dis. 8*, 69-80.

12. Ratcliff, R. M., Chang, G., Kok, T., and Sloots, T. P. (2007) Molecular diagnosis of medical viruses, *Curr. Iss. Mol. Biol. 9*, 87-102.

13. Alcon, S., Talarmin, A., Debruyne, M., Falconar, A., Deubel, V., and Flamand, M. (2002) Enzyme-linked immunosorbent assay specific to Dengue virus type 1 nonstructural protein NS1 reveals circulation of the antigen in the

blood during the acute phase of disease in patients experiencing primary or secondary infections, *J. Clin. Microbiol. 40*, 376-381.

14. Owen, T. W., Al-Kaysi, R. O., Bardeen, C. J., and Cheng, Q. (2007) Microgravimetric immunosensor for direct detection of aerosolised influenza A virus particles, *Sens. Actuators, B 126*, 691-699.

15. Kafka, J., Pänke, O., Abendroth, B., and Lisdat, F. (2008) A label-free DNA sensor based on impedance spectroscopy, *Electrochim. Acta 53*, 7467-7474.

16. Lee, M., and Fauchet, P. M. (2007) Two-dimensional silicon photonic crystal based biosensing platform for protein detection, *Opt. Express 15*, 4530-4535.

17. Boltovets, P. M., Snopok, B. A., Boyko, V. R., Shevchenko, T. P., Dyachenko, N. S., and Shirshov, Y. M. (2004) Detection of plant viruses using a surface plasmon resonance via complexing with specific antibodies, *J. Virol. Methods 121*, 101-106.

18. Cheng, X., Chen, G., and Rodriguez, W. R. (2009) Micro- and nanotechnology for viral detection, *Anal. Bioanal. Chem. 393*, 487-501.

19. Kurosawa, S., Aizawa, H., Tozuka, M., Nakamura, M., and Park, J. W. (2003) Immunosensors using a quartz crystal microbalance, *Meas. Sci. Technol. 14*, 1882-1887.

20. Su, C. C., Wu, T. Z., Chen, L. K., Yang, H. H., and Tai, D. F. (2003) Development of immunochips for the detection of Dengue viral antigens, *Anal. Chim. Acta 479*, 117-123.

21. Wu, T. Z., Su, C. C., Chen, L. K., Yang, H. H., Tai, D. F., and Peng, K. C. (2005) Piezoelectric immunochip for the detection of Dengue fever in viremia phase, *Biosens. Bioelectron. 21*, 689-695.

22. Chen, S. H., Chuang, Y. C., Lu, Y. C., Lin, H. C., Yang, Y. L., and Lin, C. S. (2009) A method of layer-by-layer gold nanoparticle hybridisation in a quartz crystal microbalance DNA sensing system used to detect Dengue virus, *Nanotechnology 20*, (21).

23. O'Sullivan, C. K., and Guilbault, G. G. (1999) Commercial quartz crystal microbalances - Theory and applications, *Biosens. Bioelectron. 14*, 663-670.

24. Nair, R. V., and Vijaya, R. (2010) Photonic crystal sensors: An overview, *Prog. Quant. Electron. 34*, 89-134.

25. Cunningham, B. T., Li, P., Schulz, S., Lin, B., Baird, C., Gerstenmaier, J., Genick, C., Wang, F., Fine, E., and Laing, L. (2004) Label-free assays on the BIND system, *J. Biomol. Screen. 9*, 481-490.

26. Huang, M. C. Y., Mateus, C. F. R., Foley, J. E., Beatty, R., Cunningham, B. T., and Chang-Hasnain, C. J. (2008) VCSEL optoelectronic biosensor for detection of infectious diseases, *Photonics Tech. L. IEEE 20*, 443-445.

27. Mandal, S., Akhmechet, R., Chen, L., Nugen, S., Baeumner, A., and Erickson, D. (2007) Nanoscale optofluidic sensor arrays for Dengue virus detection, San Diego, CA.

28. Myszka, D. G., and Rich, R. L. (2000) Implementing surface plasmon resonance biosensors in drug discovery, *Pharm. Sci. Tech. Today 3*, 310-317.

29. Homola, J., Yee, S. S., and Gauglitz, G. (1999) Surface plasmon resonance sensors: review, *Sens. Actuators, B 54*, 3-15.

30. Kumbhat, S., Sharma, K., Gehlot, R., Solanki, A., and Joshi, V. (2010) Surface plasmon resonance based immunosensor for serological diagnosis of Dengue virus infection, *J. Pharm. Biomed. Anal. 52*, 255-259.

31. Rosi, N. L., and Mirkin, C. A. (2005) Nanostructures in biodiagnostics, *Chem. Rev. 105*, 1547-1562.

32. Johnson, C. J., Zhukovsky, N., Cass, A. E. G., and Nagy, J. M. (2008) Proteomics, nanotechnology and molecular diagnostics, *Proteomics 8,* 715-730.

33. He, B., Morrow, T. J., and Keating, C. D. (2008) Nanowire sensors for multiplexed detection of biomolecules, *Curr. Opin. Chem. Biol. 12*, 522-528.

34. Wang, J. (2009) Biomolecule-functionalised nanowires: From nanosensors to nanocarriers, *ChemPhysChem 10,* 1748-1755.

35. Zhang, G. J., Zhang, L., Huang, M. J., Luo, Z. H. H., Tay, G. K. I., Lim, E. J. A., Kang, T. G., and Chen, Y. (2010) Silicon nanowire biosensor for highly sensitive and rapid detection of Dengue virus, *Sens. Actuators, B 146,* 138-144.

36. Stoermer, R. L., Cederquist, K. B., McFarland, S. K., Sha, M. Y., Penn, S. G., and Keating, C. D. (2006) Coupling molecular beacons to barcoded metal nanowires for multiplexed, sealed chamber DNA bioassays, *J. Am. Chem. Soc. 128,* 16892-16903.

37. Gómez-Hens, A., and Manuel Fernández-Romero, J. (2005) The role of liposomes in analytical processes, *TrAC – Trends Anal. Chem. 24*, 9-19.

38. Rongen, H. A. H., Bult, A., and Van Bennekom, W. P. (1997) Liposomes and immunoassays, *J. Immunol. Methods 204*, 105-133.

39. Zaytseva, N. V., Montagna, R. A., and Baeumner, A. J. (2005) Microfluidic biosensor for the serotype-specific detection of Dengue virus RNA, *Anal. Chem. 77*, 7520-7527.

Chapter 2: Electrochemical impedance spectroscopy characterisation of the nanoporous alumina Dengue virus biosensor.

2.1. Introduction

2.1.1. Fundamental of electrochemical impedance spectroscopy

Electrochemical impedance is usually measured by applying small amplitude perturbing sinusoidal voltage signal to an electrochemical cell and measuring the current through the cell. Normally, a small excitation signal is applied such that the current-voltage relationship remains linear and impedance is strictly defined. The excitation signal is given as:

$$E_t = E_o \sin(\omega t)$$

where E_t = potential at time (t), E_o = amplitude of the signal and ω = radial frequency.

The corresponding current in a linear system is:

$$I_t = I_o \sin(\omega t + \emptyset)$$

The impedance of the system is calculated using:

$$Z = \frac{E_t}{I_t} = \frac{E_o \sin(\omega t)}{I_o \sin(\omega t + \emptyset)} = Z_o \frac{\sin(\omega t)}{\sin(\omega t + \emptyset)}$$

where Z_o = magnitude and $\emptyset$ = phase shift (*1*)

With simplification using Eulers relationship, the impedance can be represented as a complex number:

$$Z(\omega) = Z_o(\cos\emptyset + j\sin\emptyset)$$

In this representation, impedance is composed of a real and imaginary part. The spectroscopy part is derived from the fact that impedance is generally determined at different frequencies rather than just one. At such, an impedance spectrum can be generated. There are basically 3 representations of the impedance data obtained (*1*).

1. Nyquist plot : Plot of the imaginary part (-Z") against the real part (Z')
2. Bode plot: Plot of the impedance (Z) against the log frequency (ω)
3. Phase angle plot: Plot of the phase shift (ϕ) against the frequency(ω)

Depending on the type of information that needs to be discussed, more than 1 type of the plots may be presented. Equivalent circuits are used in order to approximate the experimental impedance data with these ideal or distributed impedance elements arranged in series and/or in parallel with each other. An impedance spectrum can be fitted with numerous equivalent circuits. Likewise, an equivalent circuit can fit many impedance spectra. Theoretically, the most appropriate circuit is probably one which can fit the impedance spectrum and provide physical meanings which can best describe the system (*2*). The elements that are commonly used in circuit fitting to describe the different systems are

resistance (R), capacitance (C), Warburg element (W) and constant phase element (CPE). Table 2.1 briefly describes the properties of these circuit elements.

Table 2.1. The impedance, phase shift and the frequency dependence of the impedance elements most often used to describe an electrochemical system.

Circuit element	Impedance	Phase angle	Frequency dependence
Resistor (R)	$Z = R$	0^o	No
Capacitor (C)	$Z = 1/Cj\omega$	90^o	Yes
Constant phase element (CPE)	$Z = 1/Q(j\omega)^n$	0^o and 90^o	Yes
Warburg element (W)	$Z = \sigma/(\omega)^{1/2}(1-j)$	45^o	Yes

The solution resistance (R_s) represents the resistance between the working and the reference electrode. It arises from the infinite conductance of the ions in the bulk solution, and thus is generally not affected by binding. The resistance of the ionic solution commonly depends on the ionic concentration, type of ions, temperature and the geometry of the area in which the current is carried. The electron transfer resistance (R_{et}) accounts for the rate of electron transfer of the redox electrolyte at the working electrode. The capacitance (C) between the metal electrode and the ions in solution can be modelled as a series combination of the surface modification capacitance and the double layer capacitance. The capacitance is often replaced by the constant phase element (CPE) as it has been known that the impedance of solid surfaces/electrodes usually deviates from purely capacitive behaviour. The impedance of CPE is defined as $Z_{CPE}=1/(Q(j\omega)^n)$ where Q is the analogous of capacitance, ω is the frequency expressed in rad s^{-1}, governed by an exponent value n. The values of n vary between 0 and 1, where n=1 corresponds to a pure capacitor and n=0 represents a pure resistor. The Warburg element (W) represents the semi-

infinite diffusion of the ions towards the interface/working electrode surface from the bulk electrolyte. The Warburg element is essentially a constant phase element, with a constant phase of 45° and n=0.5. The solution resistance and Warburg element represent the properties of the electrolyte solution and diffusion of the redox probe, thus they are not affected by modification of the surfaces (*2*).

Equivalent values of the various circuit elements are often extracted after the fitting process. The changes in these values are often used for the characterisation of surfaces, layers of membranes as well as exchange and diffusion processes. They can also be used as a parameter for analytical purposes such as relating the overall impedance or the change in the resistance with the concentration of the analyte of interest in calibration and for explanation/postulation of processes that have occurred in the system.

The typical setup for the electrochemical impedance spectroscopy comprises working, reference and auxiliary electrodes. The electrolytes used usually include an electroactive redox couple such as the ferri/ferrocyanide with well-defined oxidation and reduction properties. Electrochemical impedance spectroscopy is a non-destructive, rapidly developing electrochemical technique for the investigation of bulk and interfacial electrical properties of solid and liquid materials. For the development of a handheld device, electrochemical sensors are promising alternative as they are usually inexpensive, sensitive, require minimal instrumentation and are readily integrated with microelectronics for miniaturisation.

Oliveira *et al.* (*3*) presented an interesting method to identify the patients with Dengue and Dengue Hemorrhagic Fever based on the recognition of the glycoprotein pattern in the serum samples using a gold electrode modified with concanavalin A. Fang *et al.* (*4*) developed a novel impedimetric immunosensor based on sol-gel derived strontium titanate thin film and interdigitated electrodes for the diagnosis of Dengue infection using non-electroactive electrolyte. The low production cost and use of non-faradic processes make the system highly favorable to be handled by end users.

2.1.2. Nanopores

Nanometer-scale pores have been extensively utilised in recent times to solve urgent problems concerning health and environmental related issues. One obvious advantage of nanopore technology is the ability to utilise pore dimensions comparable with the size of many macromolecules to interrogate the interaction of these macromolecules with the porous materials, besides controlling their adsorption and transport behaviour. There are mainly two types of nanopores, the biological pores and the solid-state pores.

Among the biological pores are self-assembling peptides with low selectivity, large transmembrane ion channel proteins with high selectivity for specific ions and porins with porous channels. Ion channel proteins are ideal choice for sensing applications since these allow signal transduction and amplification (*5*). Recent advancements in protein engineering and grafting of functional groups have opened wide possibilities for applications of biological

pores including high sensitivity detection, monitoring of chemical and biochemical reactions at single molecular level, targeted cytolysis of cancer cell and potential sequencing of long strand DNA or RNA (*5*).

Bayley and Cremer (*6*) had used biological nanopores staphylococcal alpha-hemolysin and engineered pores based on alpha-hemolysin to detect analytes such as metal ions, organic compounds and in particular DNA using the resistive-pulse sensing method. The different strands of DNA can be identified using the signals produced as the DNA strands translocate through the nanopores. Recently, they had also attempted to sequence DNA using the nanopores (*7*). However, for most biological pore applications, these proteins must be reconstituted into the lipid bilayer membrane. The stability of the lipid bilayer is known to be strongly affected by pH and concentration of the solutions (*8*) which somehow limits the use of biological pores as a versatile diagnostic tools.

On the other hand, solid-state pores whose lengths and diameters that can be readily adjusted using appropriate pore formation conditions are highly attractive. In addition, these solid-state pores can be functionalised with different surface groups and exhibit significantly higher thermal, chemical and mechanical stabilities compared to biological pores (*8*). These solid-state nanopores can be made of polymer, silicon, alumina, metallic or glass materials, using various top-down methods such as ion-beam sculpting, micromolding, latent track etching, and electron beam induced fine tuning (*9*). Alternatively,

they can also be fabricated using bottom-up methods such as sol gel process (*10*), template synthesis (*11*) and anodisation (*12*).

The applications of solid-state nanopores are similar to biological pores since they are fabricated largely to mimic the biological pores. The translocation and differentiation of DNA/RNA strands had been investigated using nanopores drilled into a silicon nitride membrane by Dekker (*8)* and Skinner *et al. (13*). Kohli *et al.* (*14*) used gold and alumina nanotubule membrane to detect analytes through a resistive-pulse sensing and biomimetic ion-gated channel mechanism. Recently, the group had also developed conically shaped nanopores and nanotubes that can mimic functions of biological nanopores (*15*). Sensing work can be carried out with these types of conical nanopores using molecular recognition elements that are bound to the tip of the conical nanopores. The tip is selectively blocked as the target analyte binds to the recognition element leading to a decrease in the ion current (*16*). Other recent interesting works using solid-state pores include separation of analytes with mutilayer alumina membranes (*17*) and transportation of drugs through polypropylene membrane (Fig. 2.1).

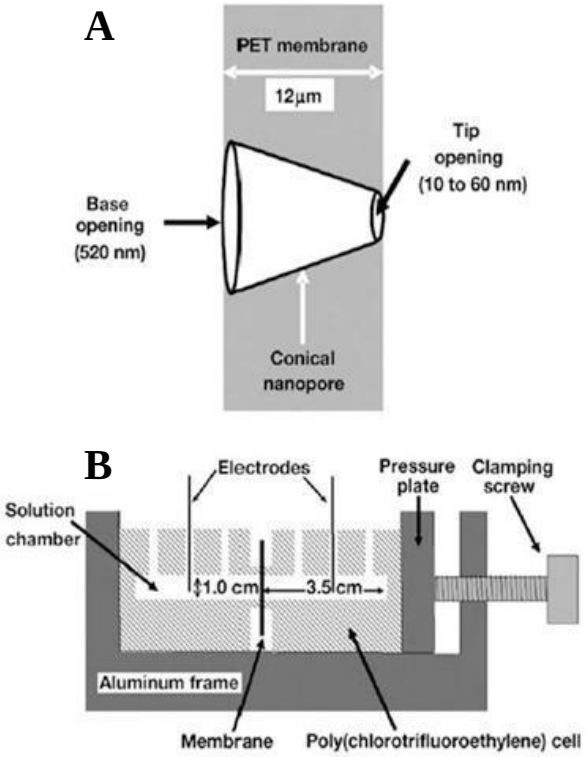

Fig. 2.1. (A) Schematic diagram of a conical nanopore which mimics functions of biological nanopores formed by the track-etch method in a polyethylene terephthalate (PET) membrane; (B) Schematic diagram of the experimental setup used for the electrochemical measurement of ion currents traversing across a single conical nanopore within a PET membrane. (Re-printed with permission from *(16)*. Copyright (2007) WILEY-VCH Verlag GmbH & Co.KGaA, Weinheim).

Development of nanochannel array-based bioanalytical devices is an alternative approach to achieve highly sensitive detection of biomolecules. The sensitivity is achieved due to the high pore density of the membrane as well as the close interaction of the target biomolecules with the nanochannels. The similarity in size between the nanopores and the analytes allows their interactions to be amplified, which can be easily detected with an electrochemical method using the resistive-pulse sensing method. Thus, the combination of nanopore membrane coupled with an electrochemical method is an attractive system for sensitive detection of analytes typically present in low

concentration. Although this type of system may be less sensitive than the mass spectrometry systems such as those of LC-MS and ICP-MS, the small size of the electrochemical station, the simplicity in operation and its relative robustness make it more appropriate to be used for on-site testing.

Previously, our group had fabricated an alumina membrane biosensor based on the anodisation method and the nanobiosensor was sensitive toward whole virus particles for the detection of West Nile virus (*18*). In this project, we extent the use of this system for the detection of Dengue virus. However, electrochemical impedance spectroscopy will be used as the detecting platform in replacement of the differential pulse voltammetry. The main aim of this project is to demostrate that this system can be used for the detection of Dengue virus and to understand the sensing mechanism governing the system with impedance.

2.2. Materials and methods

2.2.1. Materials and Reagents

Anti-Dengue serotype 2 antibody, (clone 3H5, isotype IgG, 1.0 mg mL^{-1}) was purchased from (Millipore). Bovine Serum Albumin (BSA,>98%), ferrocenemethanol (FeMeOH,>99%) and phosphate buffered saline (PBS, 10X) were purchased from (Sigma Aldrich). Phosphoric acid (85%) was purchased from (Lancaster Synthesis). All chemicals and solvents were of analytical grade and used as received. Ultrapure water (Sartorius Ultrapure Water System) was used for all preparations.

2.2.2. Virus cultivation and inactivation

Aedes mosquito cells (C6/36) were infected with Dengue serotype 2 viruses at a multiplicity of infection (MOI) of 0.01 for 1 h at 28°C. Following this, the medium was removed and fresh growth medium (RPMI, 5% heat-inactivated fetal bovine serum (FBS) and 5 mM 2-mercaptoethanol) was added. After which, the cell culture was incubated at the same temperature for 5 days. After 5 days, the medium was collected and a plaque assay was carried out to determine the concentration of the Dengue virus in terms of plaque forming unit (PFU mL^{-1}). The Dengue virus sample was subsequently heat inactivated at 56 °C for 30 min. All experiments were carried out in a biosafety level 1 laboratory since the Dengue virus is not an air-borne virus. As an additional

safety precaution, chlorine tablet was added before the Dengue virus solution was discarded.

2.2.3. Preparation of the nanobiosensor

The preparation procedure of the nanoporous alumina electrode follows the previous report (*19*). Nanoporous alumina membrane electrodes were fabricated using platinum wires embedded in epoxy sheaths and micropipette tips. The electrode tip was polished with 1.0 μm and 0.3 μm diameter alumina powder before coating with an aluminium metal film. Submicrometer thick aluminium films in the thickness range of 300–500 nm were sputter-coated onto the platinum electrodes using 99.999% purity aluminium target, Denton discovery® 18 Sputtering System and sputtering power of 100 W in an atmosphere of research-grade Ar at 5×10^{-3} Torr.

Anodisation of the aluminium coated electrodes were conducted using the previously described pipette contact anodisation method. This was carried out by positioning a glass pipette coated with a ~ 40 nm thick platinum layer, above and in contact with the surface of the aluminium coated electrode. 0.1 M oxalic acid solution was then added into the interior portion of the platinum coated glass pipette. The aluminium coated layer was anodised potentiostatically in the 0.1 M oxalic acid at 40 V versus the platinum counter electrode placed in the glass pipette to produce nanopores.

To prepare the biosensor, the nanoporous alumina electrode was first etched in 3% phosphoric acid for 15 min and washed thoroughly with copious amount of PBS to produce the pores (Fig. 2.2A). Solutions of 3H5 antibody, BSA and Dengue virus were prepared in PBS. BSA was used as blocking agent for nonspecific binding sites. Immobilisation of the respective reagents was subsequently carried out by spreading 5 µL of the reagent solution across the alumina electrode surface. The antibody was immobilised for 1 h followed by BSA while the virus capture was carried out with 30 min incubation time (Fig. 2.2B). After each immobilisation step, the alumina electrode was rinsed extensively with PBS and then characterised using cyclic voltammetry.

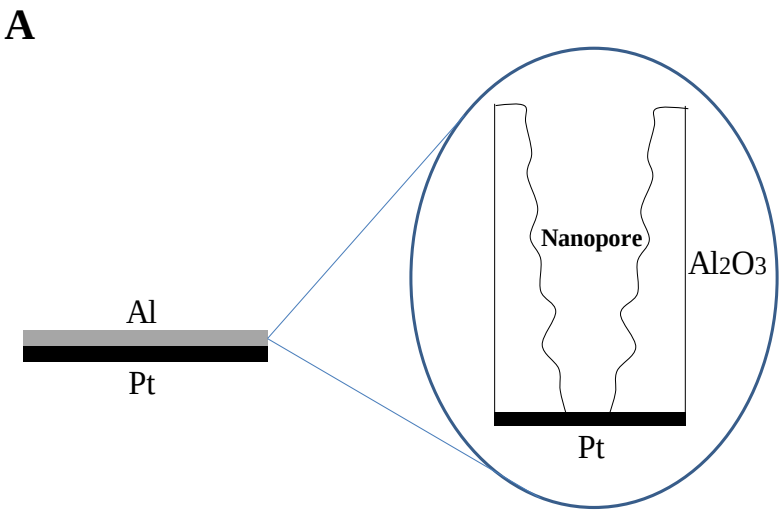

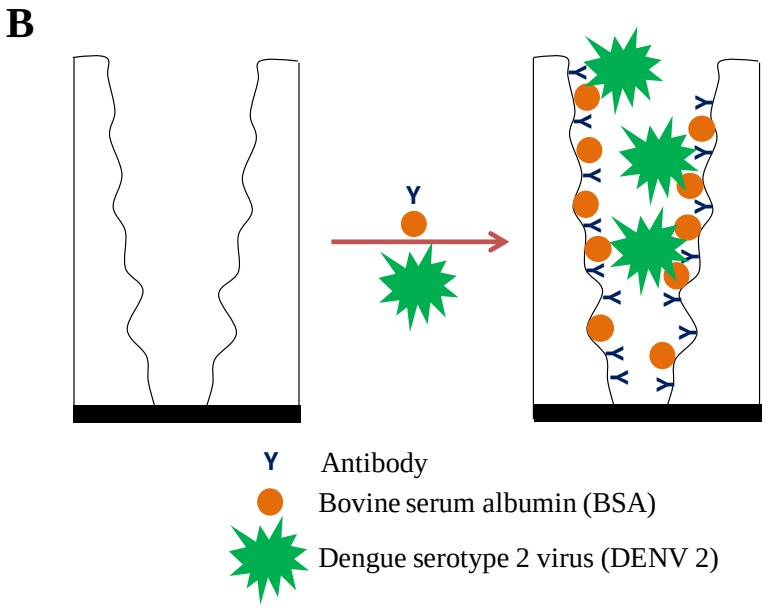

Fig. 2.2. (A) Schematic diagram illustrating the formation of one nanopore after anodisation with oxalic acid solution and etching with 3% phosphoric acid; (B) Schematic diagram showing the immobilisation of the antibody, BSA and Dengue virus along the wall of the nanoporous membrane.

2.2.4. Characterisation of the nanobiosensor

All electrochemical measurements were carried out on an autolab potentiostat/galvanostat (Eco Chemmie, Netherland) using a three electrode cell containing a nanoporous alumina working electrode, a silver/silver chloride reference electrode and a platinum wire counter electrode in PBS pH 7.4 solution containing 1 mM ferrocenemethanol (Fig. 2.3). Cyclic voltammetry was carried out at a potential range from −0.2 to 0.6 V with a scan rate of 0.05 V s^{-1}. Impedance measurements were performed over the frequency range from 0.1 Hz to 100 kHz at the mid-peak potential of ferrocenemethanol derived from cyclic voltammetry (~0.19 V versus Ag/AgCl, 1 M KCl) with an alternating current potential amplitude of 50 mV. The impedance data was fitted to an equivalent circuit model using the EIS spectrum analyser (Minsk, Belarus). The

fitting quality was evaluated by the chi-squared (R^2) value and error percentage corresponding to each component of the equivalent circuit model.

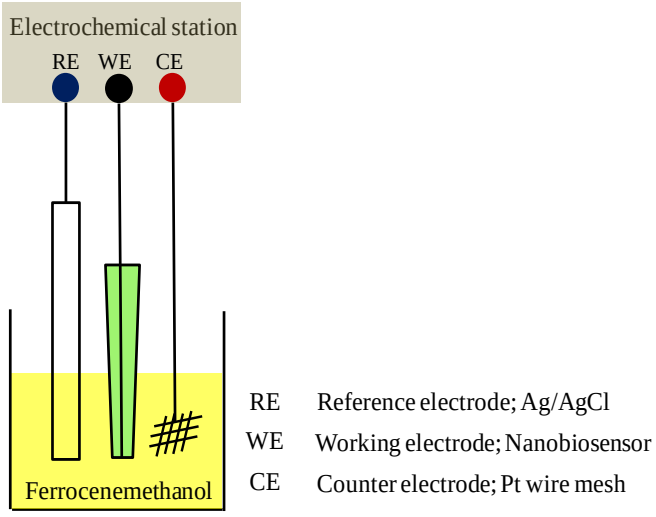

Fig. 2.3. Schematic diagram showing the three electrode system used in the electrochemical detection.

2.3. Results and discussion

2.3.1. Characterisation using cyclic voltammetry

Fig. 2.4 shows the typical cyclic voltammograms of the alumina electrode after each step of the nanobiosensor preparation procedure: before and after chemical etching, antibody immobilisation, BSA immobilisation and virus capture in PBS (pH=7.4) containing 1 mM ferrocenemethanol redox probe. It is observed that the current transmission of the alumina electrode is increased by etching. This is attributed to the further widening of the alumina nanopores (or nanochannels) with phosphoric acid thus allows more redox probes to enter the nanochannels and increases the Faradaic current.

The magnitude of the current decreases after each of the following antibody immobilisation, BSA immobilisation and virus capture steps, due to enhanced barriers either at the electrode–electrolyte interface and/or the thin alumina layer. Though the peak height decreases, the anodic and cathodic peak positions remain relatively unchanged after the several immobilisation steps, which strongly suggest that the loading of antibodies and subsequent virus capture do not influence the charge transfer kinetics significantly at the electrode–electrolyte region (*20*). It is also observed that there is a gradual decrease in the current with increasing amount of the Dengue virus added. Presumably, this decrease in current is related to the amount of the immunocomplexes formed within the nanochannels so ought to provide a close

correlation between the signal change and the virus concentration using an equilibrium binding theory.

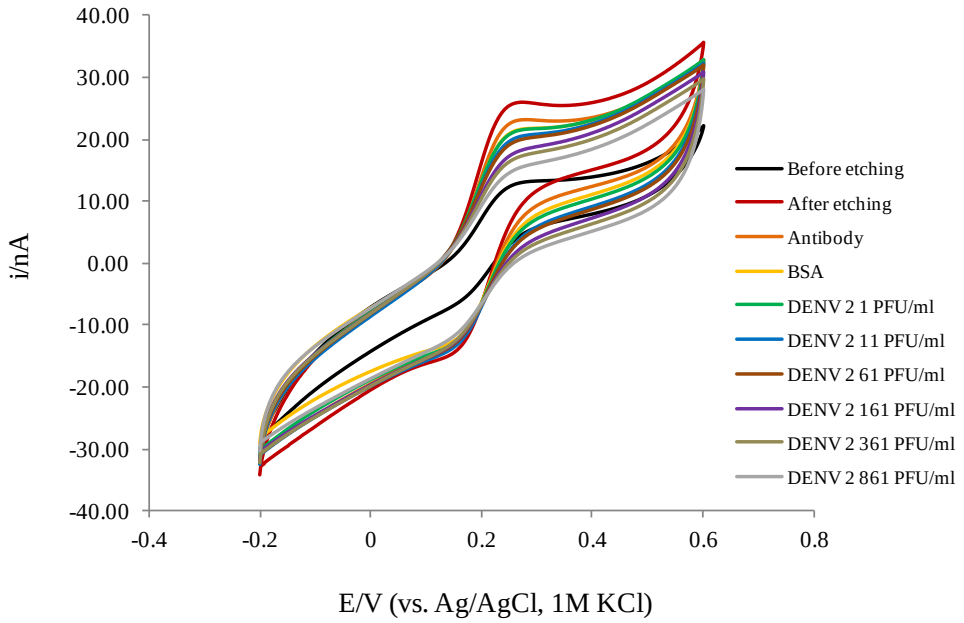

Fig. 2.4. Cyclic voltammetries of the alumina electrode after each step of the nanobiosensor preparation procedure: before and after chemical etching, antibody immobilisation, BSA immobilisation and virus capture in PBS containing 1 mM ferrocenemethanol.

2.3.2. Characterisation using electrochemical impedance spectroscopy

Electrochemical impedance spectroscopy is used to investigate the processes that occur within the thin nanoporous alumina coated biosensor which are highly relevant to understand several recent biosensing works involving thin film and membrane-based biosensors for viruses, living cells and other biological species. Unlike cyclic voltammetry and differential pulse voltammetry which derive mass transfer limited signal responses at high overpotentials, EIS data are derived at near equilibrium conditions close to the formal potential of the redox probe. Thus, EIS can probe other physical

processes that occur during the virus capture events within the nanoporous structure of the thin alumina layer of the biosensor, and possibly construct an alternative method for direct virus detection in contrast to the mass transfer limiting approach.

Fig. 2.5A and B show the real and imaginary parts of the impedance of the nanobiosensor with respect to frequency in the presence of increasing virus concentrations from 1 to 900 PFU mL^{-1}. The real and imaginary parts of the impedance are calculated from the overall impedance (Z*): $Z^*(\omega) = Z'(\omega) + jZ''(\omega)$ where ω is the angular frequency and equals $2\pi f$ (f/Hz is the frequency). It is shown that at frequencies lower than 1 Hz, both the real impedance Z' and imaginary impedance Z'' are increased after exposure to the virus particles. At the lowest frequency, the change in the overall impedance Z* at 1 PFU mL^{-1} virus concentration is ~10 times larger than that of the BSA solution. Clearly, the biosensor presents sensitive response towards the presence of immobilised proteins and virus particles in the low frequency range.

In contrast, at higher frequencies, all the traces overlapped which indicates the curves do not depend on the presence of virus particles, and are thus not useful for virus detection. This differential change in Z* at increasing virus concentration is clearly indicated by the enlarging traces of the Nyquist plot (Fig. 2.5C). No straight line tails are observed at low frequency range probably suggested the absence of a Warburg element (*21*). This indicates diffusion of the redox probe is not rate-limiting under the conditions of the impedance measurements in this system, unlike voltammetric measurements.

Interestingly, two maxima in the phase angle plot well separated in the frequency domain are observed for the etched alumina electrode (Fig. 2.5D), which clearly indicate two time constants. Since the physical structure of the alumina electrode comprises the alumina/nanochannel-electrolyte and the electrode–electrolyte interfaces, the interactions of virus particles can change the impedimetric responses of these two interfaces. Thus, the time constant at high frequency range is attributed to the faster charge transfer at the conductive electrode-electrolyte interface while the low frequency region presents the movement of ions along the nanochannels. The phase shift of the first maximum at ca. 14 Hz increases with immobilisation of the antibody probes and subsequent addition of the virus particles. In contrast, the second maximum at ca. 400 Hz decreases significantly upon immobilisation of the antibody probes and a less obvious change when more virus particles are added to the solution.

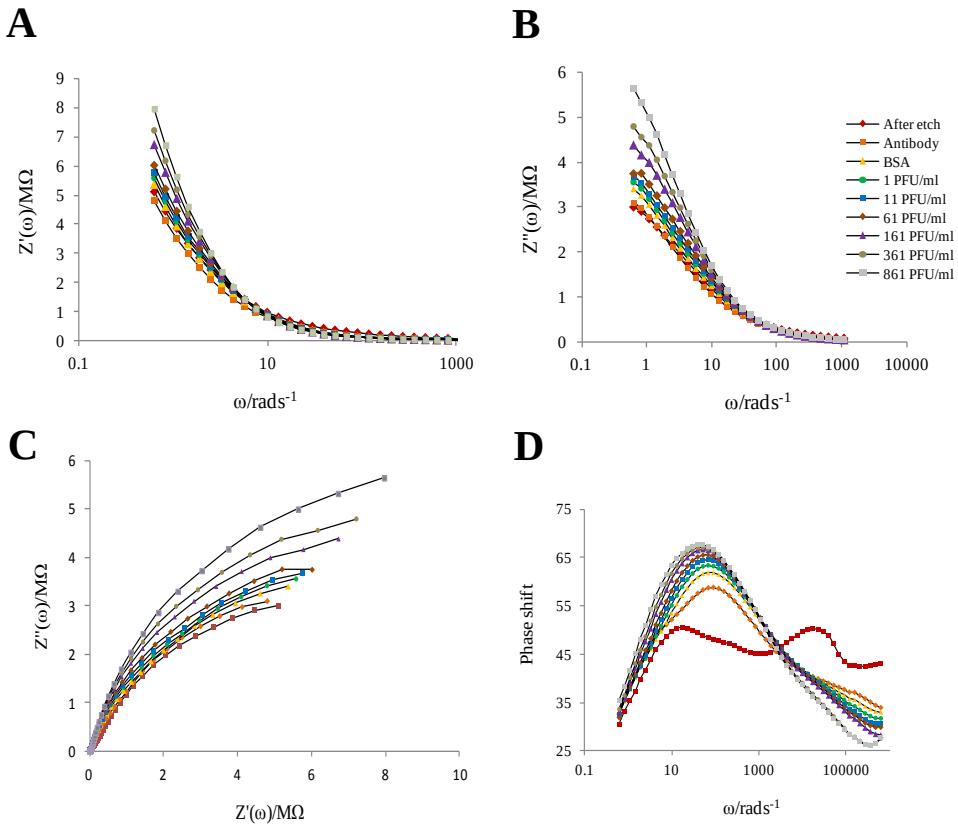

Fig. 2.5. (A) Real (in-phase) impedance Z′ and (B) imaginary (out-of-phase) impedance Z″ versus angular frequency, ω, (C) Nyquist plot and (D) Bode-phase plot of the nanobiosensor after Dengue 2 virus capture from solutions of increasing virus concentration. Measurements were conducted in PBS (pH=7.4) containing 1 mM ferrocenemethanol.

The optimal model that matches the impedimetric responses of the thin nanoporous alumina biosensor comprises a series of two constant phase elements (CPE) in parallel with two resistances (R), which is consistent with an insulating porous layer on top of a conductive layer (Fig. 2.6). Three distinct regions can be identified: the electrolyte solution resistance (R_s), the porous alumina channels (including proteins and virus particles) (CPE_1, R_1) and the conductive electrode substrate layer (CPE_2, R_2). The constant phase element (CPE) is used to describe the non-Faradaic process at the alumina-electrolyte and electrode-electrolyte layers, in contrast to the capacitance element to take into account of the topological imperfection of the alumina porous layer and the conductive electrode layer. This is in agreement with previous works on porous

structures such as a thin nanoporous alumina membrane which had been modelled using non-Faradaic components comprising a channel resistance in parallel with a constant phase element which represents the channel capacitance (*22*, *23*).

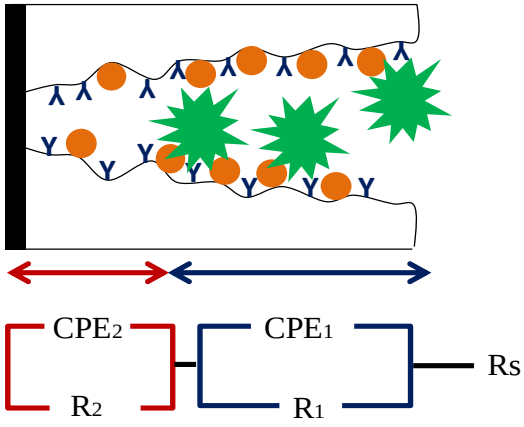

Fig. 2.6. Schematic diagram of the alumina nanobiosensor for Dengue 2 virus detection mapped with the equivalent circuit model showing the 3 distinct regions.

Table 2.2 shows the values of the circuit elements obtained by fitting the experiment data in fig. 2.5 and two other repeated experiments. The fitted R_1 and R_2 parameters are attributed to the channel resistance and slow charge transfer kinetics respectively at the alumina electrode. In the presence of increasing virus concentrations, the charge transfer resistance R_2 increases. This is most probably due to nonspecific physical adsorption of proteins and cell fragments at the electrode–electrolyte interface which can reduce the electrode area, causing an increase in the charge transfer resistance. The heterogeneous rate constant for the ferrocenemethanol Faradaic reaction can be described using the following relation between the heterogeneous rate constant k_{ct}, the concentration of redox species C, the electrode area A and the change in charge transfer resistance R_2 (Eq. (1)):

$$R_2 = RT/n^2F^2k_{ct}AC \quad (1)$$

where R is the gas constant, T is the absolute temperature, n is number of electrons transferred and F is the Faraday constant. From an average R_2 value of 10 MΩ, it is estimated that the heterogeneous rate coefficient $k_{ct} = 0.66 (\pm 0.03) \times 10^{-3}$ cm s^{-1} which agrees closely with previous values determined from the voltammetric peak-to-peak distance (*20*).

From the fitted impedance values of R_1 in table 2.2, we estimate the channel resistivity, ρ_c=420(±21) MΩ cm using the relation $R_1=\rho_c l_c/A_c$ between ρ_c/Ωcm, channel length l_c (~300 nm), channel cross-section area A_c and channel resistance, R_1. This resistivity value is similar to the channel resistivity of a 60 μm thick alumina membrane placed in a solution of similar ionic strength (*24*). We observe an increase in the channel resistance R_1 responses in the presence of increasing virus concentration which is attributed to specific Dengue virus particles interaction with the immobilised antibodies. The immobilisation of the Dengue viruses along the nanochannels can reduce the channel area thus causes the increase in channel resistance. The calibration plot of the change in resistance, $R_1(R_{Dengue2\ virus} - R_{BSA})$ against the concentration of the Dengue viruses shows a good correlation with a detection limit of 1 PFU mL^{-1} (Fig. 2.7).

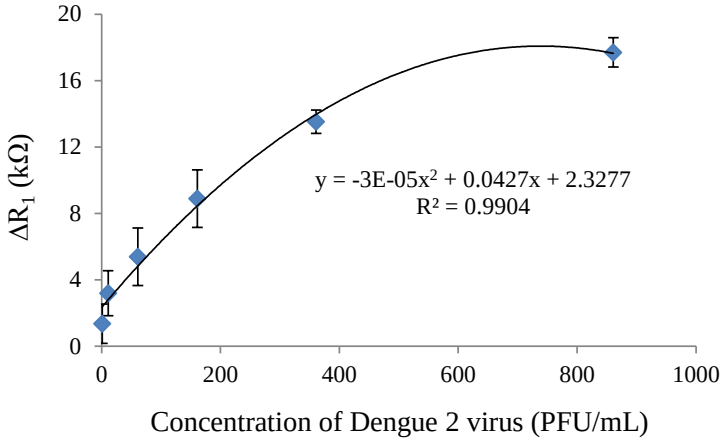

Fig. 2.7. Calibration plot of the change in channel resistance against the concentration of Dengue 2 virus (PFU mL^{-1}).

Interestingly, the channel capacitance CPE_1 changes significantly in the presence of virus, for example, 100% increase is observed from 1 to 900 PFU mL^{-1} virus concentration. Similar effects on surface capacitance of alumina had been observed due to binding of charged species (*25*). In this case, the capture of negatively charged Dengue virus particles with pI of 5 in pH 7.4 PBS solution, to the antibody-coated alumina nanochannel walls, is the most likely cause of this increase in channel capacitance. In contrast, the change in the electrode–electrolyte capacitance CPE_2 remains relatively similar when the Dengue 2 virus concentration is changed from 1 to 900 PFU mL^{-1}. The significant change in the value of n_1 further corroborates with binding of the virus particles or other species within the channels, since any deviation of n_1 from 1 represents a non-smooth surface. In comparison, the n_2 values are closer to 1 than those of n_1 as expected for the more homogeneous metal electrode surface compared to the antibody-coated nanochannel walls.

Table 2.2. Fitted EIS results of the nanobiosensor using the equivalent circuit shown in fig. 2.6 and an average bulk solution resistance R_s =1.9 KΩ.

	R_1/KΩ	R_2/KΩ	CPE_1/μF	n_1	CPE_2/μF	n_2	χ^2
BSA/Ab	16.91	9.08	0.46	0.51	0.12	0.72	0.16
DENV 2 1 PFU mL^{-1}	18.26	9.08	0.57	0.50	0.12	0.73	0.13
DENV 2 11 PFU mL^{-1}	20.10	9.24	0.65	0.49	0.11	0.75	0.16
DENV 2 61 PFU mL^{-1}	22.30	9.62	0.69	0.48	0.10	0.76	0.18
DENV 2 161 PFU mL^{-1}	25.80	10.84	0.67	0.49	0.10	0.78	0.15
DENV 2 361 PFU mL^{-1}	30.43	11.57	0.95	0.44	0.09	0.79	0.12
DENV 2 861 PFU mL^{-1}	34.61	13.46	1.08	0.43	0.09	0.79	0.19

2.3.3. Dengue virus-antibody binding affinity

The specific binding interaction between the Dengue 2 virus and its antibody is as follows:

$$\text{Ab} + \text{Dengue 2 virus} \leftrightarrow [\text{Dengue 2 virus} - \text{Ab}], \text{ where}$$

$$K/M^{-1} = [\text{Dengue 2 virus} - \text{Ab}] / ([\text{Ab}][\text{Dengue 2 virus}]) \quad (2)$$

where K/M^{-1} is the binding constant which describes the strength of the antigen–antibody interaction. The binding of virus particles on planar surfaces can be described using a simple Langmuir model (*26*) in which the antibody-antigen binding site is equivalent to an active surface site. Using the membrane's cylindrical surface as the sensing platform, we find that the Freundlich isotherm (*27*) is more suitable to explain the relation between the sensor signal response and the virus concentration when compared to the classical Langmuir isotherm as well as the Langmuir-Freundlich isotherm (Fig. 2.8).

$$\theta = (K)^{1/n_2}(C)^{n_1/n_2} \quad (3)$$

where fractional coverage $\theta = (R_{\text{Dengue 2 virus}} - R_{\text{Dengue 2 virus}} = 0)/ (R_{\text{Dengue 2 virus max}} - R_{\text{Dengue 2 virus}} = 0)$, while n is the fractal order of the reaction, K is the antibody-virus binding constant and C/PFU mL^{-1} is the Dengue 2 virus concentration. The Freundlich isotherm is often used to describe adsorption within porous media which is distinctly different from the planar surface. This distinction is that in porous media, not all the adsorption sites have equal access to the bulk

solution (*28*). Since the antibodies are immobilised within the porous membrane, the situation is similar to what the Freundlich isotherm describes, where the Dengue viruses may not have access to the antibodies immobilised.

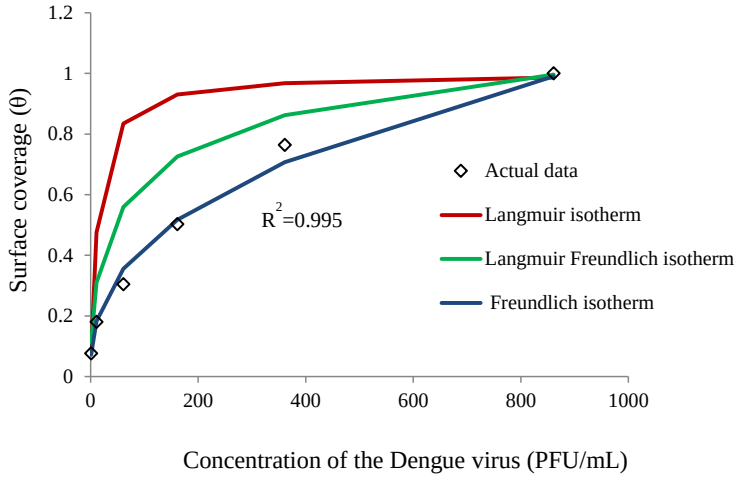

Fig. 2.8. Diagram showing the goodness-of-fit for the three isotherms: Langmuir, Langmuir-Freundlich and Freundlich isotherm against the actual data.

2.3.4. Selectivity experiment

To utilise the nanobiosensor in Dengue virus diagnosis using impedance measurement, the biosensor has to demonstrate selective responses against other viruses. Table 2.3 shows the response of the nanobiosensor towards consecutive exposure to non-flavivirus Chikungunya virus (CHIKV), flavivirus West Nile virus (WNV), followed by Dengue 2 virus which is also member of the flavivirus family. All virus concentrations are 100 PFU mL^{-1} and the incubation procedure for virus capture followed by the impedance measurement is identical for all three viruses and the control solution. The control solution is the supernatant of the cell culture medium after cell cultivation.

Using the Student's t-test with a p value cutoff of 0.05, the p-analysis indicates the channel capacitance CPE_1 is selective for Dengue 2 virus over Chikungunya virus and West Nile virus since p values are <0.05: Dengue 2 virus and Chikungunya virus (p=0.009); Dengue 2 virus and West Nile virus (p=0.007), but cannot differentiate between Chikungunya virus and West Nile virus: Chikungunya virus and West Nile virus (p=0.44). In contrast, p-analysis for the other three parameters indicates no clear trend in selectivity. The p-values for channel resistance R_1, charge transfer resistance R_2 and electrode-electrolyte capacitance CPE_2 are as follows: Dengue 2 virus and Chikungunya virus (R_1: p=0.14; R_2: p=0.003; CPE_2: p=0.043); Dengue 2 virus and West Nile virus (R_1: p=0.014; R_2: p=0.002; CPE_2: p=0.74); Chikungunya virus and West Nile virus (R_1: p=0.107; R_2: p=0.047; CPE_2: p=0.060).

Clearly, the selectivity for Dengue 2 virus is most evident for channel capacitance CPE_1 (Table 2.3) where the channel capacitance CPE_1 is unchanged in the presence of Chikungunya virus and West Nile virus but doubles when Dengue 2 virus was added. This suggests that the Dengue 2 virus particle interacts specifically with the antibody 3H5 along the nanochannels, unlike the other two viruses. However, the channel resistance R_1 is also responsive to nonspecific viruses, which we attribute to the blocking of the nanochannels by the large viruses at narrower parts of the nanochannels, which limits the mass transfer of the redox probes throughout the entire length of the blocked nanochannels.

The pore size distribution of the alumina layer has been previously shown to be largest at the exterior (~70-120 nm) and smallest at the interior part (~10-30 nm) close to the electrode-alumina interface. Since the size of the virus particles (~50 nm) are in general larger than the smaller nonspecific proteins and cell fragments, and therefore, unable to access the electrode surface covered with smaller diameter nanochannels compared to the exterior part of the alumina layer. Thus, it is reasonable to conclude that changes in the charge transfer resistance R_2 and capacitance CPE_2 of the electrode-electrolyte region are due to nonspecific bindings at the electrode surface by these smaller proteins and cell fragments present in the viral solution.

These observations appear different to most other works which measure impedimetric changes of surface bound species. We attribute this apparent discrepancy to the additional alumina overlayer of the membrane-based nanobiosensor which captures most of the specific virus particles before they reach the electrode-electrolyte interface. In contrast, nonspecific viruses and other constituents of the viral solution can reach the underlying electrode-solution interface and thus influence R_2 and CPE_2.

Table 2.3. Fitted EIS results of the nanobiosensor placed in the following solutions: pure culture medium, CHIKV, WNV and DENV 2, respectively in consecutive steps, using the equivalent circuit presented.

	R_1/KΩ	R_2/KΩ	CPE_1/μF	CPE_2/μF	χ^2
Control	43.0	191.2	39.7	79.8	0.03
CHIKV	45.1	199.9	48.2	83.9	0.03
WNV	43.0	213.4	44.6	89.2	0.03
DENV 2	47.8	228.7	114.8	90.0	0.04

2.3.5. Real sample analysis

The nanobiosensor was utilised to detect Dengue viruses in spiked human serum samples. The human serum was diluted 100 times and spiked with 1, 10 and 20 PFU mL^{-1} of Dengue viruses. Similarly, the various spiked solutions were immobilised onto the electrode for 30 min before washing off the unbound Dengue viruses with a copious amount of PBS. Subsequently, impedance measurements were carried out. Despite the complicated matrix, the results (Fig. 2.9) indicate the plausibility of using the nanobiosensor for qualitative and quantitative determination of Dengue viruses in infected human serum samples with a short total analysis time of 40 min.

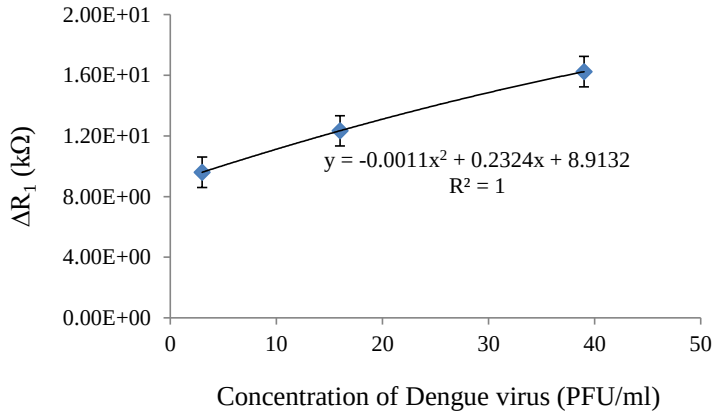

Fig. 2.9. Plot of the signal response against the concentration of Dengue 2 virus in the spike serum samples.

2.4. Conclusion

We have characterised the nanoporous alumina Dengue virus biosensor using EIS and a circuit model comprising two R-CPE units arranged in series to delineate the responses of the alumina/nanochannel-electrolyte component from the electrode-electrolyte interface. Fitted results of the pore resistance R_1 can be correlated to the Dengue 2 virus concentration using the Freundlich isotherm. In addition, the fitted pore capacitance CPE_1 data allow the specific identification of Dengue 2 virus from two other mosquito-borne viruses; West Nile virus and Chikungunya virus. These results indicate that the pore resistance and capacitance are highly useful for quantitative and specific detection of Dengue 2 virus in contrast to the electrode-electrolyte capacitance and charge transfer resistance. Significantly, the fitting circuit model ought to be applicable in general to other biosensors utilising antibody-loaded porous thin films to capture analyte targets. The capacitance change within the nanochannels upon specific virus antibody binding further suggests that monitoring of capacitive signals could be useful for the development of highly specific biosensors.

2.5. References

1. Lisdat, F., and Schäfer, D. (2008) The use of electrochemical impedance spectroscopy for biosensing, *Anal. Bioanal. Chem. 391*, 1555-1567.

2. Daniels, J. S., and Pourmand, N. (2007) Label-free impedance biosensors: Opportunities and challenges, *Electroanal. 19*, 1239-1257.

3. Oliveira, M. D. L., Correia, M. T. S., and Diniz, F. B. (2009) Concanavalin A and polyvinyl butyral use as a potential Dengue electrochemical biosensor, *Biosens. Bioelectron. 25*, 728-732.

4. Fang, X., Tan, O. K., Tse, M. S., and Ooi, E. E. (2010) A label-free immunosensor for diagnosis of Dengue infection with simple electrical measurements, *Biosens. Bioelectron. 25*, 1137-1142.

5. Majd, S., Yusko, E. C., Billeh, Y. N., Macrae, M. X., Yang, J., and Mayer, M. (2010) Applications of biological pores in nanomedicine, sensing, and nanoelectronics, *Curr. Opin. Biotechnol. 21*, 439-476.

6. Bayley, H., and Cremer, P. S. (2001) Stochastic sensors inspired by biology, *Nature 413*, 226-230.

7. Clarke, J., Wu, H. C., Jayasinghe, L., Patel, A., Reid, S., and Bayley, H. (2009) Continuous base identification for single-molecule nanopore DNA sequencing, *Nat. Nanotechnol. 4*, 265-270.

8. Dekker, C. (2007) Solid-state nanopores, *Nat. Nanotechnol. 2*, 209-215.

9. Rhee, M., and Burns, M. A. (2007) Nanopore sequencing technology: nanopore preparations, *Trends Biotechnol. 25*, 174-181.

10. Barton, T. J., Bull, L. M., Klemperer, W. G., Loy, D. A., McEnaney, B., Misono, M., Monson, P. A., Pez, G., Schere, G. W., Vartuli, J. C., and Yaghi, O. M. (1999) Tailored porous materials, *Chem. Mater. 11*, 2633-2656.

11. Meynen, V., Cool, P., and Vansant, E. F. (2009) Verified syntheses of mesoporous materials, *Microporous Mesoporous Mater. 125*, 170-223.

12. Bwana, N. N. (2008) Synthesis of highly ordered nanopores on alumina by two-step anodisation process, *J. Nanopart. Res. 10*, 313-319.

13. Skinner, G. M., Van Den Hout, M., Broekmans, O., Dekker, C., and Dekker, N. H. (2009) Distinguishing single-and double-stranded nucleic acid molecules using solid-state nanopores, *Nano Lett. 9*, 2953-2960.

14. Kohli, P., Wirtz, M., and Martin, C. R. (2004) Nanotube membrane-based biosensors, *Electroanal. 16*, 9-18.

15. Wharton, J. E., Jin, P., Sexton, L. T., Horne, L. P., Sherrill, S. A., Mino, W. K., and Martin, C. R. (2007) A method for reproducibly preparing synthetic nanopores for resistive-pulse biosensors, *Small 3*, 1424-1430.

16. Siwy, Z., Trofin, L., Kohli, P., Baker, L. A., Trautmann, C., and Martin, C. R. (2005) Protein biosensors based on biofunctionalised conical gold nanotubes, *J. Am. Chem. Soc. 127*, 5000-5001.

17. Yamashita, T., Kodama, S., Ohto, M., Nakayama, E., Takayanagi, N., Kemmei, T., Yamaguchi, A., Teramae, N., and Saito, Y. (2007) Use of porous anodic alumina membranes as a nanometre-diameter column for high performance liquid chromatography, *Chem. Commun.(11)*, 1160-1162.

18. Nguyen, B. T. T., Koh, G., Hui, S. L., Chua, A. J. S., Ng, M. M. L., and Toh, C. S. (2009) Membrane-based electrochemical nanobiosensor for the detection of virus, *Anal. Chem. 81*, 7226-7234.

19. Koh, G., Agarwal, S., Cheow, P. S., and Toh, C. S. (2007) Development of a membrane-based electrochemical immunosensor, *Electrochim. Acta 53*, 803-810.

20. Bard, A. J., and Faulkner, L. R. (2001) Electrochemical methods: fundamentals and applications, 2nd ed, John Wiley, New York.

21. Lasseter, T. L., Cai, W., and Hamers, R. J. (2004) Frequency-dependent electrical detection of protein binding events, *Analyst 129*, 3-8.

22. Hitzig, J., Juettner, K., and Lorenz, W. J. (1986) AC-impedance measurements on corroded porous aluminum oxide films, *J. Electrochem. Soc. 133*, 887-892.

23. Girginov, A., Popova, A., Kanazirski, I., and Zahariev, A. (2006) Characterisation of complex anodic alumina films by electrochemical impedance spectroscopy, *Thin Solid Films 515*, 1548-1551.

24. González, J. A., López, V., Bautista, A., Otero, E., and Nóvoa, X. R. (1999) Characterisation of porous aluminium oxide films from a.c. impedance measurements, *J. Appl. Electrochem. 29*, 229-238.

25. Varghese, O. K., Gong, D., Paulose, M., Ong, K. G., Grimes, C. A., and Dickey, E. C. (2002) Highly ordered nanoporous alumina films: Effect of pore size and uniformity on sensing performance, *J. Mater. Res. 17*, 1162-1171.

26. Langmuir, L. (1916) The constitution and fundamental properties of solids and liquids. Part 1. Solids, *J. Am. Chem. Soc. 38(11)*, 2221-2295.

27. Freundlich, H. M. F. (1906) Über die adsorption in lösungen, *Z, Phys. Chem. 57(A)*, 385-470.

28. Skopp, J. (2009) Derivation of the Freundlich adsorption isotherm from kinetics, *J. Chem. Educ. 86*, 1341-1343.

Chapter 3: Dengue virus detection using impedance measured across the nanoporous alumina membrane

3.1. Introduction

3.1.1. Replication of Dengue virus

The Dengue viruses enter the host cells by receptor-mediated endocytosis. The acidic environment of the endosomes triggers an irreversible trimerisation of the E protein that results in the fusion of the viral and cell membrane. After the fusion has occurred, the nucleocapsid (NC) of the Dengue virus containing the capsid protein and RNA dissociates is released into the cytoplasm (*1*). Consequently, the replication of the RNA genome and new Dengue particles assemblies are initiated. Here, immature Dengue virus particles are formed in the lumen of the endoplasmic reticulum (ER). These particles contain protein E, a precursor form of M protein (prM), lipid membrane and nucleocapsid. They mature by passing through the Golgi and trans-Golgi network (TGN). In the acidic environment of the TGN, the virions undergo conformational change and the cellular protease furin cleaves the prM into M and a peptide pr that remains associated with the virions. Upon release, the pr peptide dissociates from the virions, resulting in the formation of mature progeny virions (*2*)(Fig. 3.1).

3.1.2. The immature Dengue virus particles

In the recent 5 years, it was demonstrated that cells infected with Dengue viruses tend to secrete high level (~30%) of prM-containing immature Dengue virus particles (*3*). Neutralisation test with anti-prM antibodies showed that the prM antibodies that were found in the patients during infection were unable to completely neutralise the Dengue infection (*3*). These results highly suggested that three populations of Dengue virus appear to be produced and released from the infected cells. The first population is the immature Dengue viruses containing relatively high levels of prM that are inherently non-infectious. The second population is the partially mature Dengue viruses with an intermediate density of prM at the surface that can infect but susceptible to neutralisation at high antibody titer. The last population is the fully matured Dengue viruses with low or absent of prM at the surface that will not normally be susceptible to neutralisation (*4*). These immature particles were discovered to be non-infectious due to insufficient binding of the immature virions to the cell surface. In addition, the presence of the PrM obstructs the low-pH induced conformational change in the viral glycoprotein required for membrane fusion of the virus (*5*).

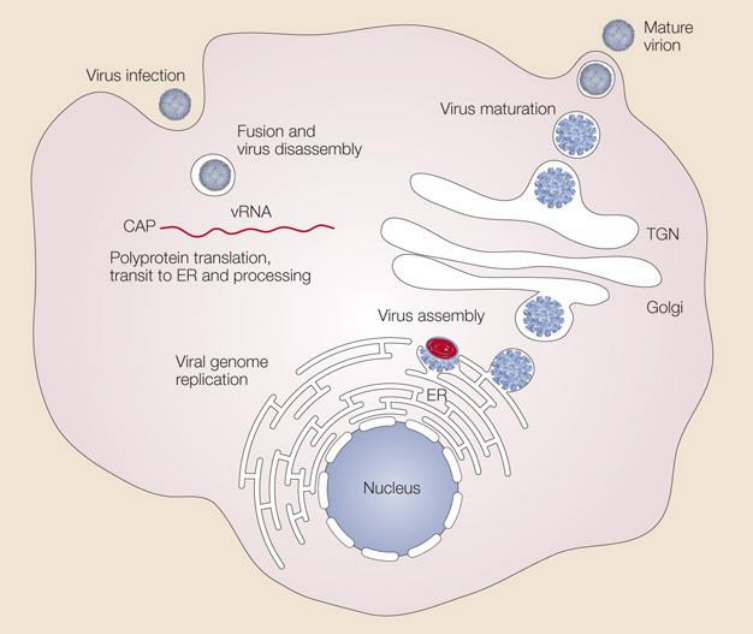

Fig. 3.1. The general life cycle of a flavivirus adopted from ref *(1)*. (Re-printed with permission from *(1)*. Copyright (2013) of Nature Publishing Group)

The question remains, why did the replication of the Dengue virus result in the inefficient cleavage of PrM, and consequently produce immature viruses which had been deduced as non-infectious in nature. Further studies revealed that the prM antibodies render essentially non-infectious immature Dengue virus nearly as infectious as the wild type virus. This enhancement of the immature Dengue virus infectivity was observed in a wide concentration range of the prM antibodies (*4*). The prM antibodies served to facilitate efficient interaction and cell entry of the virus-immune complexes via the FcγII-receptor (*3*). Upon entry, the immature Dengue virus particles became highly infectious presumably due to the efficient intracellular processing of prM to M by endoprotease furin.

3.1.3. Porous anodic aluminium oxide (AAO)

Porous anodic aluminium oxide (AAO) is an interesting nanostructured material. It is formed upon anodic oxidation of aluminium as an oxide layer that has a well-defined porous structure in which parallel pores of uniform diameter run perpendicularly to the surface. By optimising the anodisation conditions, the pore diameter can be tuned in the range of 10-450 nm (*6*). Because of its high density, well-ordered structure, ease of fabrication, and good mechanical properties, the alumina membrane has found applications in many fields (*6*). It had been used as a structural template in the fabrication of carbon nanotubes (*7*) and metal nanowires (*8*); as a mold for self-assembly (*9*); as a membrane to study the transport of molecules across it (*10*); for the filtration of proteins (*11*) and as a substrate for cell cultivation (*12*). The alumina membrane is also an excellent substrate material in biosensor systems based on optical waveguide sensing (*13*), surface plasmon resonance (*14*), and surface-enhanced Raman spectroscopy (*15*).

Compared with other porous membranes adopted in sensors, the use of AAO filter as a sensing membrane offers several advantages. The fabrication process is relatively inexpensive and highly reproducible. In addition, the three-dimensional structure of the AAO membrane provides a much higher surface area available for probe immobilisation for the same spot diameter as compared to flat surfaces (*16*). The mechanical stability of the material also allows a thin layer of metal to be deposited onto its surface (*17*). This matrix is also a suitable

and protective environment for biomolecule immobilisation and can transduce a biorecognition event such as DNA hybridisation into an electrical signal (*16*).

In the previous chapter, we had fabricated a nanoporous alumina membrane biosensor through anodising and etching of the aluminum metal deposited. The major disadvantage of the biosensor is the dislodging of the alumina layer during rinsing of the electrode. This is probably due to the weak adhesion of the alumina to the plastic surface of the pipette tip upon etching. In this chapter, commercially available alumina membranes (AAO) are used. The alumina membranes are made conductive by sputtering a submicron layer of inert Pt onto both sides of the membrane. Here, the biosensor is more robust as the alumina membrane is mechanically stable and a good material for the deposition of metal. Consequently, the conductive Pt layer does not dislodge easily with washing. The generally inert nature of both the Pt and the alumina allows the biosensor to be stored for months.

We present the use of a small and thin piece of alumina membrane, 60 μm thick and 13 mm in diameter as the sensing platform for the detection of Dengue infection using electrochemical impedance spectroscopy. The electrochemical setup is simplified by using the membrane as both the working and the counter electrode. This is achieved by coating both sides of the membrane with a submicron layer of platinum. Anti-prM antibody 2H2 is employed for the detection of Dengue virus. This antibody is highly specific towards all the Dengue complexes and recognises a conformational epitope. Even though the 2H2 antibody is not Dengue serotype specific, it can be

extremely useful for fast screening of probable Dengue cases in hospitals when a Dengue outbreak due to an unknown Dengue virus strain occurs. The transduction principle is based on the resistive-pulse sensing method, where the formation of immunocomplexes within the nanochannels reduces the ion current, resulting in a downward current pulse which will be reflected as an increase in resistance in the impedance measurement.

3.2. Materials and methods

3.2.1. Materials and reagents

Porous anodic alumina membranes (Anopore^{TM}) with nominal size of 20 and 200 nm were purchased from (United Scientific). Bovine serum albumin (BSA, >98%), potassium ferricyanide ($K_3Fe(CN)_6$**,** >99%) and phosphate buffered saline (PBS, 10X) were purchased from (Sigma Aldrich). Potassium hexacyanoferrate(II) trihydrate (>99.5%) was purchased from (Merck). Monoclonal anti-Dengue complex antibody (2H2) was purchased from (Merck-Millipore). Dengue serotype 2 and 3 viruses were obtained from Singapore Immunology Network-Agency for Science, Technology and Research (SIgN-A*STAR, Singapore). Chikungunya viruses (CHIKV) were kindly provided by Professor Vincent Chow (National University of Singapore, Microbiology). All chemicals and solvents used were of analytical grade and used as received. Ultrapure water from Sartorius Ultrapure Water System (Gottingen, Germany) was used for all preparations.

3.2.2. Fabrication of the Pt film working and counter electrode on the alumina membrane

A 100 nm thick Pt film was sputtered on both sides of the alumina membrane using JEOL JFC-1600 Auto Fine Platinum Coater (Tokyo, Japan). The Pt sputtering was performed using a current of 20 mA for 600 s. A 1 mm thick ring along the outer edge of the membrane was left uncoated on both sides

to prevent short circuiting. The effective pore size after Pt coating was determined using JEOL JSM-6701F field emission scanning electron microscopy (FESEM) (Tokyo, Japan). Aluminium tapes of suitable size were placed in electrical contact with the Pt coated alumina membrane such that it can be used as the working and counter electrodes.

3.2.3. Cell assembly and electrochemical measurement

The Pt coated alumina membrane was mounted between 2 home-made half-cell. The membrane together with an external Ag/AgCl reference electrode formed the three electrode system required for the electrochemical measurements (Fig. 3.2). Each side of the cell was filled with 10 mM of $Fe(CN)_6^{3-/4-}$ in 1X PBS (pH 7.4). Impedance measurements were performed with an autolab potentiostat/galvanostat (Utrecht, Netherlands) over a frequency range of 0.1 Hz-1 MHz, at the mid-peak potential of $Fe(CN)_6^{3-/4-}$ (~0.250 V vs. Ag/AgCl, saturated KCl), using an alternating voltage of 5 mV.

3.2.4. Preparation of the immunosensor

Each of the immobilisation step took place with the membrane held within the cell holder. The antibody, BSA and Dengue virus solutions were directly dripped onto the surface of the membrane and washed off with copious amount of PBS after the incubation time. Initially, 20 μL of the 2H2 antibodies was immobilised onto the nanochannels of the membrane for 1 h. Next, 20 μL of BSA was added for 30 min to block any available sites to prevent nonspecific

adsorption. Finally, 20 µL of the virus solution was added and incubated for 30 min. Impedance measurements were carried out after each of the immobilisation step to monitor the change in the pore resistance.

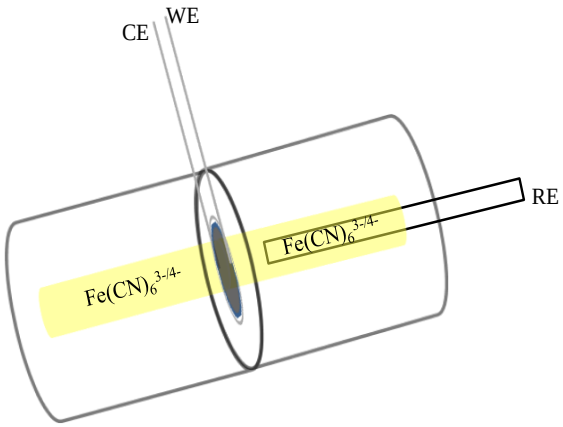

Fig. 3.2. (A) An electrochemical cell setup with the platinum coated alumina membrane acting as the working (WE) and counter electrode (CE) together with an external Ag/AgCl reference electrode (RE).

3.3. Results and discussion

3.3.1. Immunosensor fabrication

The alumina membrane was used as both the working and counter electrode. The close proximity in the distance between the electrodes reduces the resistance created by the electrodes. This helps to improve the measurement sensitivity. From the FESEM pictures (Fig. 3.3A and B), the Pt coated membrane has a pore reduction of approximately 60 nm. The effective pore size is about 140 nm where the Dengue virus (~50-60 nm) can still diffuse in. The immobilisation of the antibody, BSA and Dengue virus solutions were carried out at the face of the membrane acting as the counter electrode. This ensures that most of them are immobilised onto the nanochannels of the membrane, not the working electrode surface. Hence, the signals obtained come from the retardation of the redox probes as they transverse the partially blocked nanochannels.

A

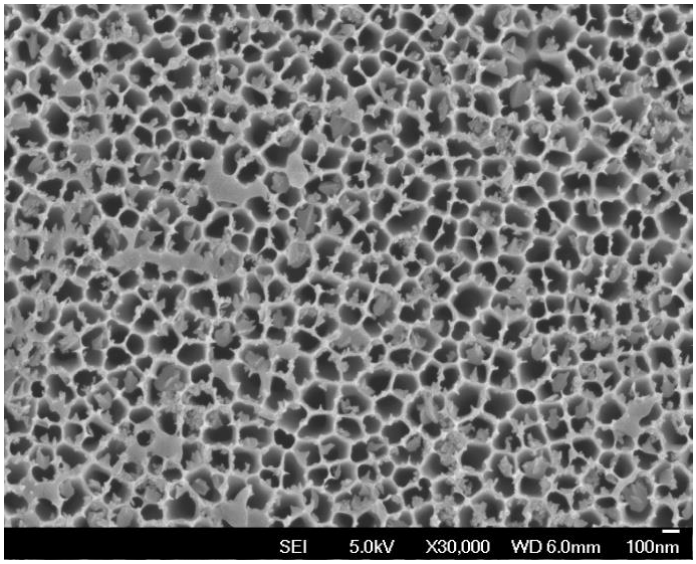

B

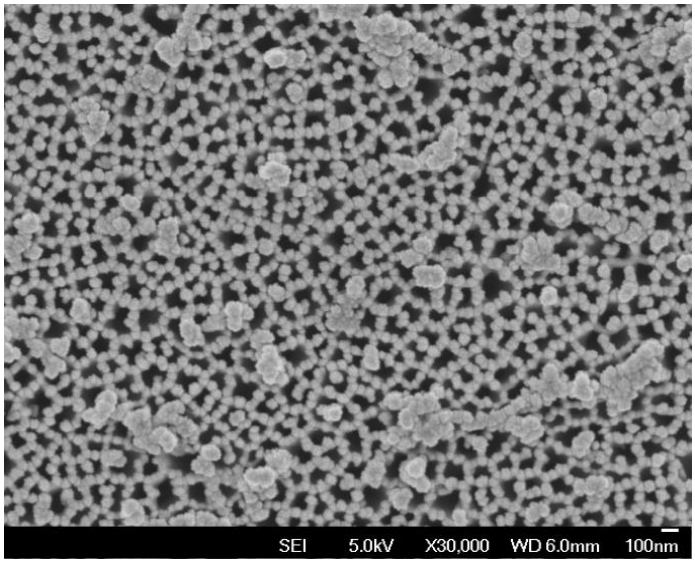

Fig. 3.3. Scanning electron micrographs of (A) Uncoated 200 nm alumina membrane (B) Pt coated 200 nm alumina membrane.

3.3.2. Impedance sensing for the detection of Dengue virus

Compared to other electrochemical techniques, electrochemical impedance spectroscopy has the advantage that the system is investigated under stationary conditions. Impedance measurement is also more sensitive to the change in ionic flow accompanying the formation of immunocomplexes between the Dengue viruses and the antibodies. In order to evaluate the interactions between the 2H2 monoclonal antibody and the Dengue virus, we exposed the immunosensors to various concentrations of Dengue 2 and Dengue 3 viruses ranging from 1 PFU mL^{-1} to 900 PFU mL^{-1}. From the Nyquist plots shown (Fig. 3.4A and B), it can be qualitatively observed that there is an increase in the resistance upon immobilisation of the antibodies, BSA and Dengue viruses. The resistance is expected to increase as the immobilised antibodies, BSA and Dengue viruses within the nanochannels of the membrane will cause the retardation of the redox probe flowing across. As a consequence,

the increase in the resistance after each of the immobilisation step is indicative that the immobilisation of the various components was successful. The increase in the resistance also correlates well with the size of the component immobilised, where the antibody (~8 nm) displayed the smallest change in resistance while the Dengue virus (~50-60 nm) showed the largest increase. It was also observed that the resistance increases with increasing concentration of the Dengue viruses added.

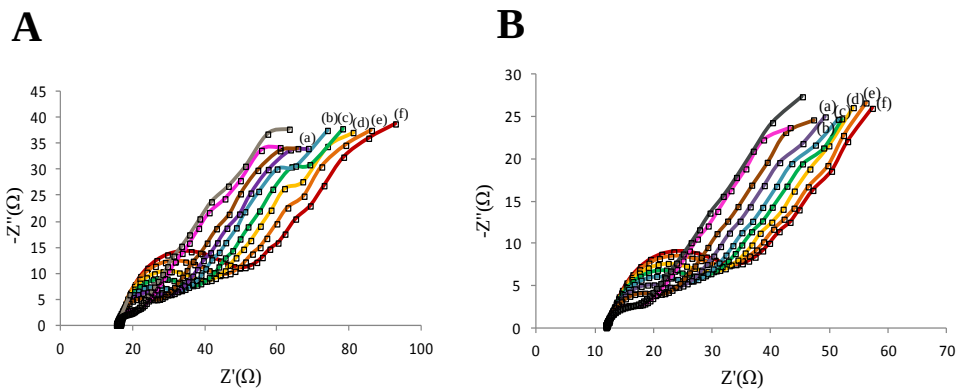

Fig. 3.4. Nyquist plots of the alumina membrane electrode after antibody immobilisation, BSA immobilisation and virus capture in PBS (pH=7.4) containing 10 mM $Fe(CN)_6^{3-/4-}$, bias potential of 0.25 V, frequency range of 0.1 Hz to 1 MHz; (A) Dengue 2 virus (B) Dengue 3 virus; (a) 1 PFU mL^{-1} (b) 11 PFU mL^{-1} (c) 61 PFU mL^{-1} (d) 161 PFU mL^{-1} (e) 361 PFU mL^{-1} (f) 861 PFU mL^{-1} of Dengue viruses.

For quantitative understanding of the impedance data, an equivalent circuit which can best address the entire physical phenomenon and describe the system needs to be constructed. The circuit most probably consists of 2 parts: the Randles circuit and the circuit for the alumina membrane joined in series (Fig. 3.5). The Randles circuit describes processes taking place at the working electrode surface. The circuit includes the following 4 elements; (a) The resistance of the solution (R_s) between the working and reference electrode; (b)

the Warburg element (W) resulting from the diffusion of ions from the bulk solution towards the working electrode; (c) the electron transfer resistance (R_{et}) and (d) the capacitance (C) of the electrode-electrolyte interface. The circuit for the alumina membrane consists of 2 elements; the resistance of the pores (R_p) and the membrane capacitance (C_m). Since the changes in the ionic flow are not affected by the electrode-electrolyte interface in the experiment, no further discussion about the Randles circuit will be done.

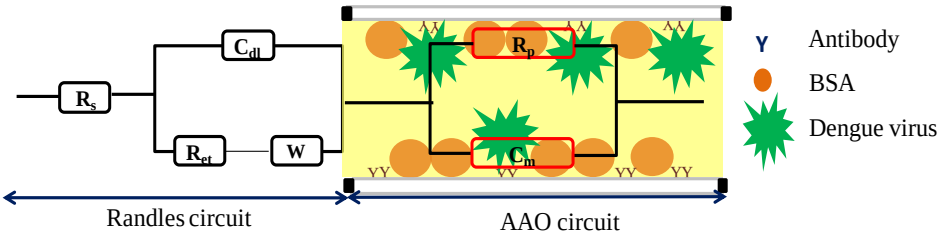

Fig. 3.5. The equivalent circuit for the Nyquist plot.

The impedance data were fitted with a commercial software EIS spectrum analyser (Minsk, Belarus). The results of the fitting are summarised in table 3.1, which mainly listed the 2 pivotal parameters R_p and C_m. The R_p responded more significantly than the C_m, thus it is a more suitable signal for sensing the changes in the ionic flow across the nanochannels. The change in R_p (ΔR_p) was calculated using the following equation:

$$\Delta R_p = R_p(\text{Dengue-Ab}) - R_p(\text{BSA})$$

where R_p (Dengue-Ab) is the resistance value after the formation of the immunocomplexes between the Dengue viruses and the antibodies and R_p (BSA) is the resistance value before any addition of the Dengue viruses. The increase

in the value of ΔR_p is associated with the blocking behavior of the assembled layer on the wall of the nanochannels. The interactions between the Dengue viruses and the antibodies resulted in the formation of immunocomplexes on the wall of the nanochannels. These immunocomplexes act as the inert electron transfer blocking layer that hinder the diffusion of the $Fe(CN)_6^{3-/4-}$ redox pair across the nanochannels. As a consequence, the pore resistance increases with the amount of Dengue viruses added due to the increase in the number of immunocomplexes formed, which will further obstruct the nanochannels. The plot of ΔR_p against the concentration of Dengue 2 (Fig. 3.6A) and Dengue 3 viruses (Fig. 3.6B) yielded calibration plots with good correlation coefficients of >0.99. The limits of detection were found to be 0.230 PFU mL^{-1} for Dengue 2 virus and 0.710 PFU mL^{-1} for Dengue 3 virus. This is actually comparable to another membrane-based virus captured sensor which reported a detection limit of 1 PFU mL^{-1} (*18*) as well as other reported techniques (Table 3.2).

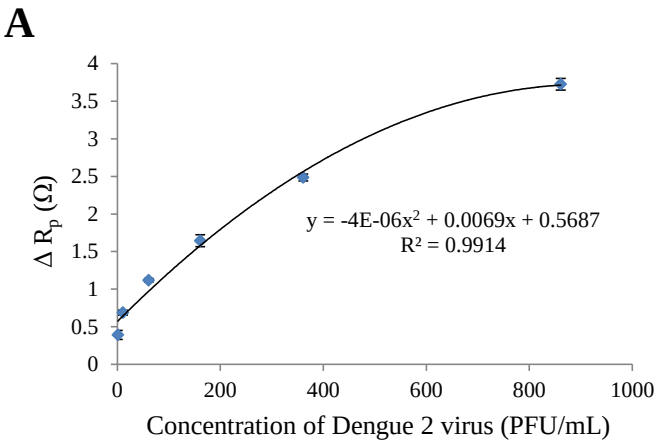

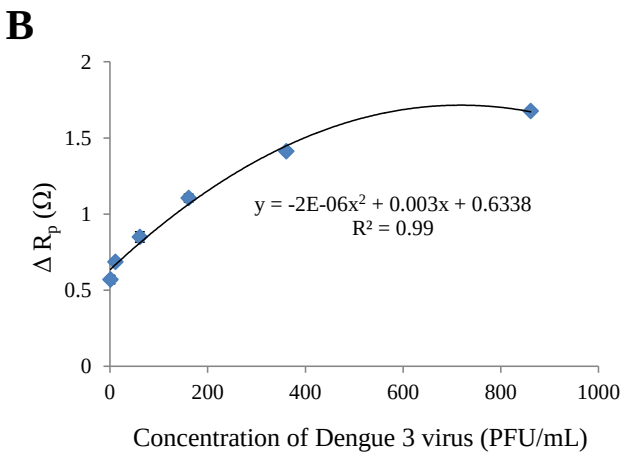

Fig. 3.6. Calibration plot of the change in pore resistance against the concentration of (A) Dengue 2 virus and (B) Dengue 3 virus.

3.3.3. Binding affinity studies of the 2H2 antibody with Dengue 2 and Dengue 3 viruses.

The 2H2 antibody is an anti-Dengue complex antibody that targets all 4 Dengue serotypes. This antibody recognises a conformational epitope on the PrM of the Dengue virus. Ideally, all the immature Dengue viruses will undergo PrM cleavage to form Pr and M prior to release during replication. However, this cleavage is usually not completed and a mixture of mature and immature Dengue viruses are often released from infected cells (*3*). This antibody was found to bind to the immature Dengue virus, and thereafter enhance Dengue infection by promoting PrM cleavage and virus fusion. Here, we demonstrate its binding affinity with the more common Dengue serotype 2 and 3 viruses under normal physiological condition of pH 7.4.

Table 3.1. Fitted values of the Nyquist plots showing pore resistance (R_p) and membrane capacitance (C_m).

DENV 2	C_m(nF)	R_p(Ω)	ΔR_p(Ω)	χ^2	DENV 3	C_m(nF)	R_p(Ω)	ΔR_p(Ω)	χ^2
BSA	0.22	1.33	0	0.06	BSA	0.11	1.87	0	0.004
1 PFU mL^{-1}	0.24	1.70	0.39	0.05	1 PFU mL^{-1}	0.13	2.27	0.38	0.004
11 PFU mL^{-1}	0.24	1.99	0.69	0.05	11 PFU mL^{-1}	0.12	2.36	0.49	0.003
61 PFU mL^{-1}	0.23	2.42	1.12	0.05	61 PFU mL^{-1}	0.15	2.53	0.66	0.01
161 PFU mL^{-1}	0.23	3.00	1.64	0.04	161 PFU mL^{-1}	0.17	2.76	0.92	0.02
361 PFU mL^{-1}	0.25	3.79	2.48	0.05	361 PFU mL^{-1}	0.18	3.09	1.22	0.02
861 PFU mL^{-1}	0.25	5.03	3.73	0.09	861 PFU mL^{-1}	0.18	3.35	1.49	0.02

Table 3.2. Summarised table showing the techniques used to detect Dengue infection, their required analysis time and limits of detection.

Method	Analyte	Limits of detection	Time required	Reference
Electrochemical alumina biosensor	DENV 2	1 PFU mL^{-1}	~ 40 min	Chapter 2
	DENV 2 & 3	0.23 & 0.71 PFU mL^{-1}	~ 40 min	Chapter 3
ELISA	DENV	1000 PFU mL^{-1}	~ 4 h	(*19*)
Microfluidics immunosensor chip	DENV	10 PFU mL^{-1}	~30 min	
Gold nanoparticle QCM biosensor	RNA	2 PFU mL^{-1}	~ 1.5 h	Chapter 1 ref (*22*)
Silicon nanowire FET biosensor	RNA	10 fM	~ 30 min	Chapter 1 ref (*35*)
Microfluidics-based fluorescence biosensor	RNA	50 pM	~ 20 min	Chapter 1 ref (*39*)

In this experiment, the immunosensor was immobilised with 50 PFU mL^{-1} of Dengue 2 and Dengue 3 virus solution with an incubation time of 30 min. The results (Fig. 3.7A and B) indicate that the Dengue 2 virus generally gives a greater response in contrast to the Dengue 3 virus. This observation is consistent with the western blot data reported (*20*), where the interactions between the 2H2 antibodies and the Dengue 2 viruses produced a greater luminescence. This suggested that the Dengue 2 virus has a stronger binding affinity to the antibody compared to the Dengue 3 virus.

At pH (~6-6.4), the immature Dengue virus was observed to undergo conformational changes when the in-vitro medium was acidified. Several researchers postulated that this change prepares the Dengue virus for the cleavage of PrM by furin to release the membrane glycoprotein and thereby allowing virus fusion (*5*). In our experiment, we observed that the structural rearrangement of the Dengue virus did not affect the recognition of the epitope on the PrM by the antibody. Interestingly, the Dengue 3 virus displayed a larger response than the Dengue 2 virus towards the antibody at this pH (Fig. 3.7C and D). It was observed that the sites of interaction between the Dengue cross-reactive antibody such as the 2H2 antibody and the 4 Dengue serotypes are commonly unique and different (*21*). The change in pH from 7.4 to 6.4 may have caused the charges around the epitope of the Dengue 2 and 3 virus to change. This change could have led to more favorable electrostatic interactions between the Dengue 3 virus and the antibody, resulting in a greater response as observed. We are not sure what causes the inconsistent results obtained after 150 PFU mL^{-1} of Dengue viruses have been added.

3.3.4. Effect of the membrane's nominal size on sensing capacity

Here, the experiment was repeated with alumina membrane of smaller nominal size (20 nm) at three concentrations; 1, 10 and 100 PFU mL^{-1}. The pores of the 20 nm membrane were almost totally covered upon sputtering with Pt at the same conditions as the 200 nm membrane. The exposed pores were those partially covered or not covered by the Pt atoms (Fig. 3.8A and B). The uncovered pores allow the BSA to enter, thus the pore resistance is expected to increase. However, the membrane showed little or no change in the pore resistance with the Dengue viruses (Fig. 3.9). The relative size of the Dengue virus is approximately 50-60 nm which is much larger than the pore opening. Being unable to enter the pores, there would be no change in the pore resistance as observed. This demonstrates that the selection of the membrane's pore size is critical for the experiment and the signals that we obtained most probably came from the retardation of the redox probes due to the partial blockage of the nanochannels with respect to the setup of the system.

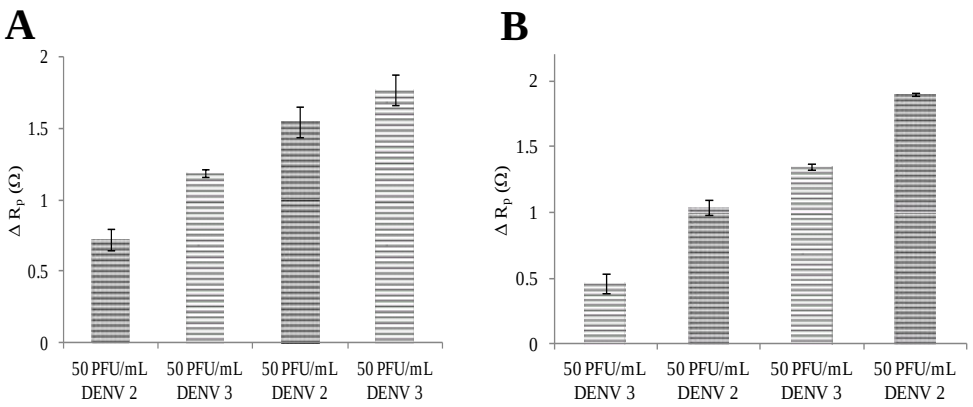

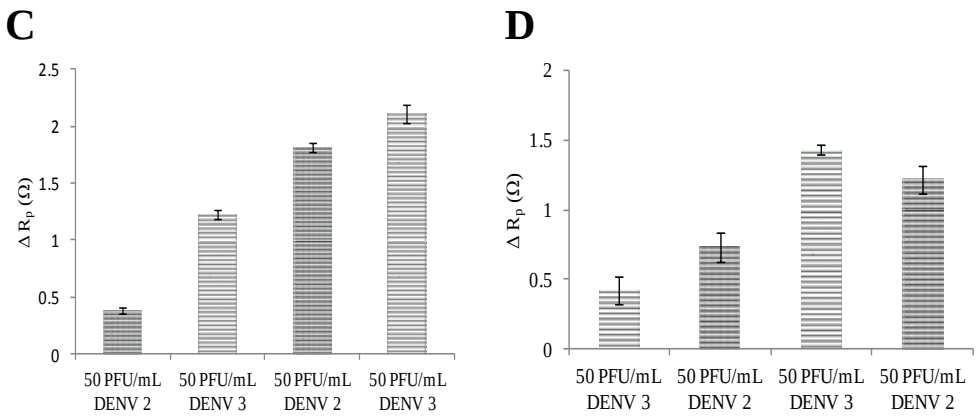

Fig. 3.7. Bar charts illustrating the difference in the interactions between the 2H2 antibody with the Dengue 2 and Dengue 3 virus at pH 7.4 (A and B) and pH 6.4 (C and D). Experiments were done in consecutive steps from left to right.

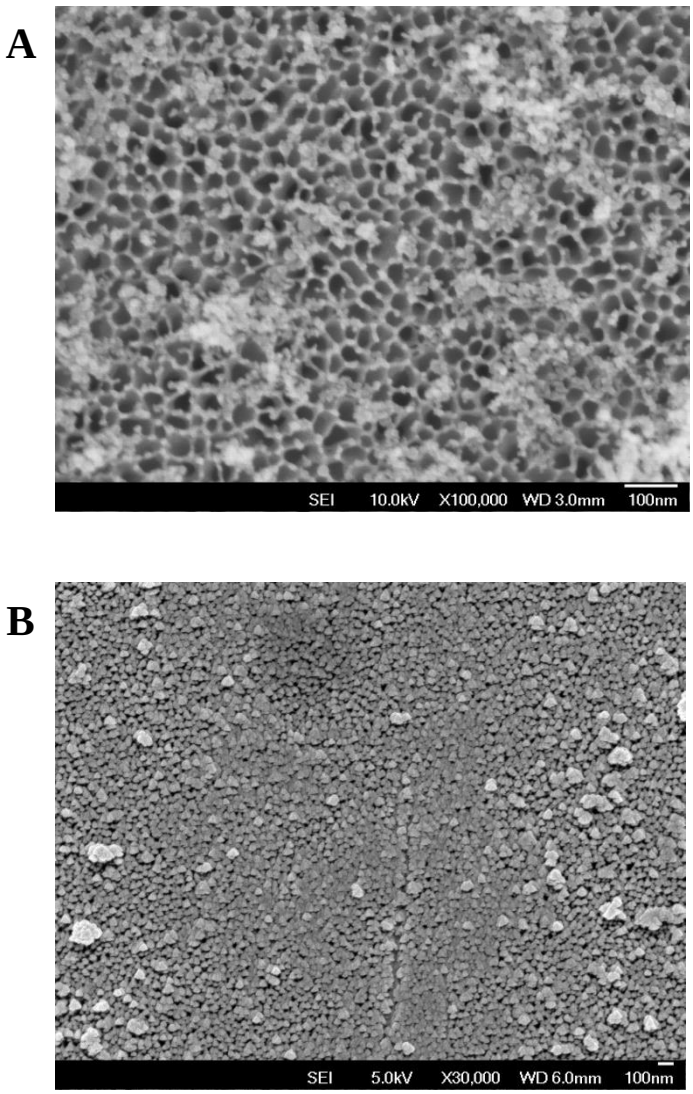

Fig. 3.8. Scanning electron micrographs of (A) Uncoated 20 nm alumina membrane (B) Pt coated 20 nm alumina membrane.

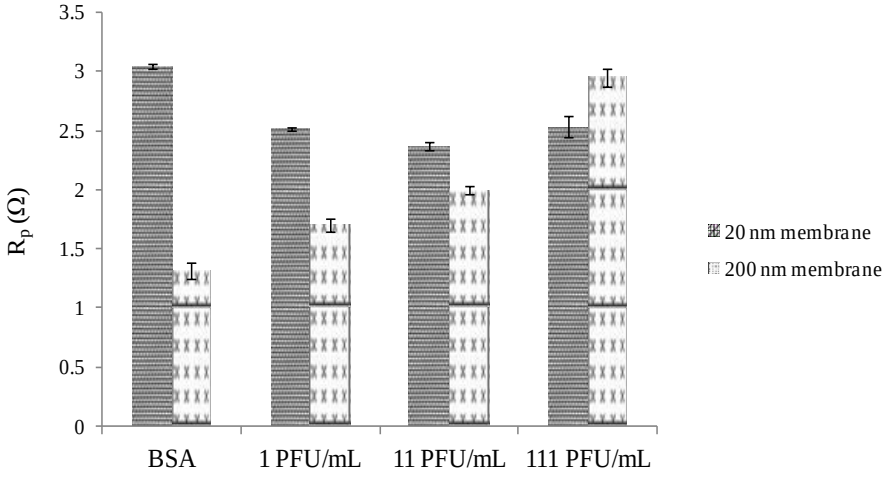

Fig. 3.9. Bar charts illustrating the response of the alumina membrane to the Dengue 2 virus at two different pore sizes: 20 nm and 200 nm. Experiments were done in consecutive steps from left to right.

3.3.5. The specificity of the immunosensor

The specificity of the immunosensor was determined by challenging it with a non-flavivirus, Chikungunya virus (CHIKV). The Chikununya virus belongs to the alphavirus family and it is also transmitted to human through Aedes mosquitoes' bites. An infection by the Chikungunya virus will result in symptoms similar to the Dengue infection. Hence, diagnosis of the true agent causing the infection is often difficult. The immunosensor showed good selectivity with the Chikungunya virus, as reflected by the small change in the pore resistance (Fig. 3.10). This result is very encouraging and indicates the potential of the sensor to clearly differentiate an infection between the two viruses.

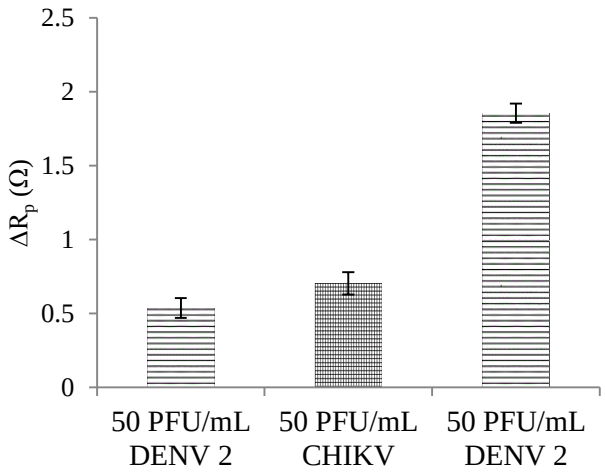

Fig. 3.10. Bar charts illustrating the selectivity of the 2H2 antibody towards the Dengue serotype 2 virus and Chikungunya virus. Experiments were carried out in a consecutive manner from left to right.

3.3.6. Real Sample analysis

The constructed immunosensor was utilised to detect Dengue viruses in spiked human serum samples. The human serum was diluted 100 times and spiked with 10, 50 and 100 PFU mL^{-1} of Dengue viruses. Similarly, the various spiked solutions were immobilised onto the electrode for 30 min before washing off the unbound Dengue viruses with copious amount of PBS. Subsequently, impedance measurements were carried out. Despite the complicated matrix, the results (Fig. 3.11) indicate the plausibility of using the immunosensor for qualitative and quantitative determination of Dengue viruses in infected human serum samples with a short total analysis time of 40 min.

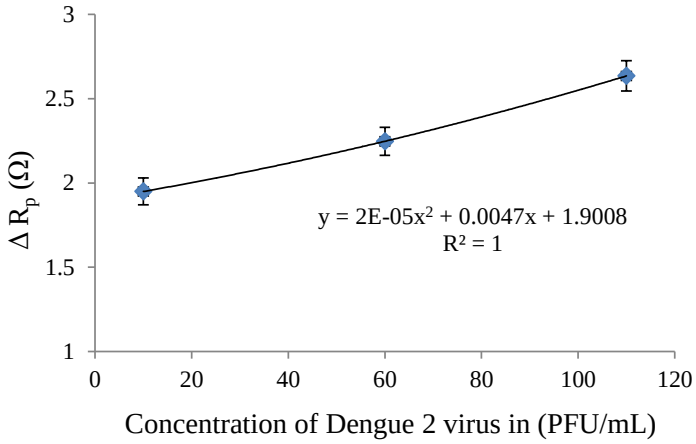

Fig. 3.11. Plot of signal response against the concentration of Dengue 2 virus in the spike serum samples.

3.4. Conclusion

We have demonstrated the possibility of using the thin piece of alumina membrane as an immunosensor for the detection of Dengue infection. This membrane sensor is label-free, sensitive towards Dengue virus and has a relatively fast data acquisition time of 40 min. This method is faster and less labour intensive than the conventional ELISA method. In addition, the small piece of alumina membrane allows it to be disposed off easily or sent for autoclaving. Hence, this membrane sensor coupled with an electrochemical detection provides opportunity for the sensor to be fabricated into a point-of-care diagnostic unit for clinical use. The future works include investigating the sensor response with Dengue 1 and Dengue 4 viruses as well as the robustness of its selectivity with other viruses.

3.5. References

1. Mukhopadhyay, S., Kuhn, R. J., and Rossmann, M. G. (2005) A structural perspective of the flavivirus life cycle, *Nat. Rev. Microbiol. 3*, 13-22.

2. Martín, C. S. S., Liu, C. Y., and Kielian, M. (2009) Dealing with low pH: entry and exit of alphaviruses and flaviviruses, *Trends Microbiol. 17*, 514-521.

3. Rodenhuis-Zybert, I. A., Van Der Schaar, H. M., Da Silva Voorham, J. M., Van Der Ende-Metselaar, H., Lei, H. Y., Wilschut, J., and Smit, J. M. (2010) Immature Dengue virus: A veiled pathogen?, *PLoS Pathogens 6*,(1).

4. Dejnirattisai, W., Jumnainsong, A., Onsirisakul, N., Fitton, P., Vasanawathana, S., Limpitikul, W., Puttikhunt, C., Edwards, C., Duangchinda, T., Supasa, S., Chawansuntati, K., Malasit, P., Mongkolsapaya, J., and Screaton, G. (2010) Cross-reacting antibodies enhance Dengue virus infection in humans, *Science 328*, 745-748.

5. Yu, I. M., Zhang, W., Holdaway, H. A., Li, L., Kostyuchenko, V. A., Chipman, P. R., Kuhn, R. J., Rossmann, M. G., and Chen, J. (2008) Structure of the immature Dengue virus at low pH primes proteolytic maturation, *Science 319*, 1834-1837.

6. Ter Maat, J., Regeling, R., Ingham, C. J., Weijers, C. A. G. M., Giesbers, M., De Vos, W. M., and Zuilhof, H. (2011) Organic modification and subsequent biofunctionalisation of porous anodic alumina using terminal alkynes, *Langmuir 27,* 13606-13617.

7. Lee, D. H., and Condrate Sr, R. A. (1995) An FTIR spectral investigation of the structural species found on alumina surfaces, *Mater. Lett. 23*, 241-246.

8. Mátéfi-Tempfli, S., Mátéfi-Tempfli, M., Vlad, A., Antohe, V., and Piraux, L. (2009) Nanowires and nanostructures fabrication using template methods: a step forward to real devices combining electrochemical synthesis with lithographic techniques, *J. Mater. Sci. – Mater. Electron. 20,* S249-S254.

9. Sakurai, M., Shimojima, A., Yamauchi, Y., and Kuroda, K. (2008) Self-assembly of amphiphilic alkyloligosiloxanes within cylindrically and spherically confined spaces, *Langmuir 24*, 13121-13126.

10. Yamashita, T., Kodama, S., Ohto, M., Nakayama, E., Takayanagi, N., Kemmei, T., Yamaguchi, A., Teramae, N., and Saito, Y. (2007) Use of porous anodic alumina membranes as a nanometre-diameter column for high performance liquid chromatography, *Chem. Commun. 11*, 1160-1162.

11. Cheow, P. S., Ting, E. Z. C., Tan, M. Q., and Toh, C. S. (2008) Transport and separation of proteins across platinum-coated nanoporous alumina

membranes, *Electrochim. Acta 53*, 4669-4673.

12. Hoess, A., Teuscher, N., Thormann, A., Aurich, H., and Heilmann, A. (2007) Cultivation of hepatoma cell line HepG2 on nanoporous aluminum oxide membranes, *Acta Biomater. 3*, 43-50.

13. Lau, K. H. A., Tan, L. S., Tamada, K., Sander, M. S., and Knoll, W. (2004) Highly sensitive detection of processes occurring inside nanoporous anodic alumina templates: A waveguide optical study, *J. Phys. Chem. B 108*, 10812-10818.

14. Kim, D. K., Kerman, K., Saito, M., Sathuluri, R. R., Endo, T., Yamamura, S., Kwon, Y. S., and Tamiya, E. (2007) Label-free DNA biosensor based on localised surface plasmon resonance coupled with interferometry, *Anal. Chem. 79*, 1855-1864.

15. Lu, Z., Ruan, W., Yang, J., Xu, W., Zhao, C., and Zhao, B. (2009) Deposition of Ag nanoparticles on porous anodic alumina for surface enhanced Raman scattering substrate, *J. Raman Spectrosc. 40*, 112-116.

16. Wang, L., Liu, Q., Hu, Z., Zhang, Y., Wu, C., Yang, M., and Wang, P. (2009) A novel electrochemical biosensor based on dynamic polymerase-extending hybridisation for E. coli O157:H7 DNA detection, *Talanta 78*, 647-652.

17. Li, S. J., Li, J., Wang, K., Wang, C., Xu, J. J., Chen, H. Y., Xia, X. H., and Huo, Q. (2010) A nanochannel array-based electrochemical device for quantitative label-free DNA analysis, *ACS Nano 4*, 6417-6424.

18. Cheng, M. S., Ho, J. S., Tan, C. H., Wong, J. P. S., Ng, L. C., and Toh, C. S. (2012) Development of an electrochemical membrane-based nanobiosensor for ultrasensitive detection of Dengue virus, *Anal. Chim. Acta 725*, 74-80.

19. Weng, C.H., Huang, T.B., Huang, C.C., Yeh, C.S., Lei, H.Y., Lee, G.B. (2011) A suction-type microfluidic immunosensing chip for rapid detection of Dengue virus, *Biomed. Microdevices 3*, 585-595.

20. Falconar, A. K. I. (1999) Identification of an epitope on the Dengue virus membrane (M) protein defined by cross-protective monoclonal antibodies: Design of an improved epitope sequence based on common determinants present in both envelope (E and M) proteins, *Archives of Virology 144*, 2313-2330.

21. Gromowski, G. D., Barrett, N. D., and Barrett, A. D. T. (2008) Characterisation of Dengue virus complex-specific neutralising epitopes on envelope protein domain III of Dengue 2 virus, *Journal of Virology 82*, 8828-8837.

Chapter 4: A nanofluidics membrane-based detection and serotyping of Dengue virus

4.1. Introduction

4.1.1. Current state-of-art in disease diagnosis

Diagnosis of diseases using antibody-antigen immune-based methods is of scientific and technological significance, because of the versatility to detect either the antibody or antigen, and the ease to generate specific antibodies and antigens using cellular and recombinant technologies (*1-3*). Importantly, antibodies are an integral part of the natural immune response and play a crucial protective role during infections. Antibodies are useful biomarkers to assess the magnitude and specificity of an immune response, besides the disease status of the patient (*4*). Consequently, several methods making use of the natural affinity of the antibody with the antigen had been reported. These methods involved labelled-free detection using sensitive instrumentations such as acoustics, surface plasmon resonance or electrochemical impedance spectroscopy as well as labelled detection with fluorescence and electrochemical methods as mentioned in chapter 1 of the thesis. In order to further improve the detection sensitivity and selectivity of the sensing system, various approaches had been taken. Different strategies had been employed for amplifying the transducing signals of the antibody–antigen interactions. Most conventional amplification strategies have relied on the use of labels, such as enzymes, electroactive molecules, redox complexes, metal ions and recently nanomaterials. While the

use of sandwich or multiple steps approach to magnify the differences between the binding affinities of the target and non-targets for the same antigen or antibody has been used to improve selectivity.

These immune-based methods which rely on capture mechanism under equilibrium conditions are traditionally prevalent. For many diseases, serological tests remain the standard for disease diagnosis. However, the cross-reactivities of antibodies are common which give false-positive results and limit the detection selectivity of these immune-based methods. Conversely, microfluidics methods when applied to the separation and detection of biological molecules provide significant advantages over the above immune-based batch analysis methods such as higher efficiencies, faster analysis time, use of a much smaller sample volume, improvement in the selectivity and multiple analytes detection (*5*). The miniaturised flow systems had reported successful two-dimensional lab-on-a-chip designs which comprise flow pumps with effective dampers and micro-sized channels grafted with antibodies for protein capture or separation (*5*). In addition, when coupled to micro- or nano-sized electrodes and nanopore structures, these microfluidics systems can achieve high sensitivity, fast response and high resolution due to improvement in sample preconcentration, purification and selection (*6*).

4.1.2. Nanofluidics

Recently, nanofluidics, the study and use of fluid flow in and around structures of nanoscale dimensions is becoming a major field of research. There are three interesting properties of fluid flow at the nanoscale which make them particularly attractive for research and development of nanofluidics-based sensors. First, the flow of fluid generally occurs in structures which are comparable to natural scaling lengths. Second, the surface-area-to-volume ratio can be amplified and together with the small cross-sectional size (the last property) of the nanochannels make diffusion an efficient mass transport mechanism at this scale (*7*). This dynamic new field has drawn attention in technology, biology, and medicine (*8, 9*) due to advances in the biomolecule preparation and analysis system, single molecular interrogations and other unique modes of molecular manipulation through making use of electrokinetic effects in the nanochannels like electro-osmosis, electrophoresis and stream potential (*10*). Some significant works in nanofluidics include nanopore (*11*) and nanowire (*12*) being used for label-free biomolecule detection.

To study the intraparticle mass transfer performance in adsorption and chromatographic processes through the nanochannels, various physical and mathematical descriptions had been proposed such as homogeneous diffusion model, pore model, pore diffusion model, surface diffusion model and parallel diffusion model. Here, structural models which consider the effects of pore size distribution, pore volume fraction, particle size distribution and other structural information about the adsorbent particle, provide a more comprehensive and

realistic descriptions for transport across porous systems (*13*). Most of these models were derived from the classical Fick's law, in which the concentration gradient is considered as the driving force. The Fick's law is definitely true for an ideal solution like those in the pore of the membrane, where the protein concentration is very low (usually less than 5 mg mL^{-1}) (*13*).

4.1.3. Adsorption of protein on surfaces

Protein adsorption to surfaces is a common event in numerous biological processes. The adsorption can trigger adhesion of particles, bacteria or cells possibly promoting inflammation cascades or fouling processes. In the field of analytical sciences, nonspecific protein adsorption on sensor surfaces, protein chips or assay platforms is a serious problem that cause the degradation of their analytical performance. Wherever proteins come into contact with a solid interface, they will most likely adsorb to it (*14*). Nakanishi *et al.* had demonstrated that it is complicated to avoid protein adsorption. From a macroscopic viewpoint, the important factors affecting protein adsorption are the structural stability of the protein and the hydrophilic/hydrophobic properties of its surface. In general, proteins with low internal stability such as IgG and BSA seemed to absorb on all surfaces irrespective of electrostatic interactions owing to a gain in conformational entropy (*15*). As the mechanism behind protein adsorption events strongly affects the adsorption kinetics, various models developed in this field are kinetic models which are usually expressed through rate equations. These models normally start from the basic Langmuir equation (*14*).

4.1.4. Use of ferrocene as an electroactive label

Ferrocene (Fc) and its derivatives are mostly neutral compounds that are particularly stable in the presence of water and air. They are pre-ionic compounds with highly reversible redox systems which may readily be switched electrochemically between the ferrocene and the respective ferrocinium cation at low potential. A unique property of metallocene is the possibility of introducing substituents on one or both of the cyclopentadienyl rings while retaining the properties of a simple one-electron redox couple. The electrochemical oxidation potential is tunable by changing the nature of the substituents (*16*). Ferrocene labelled immunoglobulin G (IgG-Fc) is of particular interest since it enables monitoring of binding events of a range of analytes to the antigen binding sites of IgG electrochemically. The conventional method for Fc-labelling involves carbodiimide coupling of Fc-COOH and the NH_2 terminated residue of an antibody (*17*). Kossek *et al.* had shown that the antibody-ferrocene conjugate has an almost unpaired binding capacity as the neat antibody (*18*). In addition, ferrocene labelled antibody was found to be stable for several weeks to months. Lim and Tanaka *et al*. had used labelled Fc-anti-human chorionic gonadotrophine IgG (*19*), Fc-anti-histamine IgG (*20*) and Fc-anti-hemoglobin IgG (*21*) for the detection of the target analyte. The method protocol involves flowing the mixture of free target antigens, label-free antibodies and labelled immunocomplexes into a column which selectively binds to those unbound species and allows the immunocomplexes to pass through. Subsequently, the immunocomplexes were detected electrochemically at the oxidation potential of the ferrocene labelled species.

Herein, we report a method which demonstrates potential in detecting the Dengue virus infecting the patient and identifying its corresponding serotype concurrently. The biosensor's design comprises a low cost potentiostat/galvanostat and an alumina nanoporous membrane separating a two compartment cell. Flow-injection instrumentations are not required (Fig. 4.1). The sensing mechanism is based on electrochemical detection coupled to a continuous diffusion flow of redox labelled antibody probes through array of nanochannels attached with the virus particles within the membrane. This is unlike the current sandwich immune-based method that adopt a static capture approach. Such approach may suffer from nonspecific bindings of other species in particular those with very similar binding affinities as the target analyte.

Common serotypes of Dengue virus with highly conserved amino acid residue sequences were used as the model analytes. This membrane biosensor method successfully achieves the identification of the Dengue 2 virus from the Dengue 3 and 4 virus, and the uninfected patient's serum samples. Its ability to identify a specific Dengue virus serotype within short analysis time of approximately 2 h is comparable to the polymerase chain reaction (PCR) method that is being used currently. By monitoring the rate at which the working electrode is fouled by the labelled proteins, a time-based result can be presented. In addition, we show that by relating with the Langmuir adsorption and Fick's first law of diffusion equation, we can adequately simulate the results observed.

4.2. Theory

4.2.1. Discussion of the sensing mechanism at the working electrode

The sensing electrode gives increasing signal toward increasing concentration of the redox labelled protein probes in the receiver solution. At the same time, significant protein adsorption occurs at the electrode which causes the differential pulse voltammetric (DPV) peak current $(\delta i)_{max}$ signal to decrease rapidly. Electrode fouling effect had been observed for many proteins including IgG and was explained above as a simultaneous process for these type of soft proteins to adsorb onto surfaces due to a gain in entropy. Assuming the adsorption rate at which a monolayer of proteins forms on an electrode surface can be described using the simple Langmuir adsorption model and that protein desorption is negligible, the overall rate of change in θ is:

$$\frac{d\theta}{dt} = k_a C_{bulk}(1-\theta)N \qquad (1)$$

where k_a is the adsorption rate constant, N is the total number of sites and θ is the fractional coverage. For simplicity, the Langmuir equation is being used here. However, we must realise that the use of Langmuir equation is less adequate since adsorption of globular proteins onto membrane surfaces is generally irreversible. The integrated form of the above equation gives the change in fraction coverage of the available sites (1-θ) with respect to time (t):

$$1-\theta = e^{-k_a C_{bulk} N(t)} \quad (2)$$

Thus over time, the surface area of the electrode that is available for binding with the proteins (A_t) decreases exponentially from the original unfouled electrode area (A_0):

$$A_t = A_0 . e^{-k_a C_{bulk} N(t)} \quad (3)$$

For a solution containing ferrocene tagged proteins kept under a continuously stirred condition, the differential pulse voltammetric (DPV) peak current $(\delta i)_{max}$ obtained at an oxidising electrode potential of ~1.0 V (vs. Ag/AgCl,1M KCl) is well described as:

$$(\delta i)_{max} = nFAmc_{bulk} \quad (4)$$

where m incorporates the mass transfer coefficient and pulse voltammetry experimental conditions, c_{bulk} is the concentration of the ferrocene tagged proteins, and A is the surface area of the electrode. Here, n=1 since oxidation of ferrocene involves one electron transfer. Combining equation (3) and (4), we obtain the overall current signal of the electrode toward a ferrocene tagged proteins which fouls the electrode surface upon reaching the electrode surface:

$$(\delta i)_{max} = nFmc_{bulk} A_0 e^{-k_a c_{bulk} N(t)} \quad (5)$$

Experimentally, the constant values of ($nFmA_0$) and (k_aN) were obtained by measuring the mass transfer limiting current of the glassy carbon electrode maintained at ~1.0 V (vs. Ag/AgCl,1 M KCl) in the presence of different concentrations of ferrocene tagged BSA (BSA-Fc) (Fig. 4.2). The obtained data was fitted with the empirical equation:

$$(\delta i)_{max} = [M] c_{bulk}\ e^{-[P] c_{bulk}(t)}$$

using the OriginPro software (Northampton, United Kingdom). By adding the average values derived in table 4.1 into equation 5, the following empirical equation adequately describes the amperometric current signal of a glassy carbon sensing electrode in response towards redox labelled proteins:

$$(\delta i)_{max} = 1.16 \text{x} 10^{-06} c_{bulk}.e^{-0.0197 c_{bulk}(t)} \qquad (6)$$

4.2.2. Mass transport of ferrocene labelled protein probes across the membrane

Having derive the equation that describes the sensing response of the electrode, we need to account for the amount of labelled proteins which has transverse the membrane from the feed compartment to the receiver compartment to reach the electrode surface. We consider the flux J (mol cm^{-2}) of the ferrocene labelled proteins across the membrane via Fick's diffusion:

$$J = -D\frac{dc}{dx} \qquad (7)$$

where D is the diffusion coefficient of the ferrocene labelled protein, dc is the change in the protein concentration and dx is the length of the nanochannel over which the concentration changes.

Within the nanochannels, the transversing ferrocene labelled antibody probes will be strongly adsorbed onto the virus particles bounded to the nanochannels. As a result of the strong binding interactions, the transversing antibody concentration within the nanochannels will be less than its initial concentration in the feed solution, since antibody-antigen binding kinetics can be considered instantaneous in the absence of mass transfer limitation. The amount of antibodies that is adsorbed onto the viruses will depend on the binding sites available on the virus surface. Saturation of the binding sites occurs gradually over time as the antibody probes move into the nanochannels from the feed solution. Assuming the adsorption follows a Freundlich adsorption as found in chapter 2, the antibody concentration within the nanochannels, near the feed solution side, changes with time as follows:

$$c_{channel,feed} = c_{feed} - y c_{feed} e^{-k_a C_{feed}{}^n (t)} \qquad (8)$$

where k_a is the adsorption rate constant; $c_{feed} e^{-k_a C_{feed}{}^n (t)}$ gives the amount of antibody that binds to the viruses in the nanochannels; y describes the ratio of the adsorbed antibody probe concentration near the feed side to the antibody

probe concentration in the feed solution; $yc_{\text{feed}}e^{-k_a C_{feed}{}^n(t)}$ is the antibody concentration removed from the nanochannels solution by adsorption onto the viruses attached to the nanochannels and the membrane wall (nonspecific adsorption). This decreases with time as the binding sites on the virus particles become saturated. Here, it is not practical to simulate the Freundlich term (n) as the exponential component generally gives a small value between 0 and 1. As a consequence, the exponential term is simplified to $yc_{\text{feed}}e^{-x(t)}$ where $x=k_a(C_{feed})^n$.

The concentration of the antibody probes within the nanochannels near the receiver side is zero at initial time. Thus, a concentration gradient of the transversing probes exists across the nanochannels as follows, which changes with time according to Fick's diffusion and saturation of the binding sites on the viruses attached within the nanochannels:

$$J = -D\frac{\{c_{\text{feed,t}} - y c_{\text{feed,t}} e^{-xt}\} - c_{\text{receiver,t}}}{l_m} \qquad (9)$$

where $c_{\text{feed,t}}$ and $c_{\text{receiver,t}}$ are the concentration of the antibody probes within the nanochannels at the feed and receiver side respectively at time (t) and l_m is the length of the nanochannel (60 μm). The concentration of the antibody probes in the receiver solution is computed using equation 9 and this is input into the empirical equation 6 to obtain the expected DPV peak current signal over time. Subsequently, the calculated DPV peak current signals are normalised against the highest DPV peak current obtained and these give the simulated biosensor's signals.

4.3. Materials and methods

4.3.1. Materials and reagents

Bovine serum albumin (BSA,>98%), ferrocenecarboxylic acid (FeCOOH), phosphate buffered saline (PBS, 10X), 1-ethyl-3-[3 dimethylaminopropyl]carbodiimidehydrochloride (EDC), 3-aminopropyltrimethoxysilane (APS), dimethyl sulfoxide (DMSO), glutaraldehyde ($CH_2(CH_2CHO)_2$) and bicinchoninic acid (BCA) protein assay kit were purchased from (Sigma Aldrich). Anhydrous sodium carbonate (Na_2CO_3) and sodium hydrogen carbonate ($NaHCO_3$) were purchased from (SCRS) and (GCE laboratory chemicals) respectively. Sodium bicarbonate buffer (SBB, pH 8.3) was prepared from Na_2CO_3 and $NaHCO_3$ solution. Propylamine (C_3H_9N) and N-hydroxysuccinimide (NHS) were purchased from (Merck), 85% phosphoric acid (H_3PO_4) was purchased from (Lancaster Synthesis), anti-Dengue serotype 2 virus antibody (clone 3H5, isotype IgG, 1.0 mg mL^{-1}) was purchased from (Millipore), hydrochloric acid (HCl, 36.5-38%) was purchased from (MSR), Econo-Pac® 10DG columns was purchased from (BioRad) and 13 mm diameter nanoporous alumina membranes (Anopore^{TM}) with 60 µm thickness, 100 nm nominal pore size and a porosity of 25–50% were purchased from (United Scientific). All chemicals and materials were used as received. All solutions were prepared in (1X PBS) with high-purity water from a Millipore milli-Q (Biocel, 18.2 MΩ) water purification system.

4.3.2. Grafting of Dengue virus particles or anti-Dengue virus antibodies onto the nanochannels of the membrane

Grafting of virus and antibody within the nanochannels of the alumina membrane were carried out using the silane-carbodiimide grafting reaction as follows. The alumina membranes were first immersed in 5% APS in acetone for 1 h. Subsequently, the membranes were washed thoroughly with acetone and dried with nitrogen gas. The membranes were further dried in oven for 30 min at 45°C. The membranes were then immersed in glutaraldehyde for 6 h, followed by thorough washing with ultrapure water and drying with nitrogen gas. 30 µL of 100 PFU mL^{-1} of the Dengue virus solution was drop-casted onto the membranes and kept at high humidity overnight. The membranes were subsequently rinsed with 1 M NaCl to remove any nonspecific absorbed Dengue viruses and dried with nitrogen gas. After which, 30 µL of 10^{-5} M propylamine was added to each membrane and kept at high humidity for 6 h to remove excess glutaraldehyde and to improve the hybridisation efficiency. Finally, the membranes were thoroughly washed using 1 M NaCl, followed by ultrapure water and dried with nitrogen gas. The same procedure was applied for the immobilisation of the 3H5 antibody onto the membrane.

4.3.3. Preparation of IgG/BSA labelled with Fc-COOH

3H5 antibody (1 mg mL^{-1}, 900 µl) was concentrated to ca. (3 mg mL^{-1}, 300 µL) using Eppendorf concentrator 5301 at 4°C (solution A). 23 mg of FcCOOH was dissolved in 1 mL of DMSO (solution B). 0.14 mmol of EDC

and NHS were dissolved in 1 mL of DMSO (solution C). Solution B was added drop-wise into solution C with stirring. Subsequently, the mixture was stirred continuously for 2 h at 25°C. After 2 h, the mixture was added to solution A and stirred continuously at 4°C overnight. Free FcCOOH molecules were removed using Econo-Pac® 10DG column. Two bands were observed in the column. The first band contained IgG labelled with FcCOOH (IgG-Fc) and the second band contained the free FcCOOH molecules. The first band was eluted out using PBS as eluent and collected in fractions of 1 mL. BCA protein assay method was used to identify the IgG-Fc fractions which were combined and concentrated to ca. 2 mL using Eppendorf concentrator 5301 at 4°C. The final concentration of IgG-Fc was determined with the BCA protein assay method using Agilent Technologies, Carry 100 UV-Visible Spectrophotometer. Cyclic voltammetry of IgG-Fc was performed using an electrochemical station (CHI Instruments, Electrochemical Analyser model 750D). For the BSA labelling, BSA solution (3 mg mL^{-1}, 300 µL) was used to react with solution B and C following the same procedure above.

4.3.4. Analysis procedure of the membrane biosensor system

All analysis were carried out at room temperature, in the custom-made acrylic cell where the modified membrane was clamped between the feed and receiver compartments (Fig. 4.1). At start of the experiment, the feed compartment contained 100 µL of IgG-Fc in PBS (pH 7.4) and the receiver compartment contained 500 µL of PBS (pH 7.4) solution. Home-made glassy-carbon (GC) working electrode (WE), Pt mesh auxiliary electrode (CE) and

Ag/AgCl (1 M KCl) reference electrode (RE) were placed in the receiver solution. The solution in the receiver compartment was stirred constantly throughout the analysis. The amount of labelled antibodies (IgG-Fc) that transverse the membrane to the receiver compartment was measured using differential pulse voltammetry (DPV) with the following parameters; potential scan from 0.3-1.3 V versus Ag/AgCl (1M KCl) reference electrode, 10 mV increment potential and a 50 mV amplitude. Repeated DPV scans were applied at an interval of 1 min to measure the increase in IgG-Fc concentration with time in the receiver compartment.

4.3.5. Real sample analysis

Four clinical serum samples derived from patients infected with Dengue 2, 3 and 4 virus and an uninfected patient were used in the real sample analysis. These serum samples were collected from patients between 3-5 days after the onset of fever and the virus serotype was validated using reverse transcriptase-polymerase chain reaction (RT-PCR) assays. 15 µL of each serum sample was first diluted 2 times with PBS (pH 7.4) buffer. The diluted sample was subsequently drop casted onto the antibody grafted membrane, followed by a 1 h incubation. Finally, the analysis procedure was carried out. The National Healthcare Group (Singapore) Domain Specific Review Boards had approved the Prospective Adult Dengue Study (Reference No.: 2009/00432) from which clinical samples were derived. Informed consent was obtained for all participants.

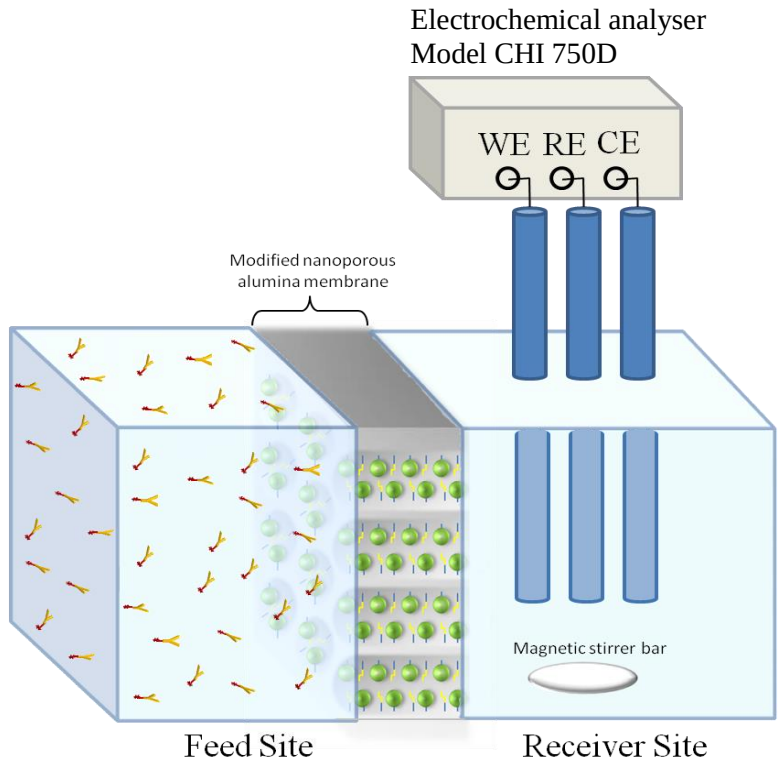

Fig. 4.1. Schematic diagram of the experimental setup (feed compartment: 100 µL of IgG-Fc, receiver compartment: 500 µL of PBS pH 7.4, WE: Glassy carbon electrode, RE: Ag/AgCl (1 M KCl), CE: (Pt wire mesh).

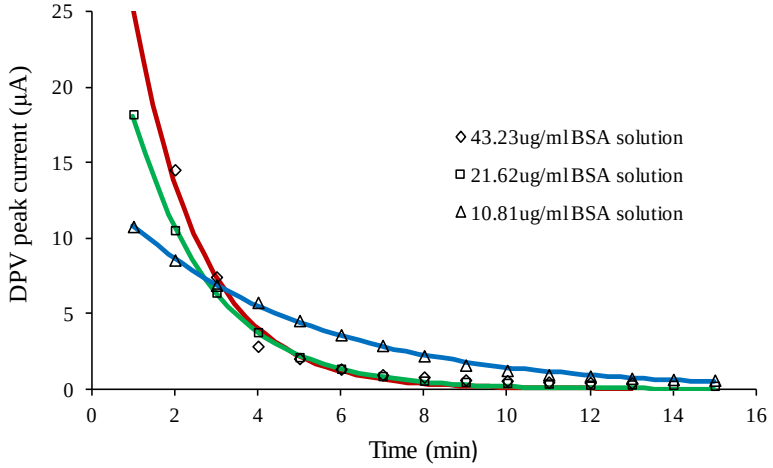

Fig. 4.2. Amperometric response of the glassy carbon electrode towards ferrocene tagged BSA proteins under stirred condition. The solid lines represent the curve fitted data using equation 5 to derive ($nFmA_0B$) and (k_aN) shown in table 4.1.

Table 4.1. Values of the ($nFmA_0B$) and (k_aN) parameters in equation 5 obtained from non-linear curve fitting.

Concentration of BSA (μg mL^{-1})	$nFmA_0B$-[M]	K_aN-[P]
43.23 (x5 dilution)	0.01416	1.156×10^{-6}
21.62 (x10 dilution)	0.02421	1.387×10^{-6}
10.81 (x20 dilution)	0.02073	0.925×10^{-6}
	Average=0.0197	Average = 1.156×10^{-6}

4.4. Results and discussion

4.4.1. Characterisation of the membrane biosensor setup

Fig. 4.3A shows the concentration level of BSA in the receiver solution of the two compartment cell as the proteins transverse the nanochannels of the membrane, measured using the BCA protein assay method. To achieve a peak signal output that varies in peak times according to the diffusion rate, the electrochemical detector which can respond sensitively to the redox labelled proteins while at same time undergoes surface fouling is selected. The opposing effects of the increasing level of redox labelled proteins in the receiver solution and the depression of the signal due to electrode fouling by the same proteins will create a peak signal. Fig. 4.3B shows the signal response of the electrochemical detector towards ferrocene labelled BSA as it passes through the same membrane from 3 different concentrations of the feed solution. As expected, the signal peak shifts toward shorter times as the protein concentration in the feed solution increases, due to faster protein diffusion and electrode fouling. Thus, the signal output can be measured as a form of elution time that depends on the rate of diffusion of the proteins transversing the nanochannels of the membrane. Such a parameter is particularly useful to describe separation efficiency, to derive physical parameter such as partition equilibrium constants between eluting species and the stationary surface, and to predict resolution of constituents in multi-components samples.

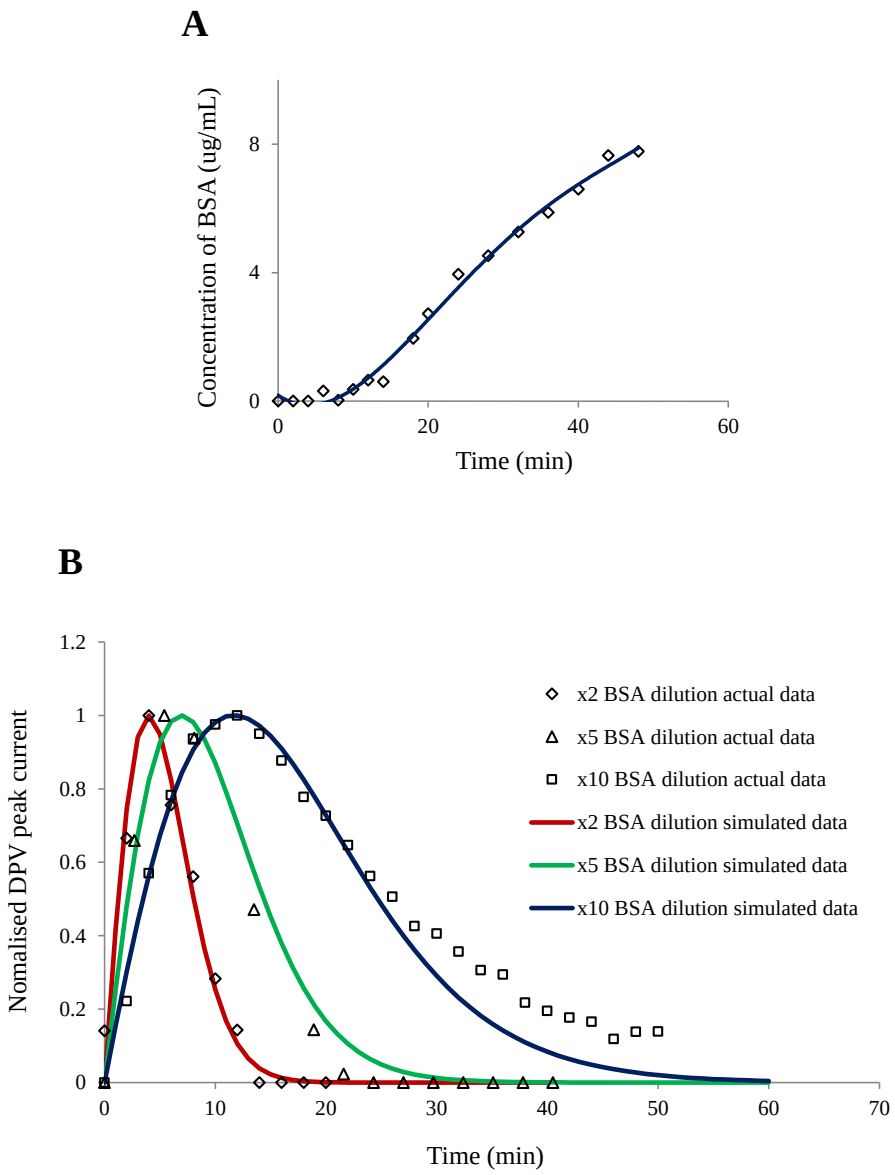

Fig. 4.3. (A) Increase in BSA concentration (determined using BCA kit assay) in the receiver solution after transversing an unmodified membrane from the feed solution; (B) Signal response of the electrochemical detector towards ferrocene labelled BSA as it transverse the unmodified membrane from 3 different concentrations of feed solution. Fitted lines represent the simulated data.

From table 4.2, we observed that the diffusion coefficient generally decreases with increasing dilution of the concentration of the labelled BSA used in the experiment. This is a strange phenomenon as the diffusion coefficient should stay the same for the same labelled protein diffusing through the bare

nanochannels. The ferrocene labelled BSA consists of a hydrophobic part (the ferrocene moiety) as well as a hydrophilic part (the BSA moiety). The increase in the number of water molecules due to dilution may impede the movement of the labelled BSA. This is due to the partial attraction by the BSA moiety as well as the partial repulsion by the ferrocene moiety. As a consequence, the diffusion of the labelled BSA was slightly slower when diluted.

Table 4.2. Values of the diffusion coefficient, (x) and ratio (y) parameters in equation 9 obtained from the simulation of the labelled BSA transvering through the bare membrane.

Concentration	Diffusion coefficient($cm^2 s^{-1}$)	y	x
X2 BSA dilution	5.50×10^{-6}	0.4	0
X5 BSA dilution	5.00×10^{-6}	0.4	0
X10 BSA dilution	3.50×10^{-6}	0.4	0

4.4.2. Selectivity and specificity of the virus grafted biosensor

The 3H5 antibody which binds exclusively to a particular region of the envelope domain III (ED III) protein of the Dengue 2 virus was used as the labelled probe to interact specifically or non-specifically with the target or non-target virus particle attached within the nanochannel respectively (Fig. 4.4). Fig. 4.5A shows that using this sensing scheme, the diffusion of the anti-Dengue 2 virus antibodies across the Dengue 2 virus grafted nanochannels, gives a peak with an elution time of 30 min. This is distinctly different from the membrane without viruses grafted (the control) which took 8 min. To test the specificity of this method, the same experiment was carried out using the nonspecific Dengue 3 virus that has high structural similarity as the Dengue 2 virus. The 3H5 antibody which neutralises the Dengue 2 virus is however not neutralising for the other three serotypes because of the differences in the ED III protein. We

observed that the Dengue 3 virus grafted membrane clearly gives a different elution time compared to the Dengue 2 virus grafted membrane.

Specific interactions with the Dengue 2 viruses grafted within the nanochannels slowed down the transversing rate of the labelled anti-Dengue 2 virus antibodies, compared to the Dengue 3 virus grafted nanochannels. The virus grafted membrane can be regenerated by passing 5 mL of 0.01 M HCl through the membrane using a simple syringe to remove the virus bound antibodies from the grafted virus particles. Fig. 4.5B shows the reproducible signal profile derived at the electrochemical detector after the regeneration procedure. The slight increase in elution time is attributed to the incomplete removal of the labelled antibodies from within the membrane.

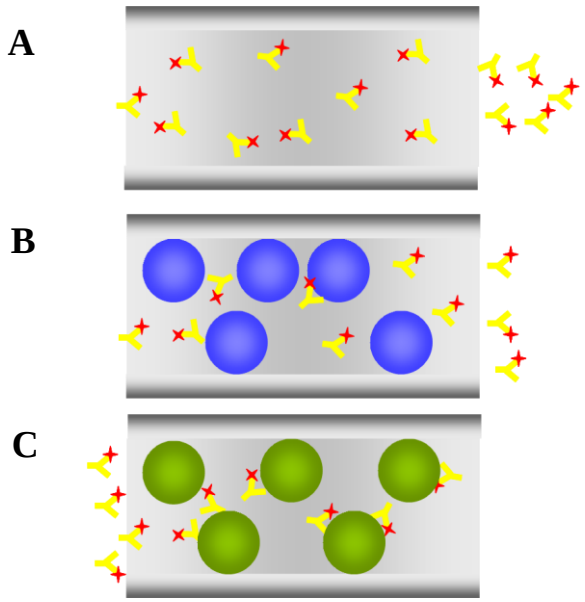

Fig. 4.4. Schematic diagram illustrating the virus grafted nanochannels; (A) Control nanochannel (B) Dengue 3 virus grafted nanochannel (C) Dengue 2 virus grafted nanochannel, followed by the addition of ferrocene labelled 3H5 anti-Dengue 2 virus antibodies on the feed side of a 2-compartment cell. Eluted redox labelled antibodies are detected at the receiver side by electrochemical detection.

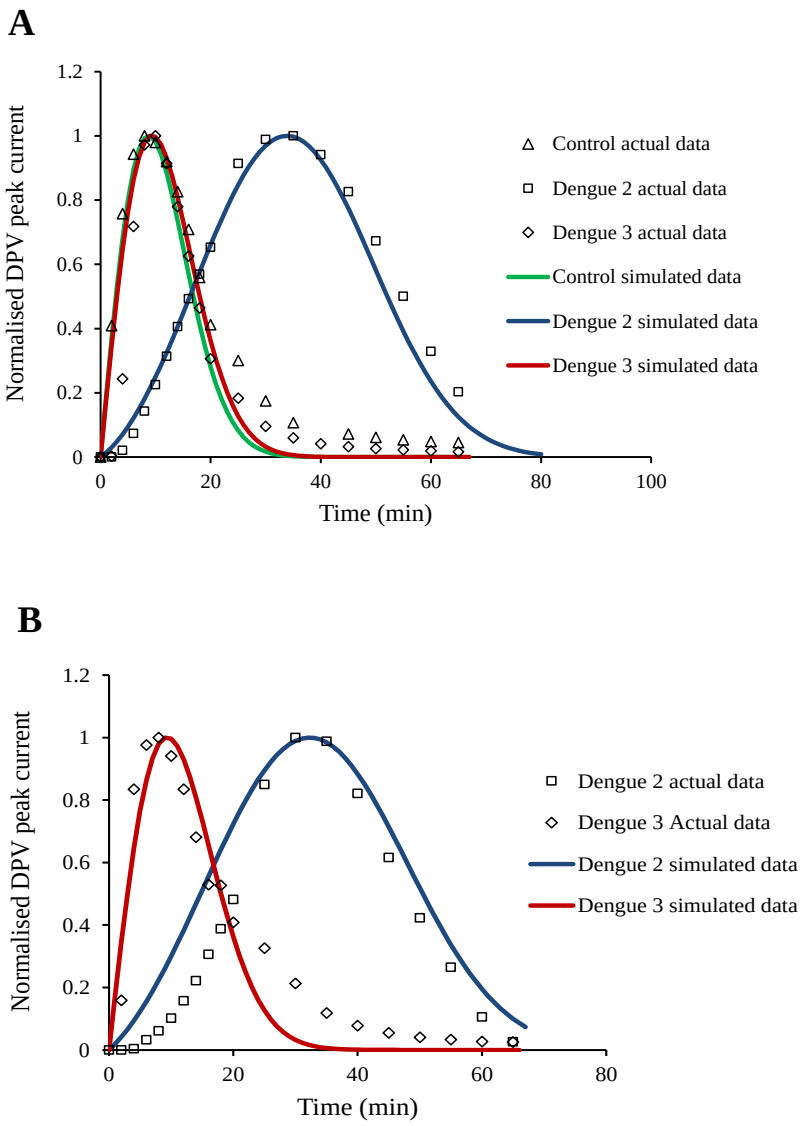

Fig. 4.5. (A) Electrode response towards ferrocene labelled anti-Dengue 2 virus antibodies as they transverse through the Dengue grafted membrane; (B) Repeated experiments after regeneration of the same membrane. Fitted lines represent the simulated data.

In the simulated data of the Dengue grafted membrane (Table 4.3), we observed that the diffusion coefficient of the labelled antibodies changes according to the conditions in the membrane. The diffusion of the labelled antibodies across the membrane is the fastest for the control membrane followed by the Dengue 3 virus grafted membrane and lastly the Dengue 2 virus grafted membrane. In general, the immobilisation of molecules within the nanochannels

of the membrane served to impede the movement of the labelled antibodies in the space constraint nanopores. The diffusion of the labelled antibodies across the control membrane is the fastest since there is no physical obstructions within the nanochannels. On the other hand, the diffusion of the labelled antibodies decreases upon immobilisation with the Dengue viruses. The chemically immobilised Dengue viruses constrict the diameter of the nanochannels being significantly large in size (50 nm) in comparison to the pore diameter (100 nm). The binding of the labelled antibodies to the immobilised Dengue 2 viruses further blocks the pores, thus diffusion of the labelled antibodies is the slowest.

The constant x was assigned 0 to the control and the Dengue 3 virus grafted biosensor since the ferrocene labelled anti-Dengue 2 virus antibodies do not bind to the bare or Dengue 3 virus grafted membrane. We noticed that in the control and Dengue 3 virus grafted membrane as well as the labelled BSA experiments, there is a small value for y (0.2 and 0.4) in the simulated data. These results indicate the presence of nonspecific adsorption which is reasonable since we cannot totally eliminate nonspecific adsorption in most sensors. The nonspecific adsorption for the labelled BSA is larger since the proteins are transversing through the bare hydrophilic membrane which provides ample sites for adsorption. This is unlike the Dengue virus grafted cases where most of the sites are occupied by the glutaraldehyde and the propylamine molecules. The specific adsorption of the labelled antibodies to the Dengue 2 viruses in the Dengue 2 virus grafted membrane is reflected by the large value of y compared to the control and Dengue 3 virus grafted membrane.

We also observed that the diffusion of the labelled BSA across the membrane is a lot faster than the labelled antibodies since the size of the BSA (~66 KDa) is much smaller than the IgG antibody (~150 KDa). The reported diffusion coefficients for the labelled BSA and antibody are slightly larger than the literature values, probably due to the short diffusion distance across the membrane (~60 um thick).

Table 4.3. Values of the diffusion coefficient, (x) and ratio (y) parameters in equation 9 obtained from the simulation of the labelled antibodies transvering through the control and the respective virus grafted membrane.

Biosensor type	Diffusion coefficient($cm^2\ s^{-1}$)	y	$x(s^{-1})$
Control	4.80×10^{-7}	0.2	0
Dengue 3	4.20×10^{-7}	0.2	0
Dengue 3 regenerate	4.20×10^{-7}	0.2	0
Dengue 2	4.00×10^{-7}	0.98	0.004
Dengue 2 regenerate	4.00×10^{-7}	0.97	0.004

4.4.3. Selectivity and specificity of the antibody grafted biosensor

Using the same grafting method, we attached the 3H5 antibodies onto the nanochannels of the alumina membrane, followed by the incubation of the membrane in the Dengue virus solution. Subsequently, the membrane was subjected to the labelled antibody probes elution experiment (Fig. 4.6). Unlike the virus grafting approach which requires overnight incubation of the membrane in the virus solution, this sandwich approach achieves virus capture within a short time of 60 min, followed by the sensing procedure of ~30 min, giving a total analysis time of less than 2 h. Since the virus is specifically captured using antibody-virus interaction, the grafted antibody approach is potentially applicable to direct detection of unlabelled virus in real sample analysis unlike the grafted virus approach.

Like the virus grafted membrane, the antibody grafted membrane also gives different elution times of the transversing antibodies according to the presence of specific or nonspecific viruses captured within the antibody grafted membrane (Fig. 4.7). In addition, we demonstrated the use of the same membrane for multiple analysis by regenerating after each experiment. In the antibody grafted experiments, the difference in the elution time between the Dengue 2 sample and the Dengue 3 sample is small compared to the virus grafted membrane. This is possibly due to the two step immobilisation in the preparation of the antibody grafted biosensor. This may lead to less Dengue 2 viruses being capture when compared to the direct chemical immobilisation of the viruses in the virus grafted membrane. As a result, the difference in the timing is smaller due to potentially less binding sites available which lead to faster diffusion of the labelled antibody probes through the Dengue 2 captured membrane.

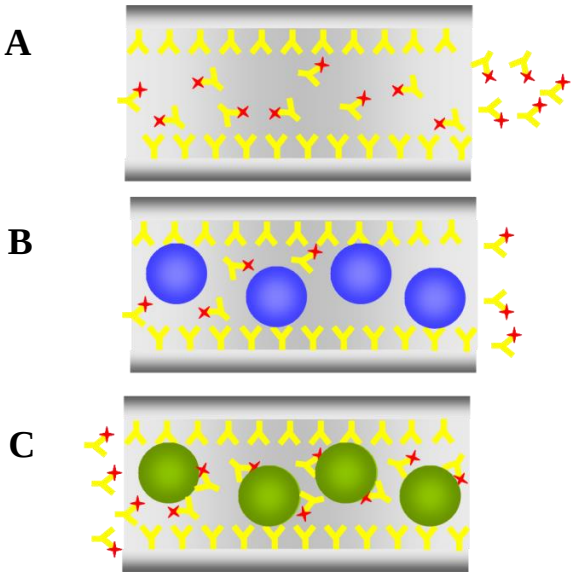

Fig. 4.6. Schematic diagram illustrating the antibody grafted nanochannels, followed by incubation in a sample containing unlabelled viruses; (A) Control nanochannel (B) Nanochannel immobilised with Dengue 3 viruses (C) Nanochannel immobilised with Dengue 2 viruses, followed by elution experiment of ferrocene labelled anti-Dengue 2 virus antibodies as in (Fig. 4.4).

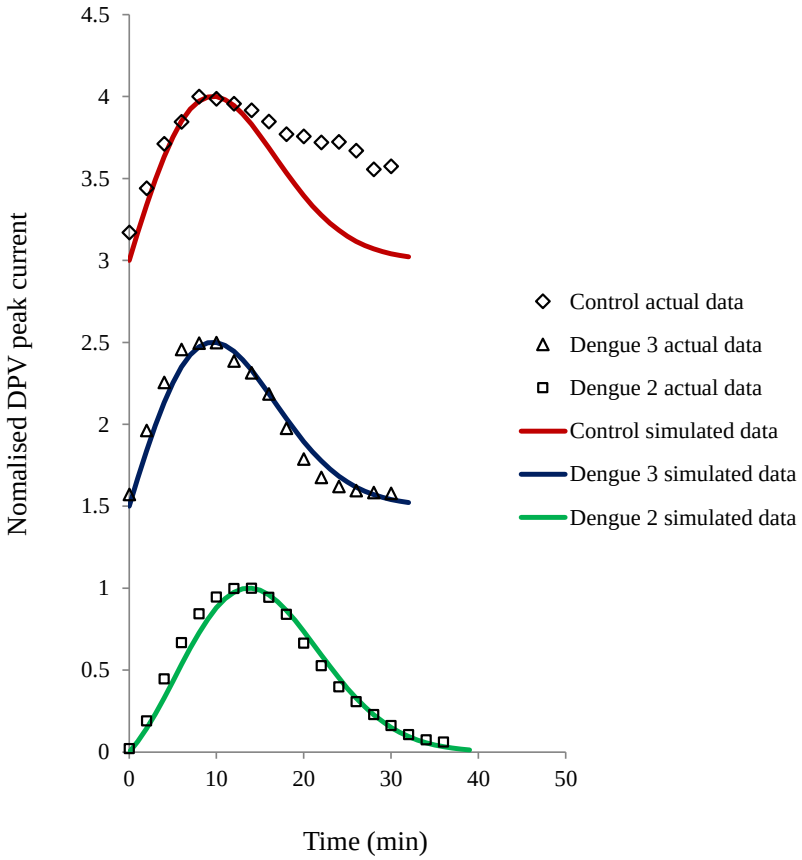

Fig. 4.7. Electrode response towards ferrocene labelled anti-Dengue 2 virus antibodies as they transverse through the antibody grafted membrane after 1 hour incubation with the Dengue 2 and 3 viruses, respectively. Regeneration of the membrane was done in consecutive steps (top-down) after each analysis. Fitted lines represent the simulated data.

In the simulated data (Table 4.4), it is encouraging that similar results were obtained like the virus grafted membrane. Again, we observed that the diffusion of the labelled antibodies is the same for the control membrane and the membrane incubated with Dengue 3 viruses but slower in the membrane incubated with Dengue 2 viruses. The diffusion of the labelled antibodies across the control membrane is slightly slower than that of the virus grafted case because the antibodies that were chemically bounded to the membrane will cause a slight retardation of the diffusing labelled antibodies. The Dengue 3

viruses do not react with the anti-Dengue 2 virus antibodies immobilised on the nanochannels, thus after washing, the condition is similar to the control membrane. As a consequence, the diffusion of the labelled antibodies across the membrane has the same diffusion coefficient as the control membrane.

Table 4.4. Values of the diffusion coefficient, (x) and ratio (y) parameters in equation 9 obtained from the simulation of the labelled antibodies transvering through the control and antibody grafted membrane, incubated with the respective Dengue virus.

Biosensor type	Diffusion coefficient($cm^2\ s^{-1}$)	y	x(s^{-1})
Control	4.40×10^{-7}	0.2	0
Dengue 2	4.00×10^{-7}	0.8	0.08
Dengue 3	4.40×10^{-7}	0.2	0

The biosensor setup is a reusable membrane-based electrochemical system. Unlike all previous redox labelled-based immunosensors, the three main components of the membrane biosensor system - the working electrode, the redox labelled antibody and the membrane are distinctly independent, which allow flexible changes to suit the sample. For example, to analyse a patient's serum sample which could probably be infected by the Dengue 2 or Dengue 3 virus, the membrane biosensor system can readily analyse both targets by switching from a Dengue 2 virus capture membrane to a Dengue 3 virus capture membrane, with the corresponding change in the transversing redox labelled antibody probes. Since the signal produced depends on the flow of redox labelled probes through the membrane, the membrane biosensor system is ideally suited for continuous monitoring. Additionally, the sensor’s unique selectivity can be achieved in a relative short analysis time of 2 h. Though various detection of unlabelled viruses by electrochemical immunosensors had been reported, they tend to suffer from false positive results as a consequence

of poorer selectivity having adopted the static immobilisation approached. This problem is potentially amplified when the specific targets are of considerably lower amount than the nonspecific interfering targets.

This type of membrane biosensor system offers significant advantages over microfluidics-based protein analysis. First, there is no pump, thus the cost of a membrane biosensor system can be significantly reduced. Second, the detector uses a conventional macro-sized electrode but can provide highly sensitive response for a small 30 μL volume of a virus sample. This can be achieved because the parallel multi-arrayed nanochannels provide significant signal output at the electrode due to simultaneous elution of the antibody probes from the large number of nanochannels at any one time. Besides lowering the overall cost, this robust design avoids laborious miniaturisation procedure and associated instrumentation, thus suggests potential utilisation in fieldwork. Third, the narrow cross-section area of each nanochannel can achieve smaller dimension compared to microfluidic devices, thus allows intimate interaction between the diffusing antibody probes and the surface-bound viruses which will greatly improve the separation efficiency.

4.4.4. Real sample analysis

In real sample analysis, direct detection of non-labelled target analytes is highly desired because it achieves minimal sample preparation and pre-treatment. To test the utility of the method in clinical analysis, four serum samples were collected from an uninfected patient and patients infected with Dengue 2, 3 and 4 Dengue virus between 3-5 days after onset of fever and were validated using RT-PCR. Fig. 4.8 shows the proof of concept results on these four clinical serum samples using the membrane biosensor system. The labelled anti-Dengue 2 virus antibody probes eluted at the longest time for the Dengue 2 virus sample which was clearly distinguished from the other samples, thus demonstrates the excellent selectivity of the simple procedure relevant to real sample analysis.

When we compare the simulated data between the virus grafted membrane (Table 4.3) and the antibody grafted membrane (Table 4.4 and 4.5), the diffusion coefficient of the labelled antibodies flowing through the two types of membrane biosensor agrees closely with each other. The values obtained are also in close agreement with those reported in literatures. We can generalise and say that for any value of $y>0.7$ is probably a positive indication that a specific antigen-antibody interaction has occurred. Alternatively, for simulated data where $x=0$ is indicative that the specific antigen to the immobilised antibody is not present in the sample.

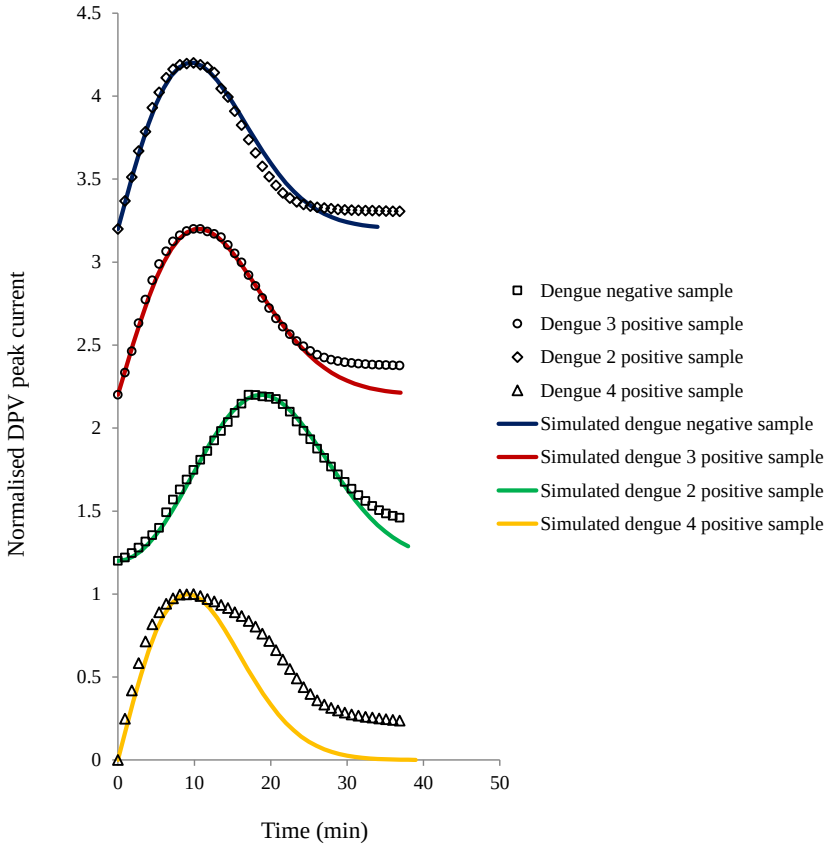

Fig. 4.8. Electrode response towards ferrocene labelled anti-Dengue 2 virus antibodies as they transverse through the antibody grafted membrane after 1 hour incubation with the uninfected human serum sample and human serum samples infected with Dengue 2, 3 and 4 viruses. Regeneration of the membrane was done in consecutive steps (top-down) after each analysis. Fitted lines represent the simulated data.

Assuming the adsorption between the Dengue virus and its corresponding antibody strictly follows the Freundlich adsorption isotherm and C^n remains approximately constant, we observed that the rate of adsorption is approximately 10 times faster in the antibody grafted membrane case. This result can be explained by two possible reasons; 1) the reduction in the binding sites available makes adsorption faster in a competitive manner; 2) the extra length of the antibody grafted pushes the antigen bounded closer to the opening

of the pore. This clearly reduces the distance required for the labelled antibodies to diffuse and makes binding more convenient.

In some experiments, we notice that the fouling is gradual. This could be due to random experimental errors or some of the adsorbed antibodies are dislodging from the electrode's surface. In many cases, the adsorption of protein to surfaces often evokes complicated processes such as changing its conformation upon attachment and repeated detaching and reattaching to the surface. Using the Langmuir equation as a start off, we have adequately simulated the data. Perhaps, detailed analysis of the ferrocene labelled antibodies' behaviour on the carbon electrode's surface may allow us to reflect whether the observed result is due to experimental errors or multiple processes occurring at the electrode due to the continuous adsorption of the labelled antibodies. The analysis will also allow us to obtain better simulation if the observed delay in fouling is due to various processes happening upon the attachment of the labelled antibodies.

.

Table 4.5. Values of the diffusion coefficient, (x) and ratio (y) parameters in equation 9 obtained from the simulation of the labelled antibodies transvering through the antibody grafted membrane, incubated with the respective real samples.

Biosensor type	Diffusion coefficient($cm^2\ s^{-1}$)	y	x(s^{-1})
Control(negative sample)	4.40×10^{-7}	0.2	0
Dengue 2	4.00×10^{-7}	0.98	0.04
Dengue 3	4.40×10^{-7}	0.2	0
Dengue 4	4.40×10^{-7}	0.2	0

4.5. Conclusion

The membrane biosensor system offers the uniqueness of analysis which can rapidly differentiate highly similar Dengue virus serotypes in short times. The overall detection scheme relies on diffusive mass transport of the labelled probes across the porous membrane and the subsequent fouling of the electrode as the probes adsorbed on its surface. The electrochemical signal output gives an ‘elution’ peak which can be adequately simulated using the Fick’s law of diffusion and Langmuir's absorption equation. Despite being similar to microfluidics-based analysis, the system does not need a precise pressure pump-valve system or highly sensitive detectors. Importantly, this simple design can be potentially miniaturised further using microelectrode arrays which are individually addressed at the end of each nanochannel to provide high throughput analysis.

4.6. References

1. Barbas, S. M., Ditzel, H. J., Salonen, E. M., Yang, W. P., Silverman, G. J., and Burton, D. R. (1995) Human autoantibody recognition of DNA, *Proc. Natl. Acad. Sci. U. S. A. 92*, 2529-2533.

2. Chanock, R. M., Crowe Jr, J. E., Murphy, B. R., and Burton, D. R. (1993) Human monoclonal antibody Fab fragments cloned from combinatorial libraries: Potential usefulness in prevention and/or treatment of major human viral diseases, *Infect. Agents Dis. 2*, 118-131.

3. Theofilopoulos, A. N., Kono, D. H., Beutler, B., and Baccala, R. (2011) Intracellular nucleic acid sensors and autoimmunity, *J. Interferon Cytokine Res. 31*, 867-886.

4. Tan, Y. J., Goh, P. Y., Fielding, B. C., Shen, S., Chou, C. F., Fu, J. L., Leong, H. N., Leo, Y. S., Ooi, E. E., Ling, A. E., Lim, S. G., and Hong, W. (2004) Profiles of Antibody Responses against Severe Acute Respiratory Syndrome Coronavirus Recombinant Proteins and Their Potential Use as Diagnostic Markers, *Clin. Diagn. Lab. Immunol. 11*, 362-371.

5. Verpoorte, E. (2002) Microfluidic chips for clinical and forensic analysis, *Electrophoresis 23*, 677-712.

6. Bo, Y. K., Swearingen, C. B., Ho, J. A. A., Romanova, E. V., Bohn, P. W., and Sweedler, J. V. (2007) Direct immobilisation of Fab′ in nanocapillaries for manipulating mass-limited samples, *J. Am. Chem. Soc. 129*, 7620-7626.

7. Gatimu, E. N., Sweedler, J. V., and Bohn, P. W. (2006) Nanofluidics and the role of nanocapillary array membranes in mass-limited chemical analysis, *Analyst 131*, 705-709.

8. Chin, C. D., Laksanasopin, T., Cheung, Y. K., Steinmiller, D., Linder, V., Parsa, H., Wang, J., Moore, H., Rouse, R., Umviligihozo, G., Karita, E., Mwambarangwe, L., Braunstein, S. L., Van De Wijgert, J., Sahabo, R., Justman, J. E., El-Sadr, W., and Sia, S. K. (2011) Microfluidics-based diagnostics of infectious diseases in the developing world, *Nat. Med. 17*, 1015-1019.

9. Rivet, C., Lee, H., Hirsch, A., Hamilton, S., and Lu, H. (2011) Microfluidics for medical diagnostics and biosensors, *Chem. Eng. Sci. 66*, 1490-1507.

10. Schoch, R. B., Han, J., and Renaud, P. (2008) Transport phenomena in nanofluidics, *Rev. Mod. Phys. 80*, 839-883.

11. Majd, S., Yusko, E. C., Billeh, Y. N., Macrae, M. X., Yang, J., and Mayer, M. (2010) Applications of biological pores in nanomedicine, sensing, and nanoelectronics, *Curr. Opin. Biotechnol. 21*, 439-476.

12. Wang, J. (2009) Biomolecule-functionalised nanowires: From nanosensors to nanocarriers, *ChemPhysChem 10*, 1748-1755.

13. Sun, Y., and Yang, K. (2008) Analysis of mass transport models based on Maxwell-Stefan theory and Fick's law for protein uptake to porous anion exchanger, *Sep. Purif. Technol. 60*, 180-189.

14. Rabe, M., Verdes, D., and Seeger, S. (2011) Understanding protein adsorption phenomena at solid surfaces, *Adv. Colloid Interface Sci. 162*, 87-106.

15. Nakanishi, K., Sakiyama, T., and Imamura, K. (2001) On the adsorption of proteins on solid surfaces, a common but very complicated phenomenon, *J. Biosci. Bioeng. 91*, 233-244.

16. Seiwert, B., and Karst, U. (2008) Ferrocene-based derivatisation in analytical chemistry, *Anal. Bioanal. Chem. 390*, 181-200.

17. Martić, S., Labib, M., Shipman, P. O., and Kraatz, H. B. (2011) Ferrocene-peptido conjugates: From synthesis to sensory applications, *Dalton Trans. 40*, 7264-7290.

18. Kossek, S., Padeste, C., and Tiefenauer, L. (1996) Immobilisation of streptavidin for immunosensors on nanostructured surfaces, *J. Mol. Recognit. 9*, 485-487.

19. Lim, T. K., and Matsunaga, T. (2001) Construction of electrochemical flow immunoassay system using capillary columns and ferrocene conjugated immunoglobulin G for detection of human chorionic gonadotrophin, *Biosens. Bioelectron. 16*, 1063-1069.

20. Lim, T. K., Ohta, H., and Matsunaga, T. (2003) Microfabricated on-chip-type electrochemical flow immunoassay system for the detection of histamine released in whole blood samples, *Anal. Chem. 75*, 3316-3321.

21. Tanaka, T., Izawa, K., Okochi, M., Lim, T. K., Watanabe, S., Harada, M., and Matsunaga, T. (2009) On-chip type cation-exchange chromatography with ferrocene-labelled anti-hemoglobin antibody and electrochemical detector for determination of hemoglobin A1c level, *Anal. Chim. Acta 638*, 186-190.

Chapter 5: Overall conclusion and future perspective

Electrochemical impedance spectroscopy has shown as a versatile technique that can be used for the characterisation of the alumina nanoporous membrane and the detection of Dengue virus. Through analysis of the Nyquist plots using equivalent circuits, we observed that binding events in the nanoporous membrane occur mainly near the pore openings. This deduction ties in with the Freundlich isotherm theory which states that the adsorption sites in the membrane may not have equal access to the bulk solution. The results of the Nyquist plot analysis have emphasised that an equivalent circuit should be constructed base on the understanding of the processes taking place in each region of the biosensor. In addition, we have shown that the constant phase element (CPE) can be used as an alternative to resistance (R) for identifying and quantifying of the target analyte due to the presence of an overall charge on the analyte.

By minimising the distance between the working, counter and the reference electrode, the sensitivity of the biosensor can be further improved. Even though immature Dengue viruses are present in lower quantities during the replication process, this amount is sufficient to be detected by the membrane sensor. The nanoscale thickness of the membrane allows diffusion to act effectively as a form of transport across the membrane. Making use of the close interactions between the antibodies and the Dengue viruses within the constraint nanopores enable us to differentiate the Dengue serotypes within a short period of time using a simple electrochemical setup. Overall, we have demonstrated

that the nanoporous membrane-based biosensor can achieve good sensitivity and selectivity required for an actual fieldwork. In addition, the small size of the membrane biosensor makes the fabricated sensor handy, easily disposable and can be carried in large numbers. All these are important factors for the development of a point-of-care diagnostic device.

The value of diagnostic can only be realised if the biosensor is able to meet the performance requirements and can be manufactured with a high volume. Having performance data does not always yield efficacy after the deployment and possible trials must establish the feasibility and cost effectiveness of the large scale production of the biosensor. For the membrane biosensor, the mere dependence on the blockage of the pores to generate signals is generally prone to unspecific binding phenomena. Besides, accuracies of the results between biosensors are often poor due to practical difficulties in controlling the physical or chemical immobilisation of the biorecognition elements as well as the blocking agents. As such, detailed optimisation and precise fabrication are required to ensure all the biosensor response fall within 5% relative standard deviation. Subsequently, numerous experiments need to be done to establish a guideline for the validation of results for non-specific and specific bindings of the Dengue virus. Lastly, a large scale clinical test with more than 50 samples is desirable to judge its benefits in routine patient care.

Although antigen-antibody interaction (immunoassay) type biosensors are highly specific and sensitive, these biomolecules are generally sensitive to the environment and susceptible to degradation at higher temperature and over

time. As a consequence, the self-life of the biosensor fabricated is often short. Besides, the use of purified antibodies and Dengue viruses will inevitably add cost to the development of the diagnostic tool. It will be advantageous to seek alternatives that can complement or replace immunoassay-typed biosensors without compromising the selectivity and sensitivity.

Large scale metallomics, metabolomics and proteomics can be carried out on healthy individuals, patients inflicted with normal Dengue and patients suffering from severe Dengue. With the results obtained, we may get fingerprints of patients infected with the different Dengue serotypes and those who had developed into severe Dengue. In addition, we can identify new potential biomarkers which can be recognised with organic or inorganic chelates that are stable over a long period of time. With the constant evolution of the Dengue virus, multidisciplinary research and collaboration are the keys to fully understand the behaviour of the Dengue virus and thereafter coming out with effective vaccines or drugs and biosensors to counter this debilitating disease.

List of Publications

1. Peh, A.E.K., Leo, Y.S., Toh, C.S. (2011) Current and nano-diagnostic tools for Dengue infection. *Front. Biosci. (Scholar edition) 3*, 806-821.

2. Nguyen, B.T.T., Peh, A.E.K., Chee, C.Y.L., Fink, K., Chow, V.T.K., Ng, M.M.L., Toh, C.S. (2012) Electrochemical impedance spectroscopy Characterisation of nanoporous alumina Dengue virus biosensor. *Bioelectrochemistry 88*, 15-21.

3. Peh, A.E.K., Li, S.F.Y. (2013) Dengue virus detection using impedance measured across nanoporous alumina membrane. *Biosens. Bioelectron. 42(1)*, 391-396.

4. Peh, A.E.K., Li, S.F.Y. (2013) Dengue virus detection using impedance measured across nanoporous alumina membrane. Singapore International Conference on Dengue and Emerging Infections, 21-23 November 2012.